Report No. UT-03.07

INFLUENCE OF SOIL SOFTENING AND LIQUEFACTION ON RESPONSE SPECTRA FOR BRIDGE DESIGN

Prepared For:

Utah Department of Transportation
Research and Development Division

Submitted By:

Brigham Young University
Department of Civil and Environmental Engineering

Authored By:

T. Leslie Youd
Ben Carter

March 2003

UDOT RESEARCH & DEVELOPMENT REPORT ABSTRACT

1. Report No. UT-03.07	**2. Government Accession No.**	**3. Recipient's Catalog No.**
4. Title and Subtitle: **Influence of Soil Softening and Liquefaction on Response Spectra for Bridge Design**	**5. Report Date** March 31, 2003 **6. Performing Organization Code**	
7. Author(s) **T. Leslie Youd** **Ben Carter**	**8. Performing Organization Report No.**	
9. Performing Organization Name and Address **Brigham Young University** **Department of Civil and Environmental Engineering** **Provo, Utah 84602**	**10. Work Unit No.** **11. Contract No.** 029008	
12. Sponsoring Agency Name and Address **Utah Department of Transportation** **4501 South 2700 West** **Salt Lake City, Utah 84119**	**13. Type of Report and Period Covered** Final Report, April 2001- March 2003 **14. Sponsoring Agency Code** 81FR0141	

15. Supplementary Notes

Clifton Farnsworth, UDOT Research Project Manager

16. Abstract: The purpose of this investigation is to assess the adequacy of seismic bridge design criteria and to suggest modifications to account for the influence of soil softening and liquefaction. To define the influence of soil softening on response spectra and assess the adequacy of LRFD seismic criteria, records are analyzed from five sites underlain by soils that liquefied. Findings are: (1) Where pore water pressures rose early during ground shaking, soil softening reduced short period (<0.7 sec) spectral accelerations. (2) Where soil softening did not occur early, softening has little influence on short period (<0.7 sec) ground motions. (3) Soil softening usually causes enhanced long-period (>0.7 to 1.0 sec) spectral values due to the onset of ground oscillation that persisted after strong ground shaking ceases. (4) For short fundamental periods (< 0.7 sec), LRFD acceleration coefficients, A, of either 0.60 g or 0.30 g and Code Soil Profile Types (CSPT) III or IV, elastic seismic design coefficients, C_{sm}, conservatively envelope calculated spectra, indicating that criteria in the LRFD code are adequate for liquefiable sites. (5) For structures with fundamental periods >0.7 sec, an A of 0.60 g and a CSPT IV generates C_{sm}, that conservatively envelope the calculated actual response spectra. (6) For design at liquefiable sites, increased ground deformation within the liquefied zone must be considered.

17. Key Words Earthquake, liquefaction, ground response, response spectra, seismic design coefficient		**18. Distribution Statement**	
19. Security Classification (of this report)	**20. Security Classification (of this page)**	**21. No. of Pages** 145	**22. Price**

THIS PAGE LEFT BLANK INTENTIONALLY

Influence of Soil Softening and Liquefaction on Response Spectra for Bridge Design

A Research Report Submitted to the
Utah Department of Transportation
UT-03.03

By

T. Leslie Youd
And
Ben L. Carter

Department of Civil and Environmental Engineering
Brigham Young University
Provo, Utah 84602

THIS PAGE LEFT BLANK INTENTIONALLY

CONTENTS

LIST OF FIGURES

LIST OF TABLES

SECTION 1

Introduction

Liquefaction has been a major cause of damage to bridges during past earthquakes. For example, 266 railway and highway bridges were severely damaged or collapsed due to liquefaction-induced lateral spread during the 1964 Alaska earthquake (Youd, 1978). Similar bridge damage has occurred during many other earthquakes as a consequence of lateral spread and other forms of ground displacement (Youd, 1993). Damage to bridges may occur due to either of two possible consequences of liquefaction: (1) Liquefaction may lead to large permanent ground displacements that distort and fracture structural elements. (2) Due to soil softening within the liquefiable layer as excess pore water pressures generate during the liquefaction process, ground response is modified changing the spectral content of the motions for which the structure must be designed. This paper addresses the second of these two possible deleterious effects.

In a past project, Youd et al.(1997) evaluated liquefaction-induced ground failure hazards to bridges in Utah, using liquefaction hazard screening procedures developed by Youd (1998). Little attention was given in that report to the influence of soil softening on ground response. As seismic design criteria were being developed for the major I-15 reconstruction project in Salt Lake County in the late 1990's, a major deficiency was discovered in engineering procedures for defining ground response for sites underlain by liquefiable layers. In the I-15 case, many bridge sites are underlain by liquefiable layers that, because the ground surface is nearly flat, pose no ground displacement hazard. At that time, design response spectra for the project were slightly enhanced for long-period motions to account for possible soil softening during earthquakes. This enhancement was

made on the basis of engineering judgment and was not supported by any analysis. Similar issues have developed for bridge sites in the Legacy Highway project.

The purpose of this investigation is to assess the adequacy of standard seismic design criteria, such as the criteria in the LRFD Bridge Code, and to suggest modifications that should be made to those criteria to account for the influence of soil softening and liquefaction. To better understand and define the influence of soil softening on response spectra at liquefiable sites and to assess the adequacy of LRFD code procedures, records are analyzed from five instrumented sites that are underlain by soils that clearly liquefied during the recorded ground shaking. Strong motion accelerometers had been installed at these sites prior to the occurrence of seismically induced liquefaction. The five sites are the Wildlife Liquefaction Array (WLA), Imperial Valley, California; the Port Island downhole instrument array (PIDA), Kobe, Japan; the Treasure Island (TI) strong motion site, San Francisco, California; the Alameda Naval Air Station (ANAS) strong motion site, Alameda, California; and the Kawagishi-cho apartment complex (NJ), Niigata, Japan**.**

Over the past 40 years liquefaction induced damage to buildings, roads, bridges, and earth dams, has alerted scientist, geologists, engineers and the general public of the danger of this phenomenon. Liquefaction is defined as "the transformation of a cohesionless material from a solid state into a liquefied state as a consequence of increased pore pressure and reduced effective stress" (Youd, 1975). One of the principal effects of liquefaction is ground softening that leads to modification of ground motions as they propagate through layers softened by the liquefaction process.

In this report, modifications of ground motions due to soil softening and liquefaction are analyzed by comparing actual ground motions and computed response spectra with motions predicted to occur at the same site in the absence of softening and liquefaction. The predicted motions are calculated from strong motion records produced by strong motion instruments either installed directly below the liquefiable layer (WLA and PDIA) or on nearby bedrock outcrops (TI and ANAS). In the case of the Niigata, Japan site, no reference records are available, so the actual ground motion and response spectra are compared with responses at the other sites noted above. The purpose of these analyses is to provide design guidance to Utah Department of Transportation bridge engineers and others responsible for design of major structures on sites underlain by subsurface liquefiable layers that have been shown to be benign with respect to generating large permanent ground deformations. In these instances, structures can be safely sited over the liquefiable deposits so long as modifications of ground motion due to softening and liquefaction are properly accounted for in the design.

SECTION 2

Investigative Procedure

As noted in the introduction, to determine the influence of soil softening and liquefaction on ground response, we collected and analyzed strong motion records from sites where other evidences, such as eruption of sand boils, ground settlement, and ground fissures, indicated that subsurface liquefaction had occurred during earthquake-induced strong ground shaking. Records from either subsurface instruments placed below the liquefiable layer or on nearby outcrops of bedrock were then used to predict ground motions that should have occurred at the sites in the absence of soil softening or liquefaction. For each site, ground motions and computed response spectra were determined from acceleration time histories measured at ground surface above the softened or liquefied layer. These motions and spectra are termed "actual" motions throughout this report. Similarly, ground motions and spectra that should have occurred at the site in the absence of soil softening and liquefaction were predicted by use of response analyses performed with the aid of the computer program PROSHAKE, a user-friendly Windows version of the program SHAKE. In these analyses, ground motions measured below the liquefiable layer or on a nearby bedrock outcrop were propagated upward through the sediment profile using shear-wave velocities and other soil properties. These were either measured prior to the earthquake or long after pore pressures had dissipated. No modulus reduction or other compensation was applied in these analyses to account for softening of liquefiable layers. Thus the predicted motions are estimates of those that should have occurred at the site in the absence of increased pore water pressures or liquefaction

Verification of Procedure

Verification of the consistency between predicted and actual motions in the absence of liquefaction, was performed by comparing actual and predicted motions from the 1987 Elmore Ranch earthquake (M=6.2). This earthquake shook the WLA site approximately 11 hours prior to the Superstition Hills earthquake, but did not generate significant measured pore water pressures (Holzer et al., 1989). Thus, according to our hypothesis, the predicted and actual ground motions and calculated response spectra should be similar for the Elmore Ranch event. Only enough records are presented in this section to verify the proposed procedure. Greater detail on the response of the WLA site is presented in the analysis contained in Section 3.

To compare motions and spectra at the WLA site, actual and predicted acceleration time histories at ground surface for the Elmore Ranch event are plotted on Figure 2.1a and b for both the North-South (NS) and East-West (EW) motions respectively. The NS and EW accelerations are nearly congruent in amplitude and period except for short intervals at about 5 sec and from 8 to 11.5 sec after instrumental triggering for the NS motions; and for the first 4 sec and an interval from 8 to 9 sec for the EW motions. In these discordinate time increments, the predicted amplitudes are slightly smaller than the measured values. Overall, the predicted accelerations appear generally compatible with the actual values.

To better assess differences between predicted and actual response of site, response spectra were calculated and plotted for these motions on Figure 2.2a and b for NS and EW directions respectively. Response spectra for both the NS and EW motions are essentially congruent at periods greater than 0.4 sec for the NS direction and 0.7 sec

for the EW direction. Actual and predicted spectra for periods less than 0.4 sec in the NS direction and 0.7 sec in the EW direction have basically the same shape, but with slightly lower predicted spectral values than measured spectral values. Based on this comparison, we suggest that for the WLA site and a condition of no pore pressure increase, predicted response spectra adequately match the actual spectra for comparative purposes.

As a second check of the procedure, we compared motions and calculated spectra at the 16 m depth that were recorded during the 1995 Kobe earthquake (M=6.9) (noted as actual motions and spectra on Figures 2.3 and 2.4) with predicted motions and spectra at that same depth that were calculated from motions recorded by a strong motion instrument that had been placed at the 32 m depth. Acceleration time histories from the 32 m depth were propagated upward to the 16 m depth using the program PROSHAKE. The soils between the 32 m and 16 m accelerometers are soft, non-liquefiable alluvial clays that did not detectably soften further during the earthquake. Comparisons of the actual and predicted accelerations at the 16 m depth, while not perfect, have amplitudes and frequencies of motions that match quite closely. Exceptions include a higher actual than predicted acceleration peak at about 8 sec in both the NS and EW records (Figure 2.3).

Calculated actual and predicted response spectra for the 16-m depth motions are plotted in Figure 2.4. Visual comparisons of these spectra indicate a close match between actual and predicted spectra for periods greater than 0.3 sec for the NS direction and greater than 0.5 sec for the EW direction. For periods less than 0.3 sec for the NS direction, the actual and predicted spectra are similar in shape, but vary in amplitude.

While in the EW direction a predicted peak is missing at a period of 0.3 sec. Again, the match appears adequate for comparative purposes.

Based on these comparisons we conclude that predicted motions and spectra generated by propagating motions upward through unsoftened soil strata, characterized by shear wave velocities and soil properties measured prior to the 1987 Elmore Ranch and 1995 Kobe earthquakes, adequately match actual motions and spectra to make the desired comparisons. Thus, major differences between actual and predicted motions in the chapters to follow are attributable to soil softening.

Procedure for sites without a down-hole accelerometer

At sites with a surface accelerometer but no down-hole accelerometers at the time of the earthquake, strong motion records from nearby bedrock outcrop stations are used to estimate predicted surface motions. In these instances, the program PROSHAKE was used to deconvolve the measured bedrock outcrop motion to motions expected at depth. The deconvolved motions were then transferred under the liquefaction site and propagated upward through an unsoftened site soil profile. Soil properties applied in these analyses included shear wave velocities and other properties measured long after earthquake-generated pore pressures had dissipated. Two liquefaction sites directly affected by the 1989 Loma Prieta (M=6.8) earthquake, Treasure Island (TI) and Alameda Naval Air Station (ANAS), were analyzed using this procedure. The bedrock outcrop record from Yerba Buena Island (YBI) was used for both of these analyses.

One site, Niigata, Japan, was analyzed with a surface ground motion record, but no corresponding down-hole or bedrock record was available. In this instance, comparisons are made only with other sites that we analyzed.

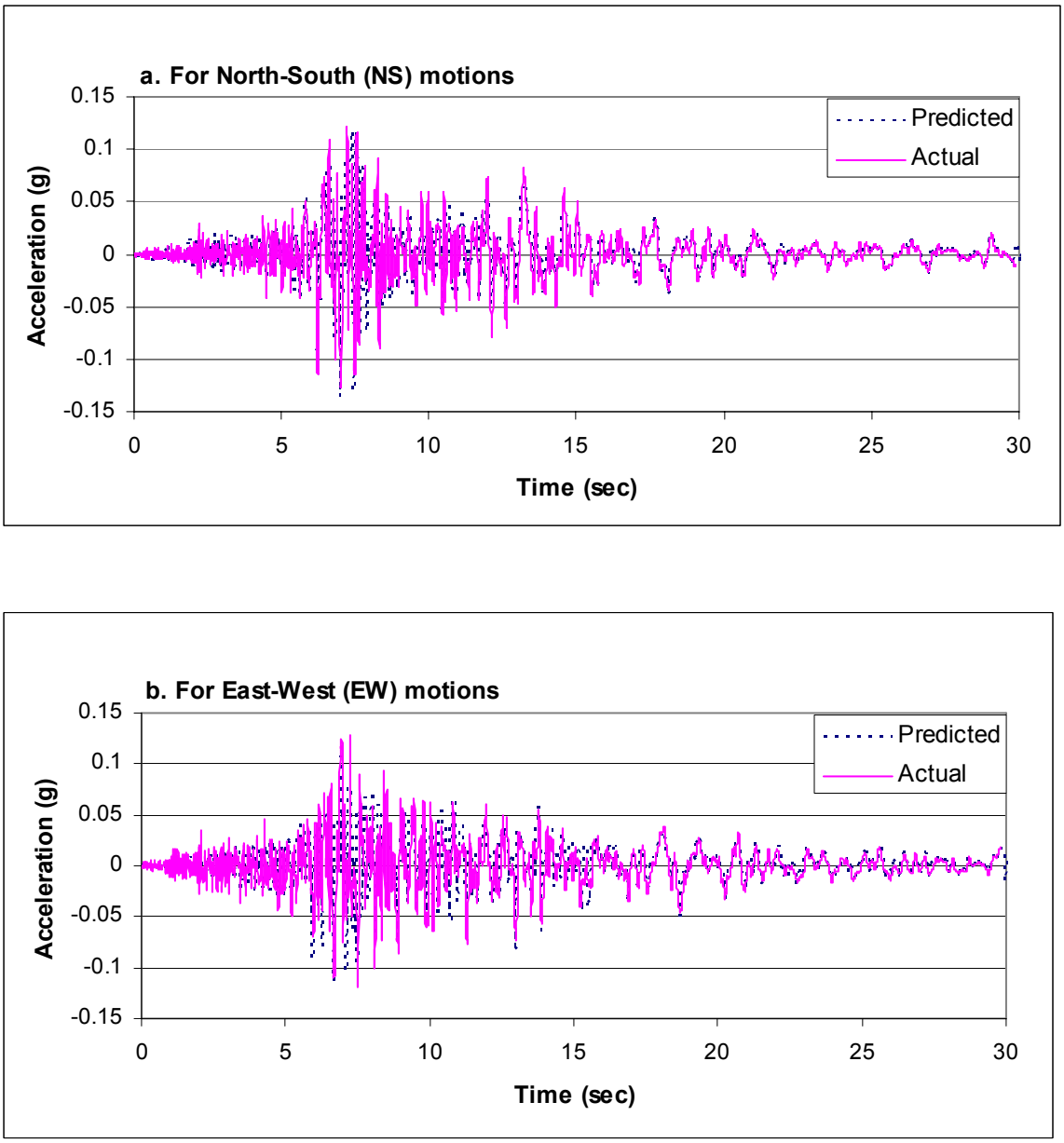

Figure 2.1. Predicted and actual acceleration time histories for WLA site during 1987 Elmore Ranch earthquake (M=6.2)

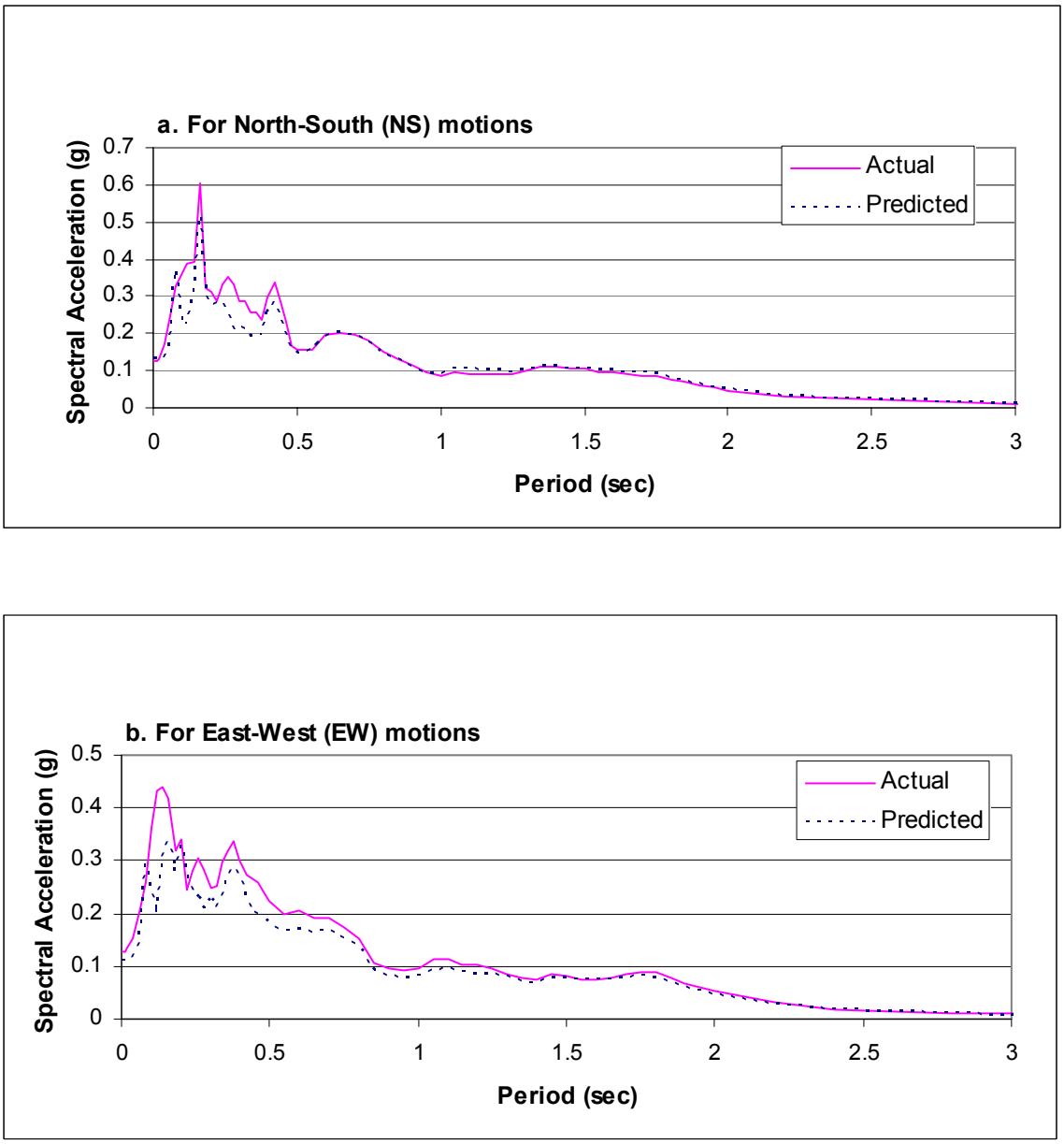

Figure 2.2. Predicted and actual response spectra for WLA site during 1987 Elmore Ranch earthquake (M=6.2)

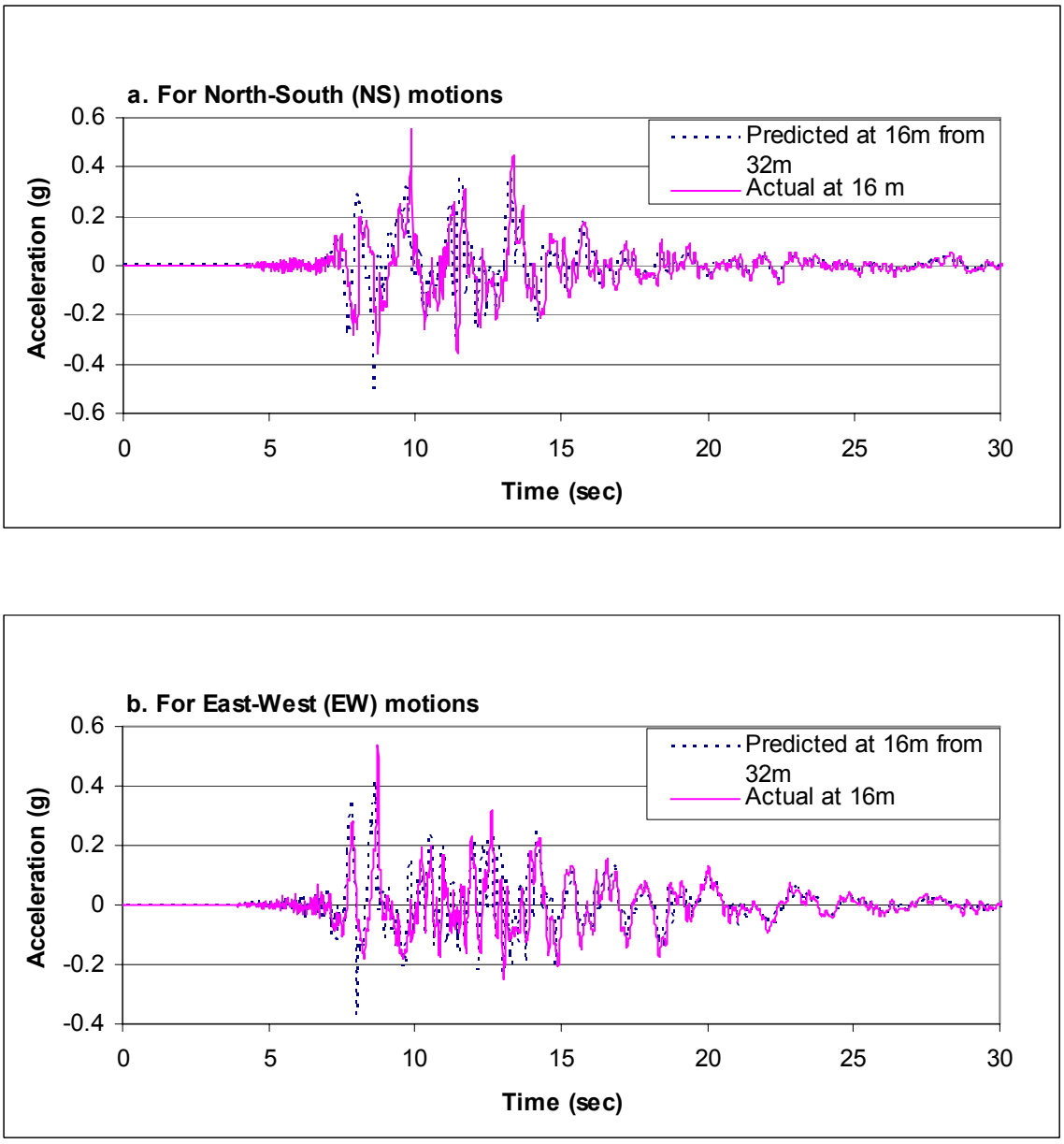

Figure 2.3. Predicted and actual acceleration time histories at 16 m depth at PIDA from 1995 Hyogoken-Nambu earthquake (M=6.9)

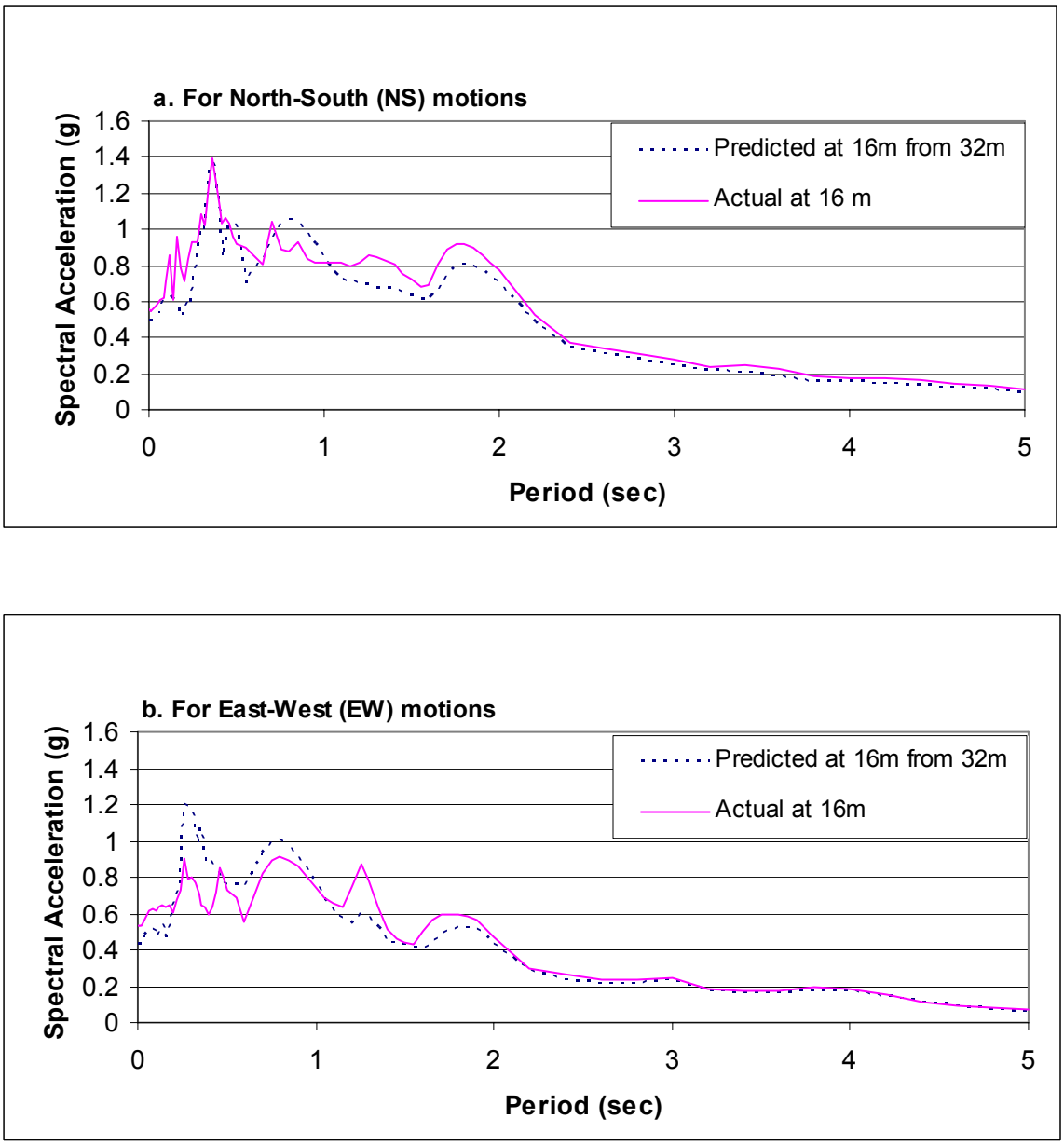

Figure 2.4. Predicted and actual response spectra at 16 m depth at PIDA from 1995 Hyogoken-Nambu earthquake (M=6.9)

SECTION 3

Wildlife Liquefaction Array

Site History, Stratigraphy, and Instrumentation

The Wildlife liquefaction array (WLA) is located in the flood plain of the Alamo River about 5 km south west of Calipatria and 160 km east of San Diego, California, in the Imperial Valley (Figure 3.1). The Imperial Valley is in a region of high seismicity, with earthquakes capable of generating liquefaction occurring, on average, about once every 12 years. In 1981, one of those earthquakes, the Westmorland event (M = 6.0), generated numerous sand boils in the flood plain of the Alamo River, including several at the WLA site (Youd and Wieczorck, 1981). In 1982, United States Geological Survey (USGS) personnel conducted cone penetration tests (CPT), standard penetration tests (SPT), and other subsurface investigations to delineate the thickness and extent of liquefiable layers beneath the site. They also installed an instrumented array (Bennett et al., 1984) (Figure 3.2).

The WLA site stratigraphy consists of about 2.5 m of silty and clayey flood plain deposits overlying a 4 m thick layer of liquefiable sands and silty sands. The liquefiable deposit is underlain by thick layers of overconsolidated clays and silts to a depth of at least 30 m (Bennett et al., 1984). The thickness and typical soil properties for these layers are listed in Table 3.1. This list includes layer thicknesses, shear wave velocities, plastic indexes, and unit weights that are applied in the response analyses conducted with PROSHAKE.

Instruments in the array consist of two three-component accelerometers (one at ground surface and one at a depth of 7.5 m, immediately below the liquefiable layer) and

six electrically transduced pore pressure piezometers (five at various depths within the liquefiable layer and one in a silt layer at a depth of 12 m) (Bennett et al., 1984). A plan view and cross sectional depiction of the instrument layout of the array is sketched in Figure 3.2.

The WLA site operates as a remote site without commercially available power. The power supplies and a data acquisition system are housed on-site in an instrument shelter. Power for the remote system is provided by batteries and solar-powered charging system. The instruments remain in a dormant state until one of the downhole accelerometers senses an acceleration greater than 0.01 g. At that instant, the instrument array is turned on and continuously records electrical signals from the various instruments until one-minute after the last acceleration pulse of 0.1 g is sensed by one of the downhole accelerometers. At that time, the power to the system turns off and the system returns to a dormant state.

1987 Elmore Ranch Earthquake (M=6.2)

At 5:54 pm local time, November 23, 1987, the Elmore Ranch earthquake shook the Imperial Valley. The epicenter was 23 km west of the WLA site. No surface fault rupture was reported for this event (Holzer et al., 1988). Peak ground accelerations of 0.13 g were recorded at ground surface at the WLA site on both the north-south (NS) and east-west (EW) components of motion. The duration of earthquake shaking was about 8 sec. No significant excess pore water pressures were recorded by the piezometers in the liquefiable layer. Because no pore water pressures were generated, this event provided

an excellent opportunity to verify and calibrate the analytical procedures used in this study.

Acceleration Time History

Without generation of significant excess pore water pressures, predicted ground responses using the program PROSHAKE should match the actual responses recorded at the ground surface. The records from the Elmore Ranch earthquake were used to verify this hypothesis. Predicted and actual acceleration time histories at ground surface from the Elmore Ranch earthquake are plotted on Figure 3.3 a and b for the NS and EW components of motion respectively. These plots indicate that the frequency characteristics of the predicted ground motions closely match those of the actual ground motions. However, many peaks of the predicted motions are smaller than those in the actual record.

Velocity Time History

Time histories of velocity, calculated by integrating time histories of acceleration, are plotted on Figures3.4 a and b for the NS and EW components of motion. Again, the frequency characteristics of the predicted motions closely match those of the actual motions, but several predicted peaks are smaller than the actual peaks. Nevertheless, the predicted velocity traces match the actual velocity traces more closely than was the case for the acceleration records.

Displacement Time History

By integrating the velocity records with respect to time, time histories of ground displacement are calculated. Time histories of ground displacement are plotted on Figures 3.5 a and b respectively, for the NS and EW components of motion. The

acceleration records apparently were not corrected sufficiently to prevent drift in the displacement time histories. Thus, both the NW and EW displacement traces drift either upward or downward. This drift indicates large permanent displacements, which did not occur. Ignoring the drift, the time histories indicate that the calculated predicted time histories of displacement closely match displacements calculated from the actual response, both in frequency and in amplitude of motion.

Acceleration Spectral Response

As a final test of the selected analytical procedure to generate predicted ground motions that match actual ground motions in the absence of significant increased pore water pressure, we calculated elastic response spectra, with 5 percent damping for both the NS and EW components of the acceleration time histories. For sand layers, average damping ratios and modulus values for sand (Seed and Idriss, 1970) provided the best matches between predicted and actual response spectra for this site. Thus average values for sand were used in these and all following computations of response spectra.

Acceleration response spectra for both the predicted and actual NS and EW components of motion are plotted in Figures 3.6 a and b respectively. The predicted spectra rather closely match those calculated from the actual time histories for periods greater than about 0.4 sec and 0.7 sec for the NS and EW motions respectively. Response spectra for shorter periods (0.0 to 0.4 sec) are sensitive to high frequency spikes in the ground motion records. These spikes are rather hard to predict, and therefore, will be ignored.

The Elmore Ranch earthquake comparisons were performed to verify and calibrate the analytical procedures used in this study. Although not perfect, the

comparisons developed for the Elmore Ranch earthquake indicate that motions and spectra can be adequately predicted for this site for comparative purposes. Thus major differences between predicted and actual responses developed in the following sections are attributed to sediment softening that occurs during the liquefaction process.

1987 Superstition Hills Earthquake

Earthquake and Seismic records

About 11 hours after the Elmore Ranch earthquake, at 5:15 am (local time) on November 24, 1987, the Superstition Hills earthquake (M=6.6) shook the WLA site, triggered the instrumentation into the active mode, and generated excess pore water pressures as large as 100 percent of the overburden pressure (r_u=1.0). This rise in pore water pressure liquefied the sand stratum (layer B, Figure 3.2) and generated nearby liquefaction effects including sand boils, ground fissures, and lateral ground displacements (Holzer et al., 1988; Youd and Bartlett, 1992; Youd and Holzer, 1992). Traces of the recorded acceleration and pore water pressure time histories are reproduced in Figure 3.7.

Using the time of triggering as reference (0 sec), the first acceleration spike greater than 0.05 g was recorded at 5 sec, the peak acceleration (0.21 g) was recorded at 13 sec. The last acceleration peak, greater than 0.05 g in the main sequence of accelerations, was recorded at 23 sec. Several subsequent acceleration spikes greater than 0.05 g were due to liquefaction induced ground oscillation as will be discussed later. Thus the duration of strong accelerations during this earthquake was about 18 sec with the peak acceleration arriving only a few sec after strong shaking began. To more clearly

illustrate the rise of pore water pressures in the liquefiable layer, the pore water pressure time histories were enlarged, normalized to yield pore pressure ratio (r_u) and plotted on Figure 3.8.

These records indicated that prior to the arrival of the peak acceleration pulse, pore pressure ratios were small, although slowly increasing. The pore pressure rise greatly accelerated following the arrival of the peak acceleration at 13 sec, but had only reached values of 0.4 to 0.5 (P2 and P5, Figure 3.8) at the top of the liquefying layer at the end of strong ground shaking (23 sec after triggering). By that time the site had softened sufficiently that ground oscillations were set in motion which continued until as long as 100 sec after triggering.

The fact that the soil system softened as pore water pressures increased is demonstrated in Figure 3.9 where recorded NS accelerations from the downhole and surface instruments are plotted on the same figure. Until 13 sec, the frequency characteristics of both records are similar with generally higher amplitudes of motions at the upper instrument due to site amplification. Beyond 13 sec, the frequency response from the surface instrument indicates a lengthening period and eventual transition to harmonic oscillation. At 18 sec, as pore water pressure ratios reach about 30 percent, coherence between the upper and lower motions is lost; thus indicating that the sediment above the liquefying layer was essentially decoupled and responding independently of the sediment layers beneath the liquefying zone. Clearly, pore water rise and eventual liquefaction of layer B greatly affected response of the ground surface at the WLA site.

Comparisons Between Records

Acceleration Time History

As was done for the Elmore Ranch earthquake records, comparisons will be made between ground motions measured at ground surface during the Superstition Hill earthquake and motions predicted using the PROSHAKE program. The same soil properties that were used in the Elmore Ranch analysis are used for the Superstition Hills analysis. The purpose for these comparisons is to determine the influence of pore-pressure-induced soil softening on ground response.

In Figures 3.10 a and b, predicted acceleration time histories are compared with actual time histories for NS and EW motions respectively. For the first 13 sec there is strong coherence between the frequency characteristics of predicted and actual records. However, the predicted amplitudes of motion are slightly less than actual amplitudes.

After arrival of the peak acceleration at 13 sec, the period of motion began to lengthen in the actual record relative to the predicted record. This lengthening was due to softening of the site as noted previously. Beyond about 20 sec there is little coherence between the two records. Also, the surface layer responded independently of the lower layer due to decoupling as a consequence of pore-pressure induced soil softening.

Velocity Time History

Similar characteristics of response occur in calculated time histories of velocity. Figures 3.11 a and b compares the predicted time history of velocity with the actual velocities motions in the NS and EW directions respectively. Prior to 13 sec, the responses are nearly congruent both in frequency and amplitude. After 13 sec, congruency is lost as long period oscillation develops in the actual velocity records.

However, in this instance low-amplitude longer period waves are evident in the predicted motions that are approximately in phase with the actual velocity waves. These longer period late arriving seismic waves apparently drove the ground oscillations to higher velocity amplitudes. In this instance, greater peak velocities were excited in the NS direction than in the EW direction.

Displacement Time History

Displacement time histories were determined by integrating the velocity time histories with respect to time. Calculated displacement time histories for WLA during the Superstition Hills earthquake are plotted on Figures3.12 a and b, for the NS and EW directions respectively. As noted with the velocity plots, the displacement plots clearly show the onset of ground oscillation and that amplitude of the ground oscillation increased with time after the cessation of strong ground accelerations about 23 sec after triggering. Youd and Holzer note that the increased displacements caused increased shear deformations within the liquefiable layer (1994). These larger cyclic shear deformations in turn generated increased pore water pressures. Hence the pore water pressures continued to rise after cessation of strong ground accelerations. The large oscillations also generated an extended train of long-period motions or oscillations that could adversely affect long-period structures, such as tall buildings and tall bridges.

As with the Elmore Ranch comparisons, the actual and predicted displacement time histories drift with time, indicating that the records were not corrected properly to eliminate drift in the displacement calculations. Although minor ground displacement (no more than a few tenths of a meter) occurred due to lateral spread at the site, the

constant rate of drift evident in Figure 3.12 indicates an error in calculation or processing of the records.

Comparison of Response Spectra

Total Spectral Acceleration Response

To examine the influence of soil softening on response spectra, acceleration response spectra with 5 percent damping were calculated from the actual and predicted ground motions. Those spectra are plotted on Figures 3.13a and b for the NS and EW directions respectively. Large predicted spectral peaks, at periods between 0.2 sec and 0.5 sec, are absent in the actual spectra, indicating that motions causing these expected peaks were absorbed in the softened layer. Conversely, at periods greater than 1.0 sec, the predicted spectra are larger than the actual spectra, indicating amplification of motions in the long period range. This amplification was due to ground oscillation that developed at the site. The greater amplification of motions in the 2.0 sec to 4.0 sec range in the NS direction compared to the EW direction was apparently due to greater oscillation in that direction, which is the approximate direction in which lateral spread displacement occurred (Youd and Bartlett, 1989).

13.6 and 15 Second Responses

To further demonstrate the attenuation of short-period motions and amplification of long-period motions as a function of sediment softening, we computed response spectra from various time segments of the actual and predicted records of ground motion. For example, predicted and actual spectra for the first 13.6 sec, up until the time of the arrival of the peak acceleration pulse and prior to significant pore-pressure rise, are plotted on Figure 3.14. These plots show that the predicted and actual spectra were

nearly congruent for this increment, an indication that significant sediment softening had not occurred at that time. By that time enough short period energy (periods less than 0.5 sec) had propagated through the site to generate spectral values nearly as large as the final spectral values illustrated in Figures 3.14 a and b. The small spectral values at periods greater than 1.5 sec on these figures indicate that very little long period seismic energy had propagated through or developed at the site by that time.

Spectra generated during the first 15 sec of record are plotted in Figures 3.15 a and b. During the 1.4 sec increment of time between 13.6 sec and 15 sec, the most intense accelerations generated by the earthquake passed through the site (Figure 3.10). These intense motions produced a spike in the predicted NS spectrum and several narrow spikes in the EW spectrum between periods of 0.3 sec and 0.6 sec. The spike in the NS spectrum had a maximum spectral value of 1.2 g. Only a muted spike, however, is evident in the spectra calculated from the actual records. Even though measured pore water pressures had risen to ratios, r_u, of only 5 to 20 percent by that time, those pore pressures apparently produced sufficient soil softening to mute the largest peak in the predicted NS spectrum.

The energy passing through the site between 13.6 sec and 15 sec was very directional. Intense motions and spectral energy occurred mostly in the NS direction. However by 15-sec time juncture, sufficient short-period seismic energy in both the NS and EW directions, had passed through the site to fill in the final response spectra up to periods of 0.6 sec. Also at 15 sec, predicted and actual spectra are almost congruent for the NS spectra for periods greater than about 0.6 sec, indicating that in the absence of ground oscillation, seismic shaking was complete for the entire earthquake. Conversely,

the greater spectral values in the final actual spectra compared to the 15 sec spectra in the NS direction indicates that significant ground oscillation had not developed at that time. The same conclusion is generally true for the EW spectra, except that the much greater spectral values in the actual spectra compared to the predicted spectra at periods between 0.6 sec and 1.0 sec indicate that some longer period energy or ground oscillation had begun to develop in the EW direction by 15 sec.

20 Second Response

An examination of the predicted acceleration time history reveals that the most intense predicted ground motions in the EW direction passed through the site between 15 and 20 sec. The site, however, had softened sufficiently by 15 sec to 20 sec (r_u between 0.2 and 0.7 from the curves in Figure 3.8) to prevent transmission of these intense motions through the liquefying layer. Although these intense motions generated a strong, spectral peak of 1.1 g in the predicted EW spectra, this peak is muted in the actual spectra (Figure 3.16). Thus, no significant increase was generated in the actual response spectrum over this period range (0.3 sec to 0.6 sec) during this time interval (15 and 20 sec after triggering).

Beyond the 20 sec time mark, ground motions measured at the ground surface were sufficient to greatly increase spectral values for periods (greater than 1.2 sec) in both NS and EW directions. For example, between the 15 sec and 20 sec time marks, sufficient energy was generated in the actual NS record to increase spectral values in the actual spectrum from roughly 0.2 g to 0.4 g for periods between 0.8 sec and 1.3 sec and completely fill in that segment of the final actual response spectrum. As noted above,

increases in the NS spectra were much greater than those in the EW spectra over the 15 to 20 sec time increment.

25 and 50 Second Response

Between time increments of 25 sec and 50 sec, while pore water pressures were increasing to values near r_u = 100 percent and the site was in a state of ground oscillation, spectral values continued to increase for periods greater than 2.6 sec for the NS actual spectrum and greater than 1.0 sec for the EW actual spectrum (Figure 3.17). By the 50 sec time mark, the actual spectra had reached its final values in both the NS and EW direction (Figure 3.18).

Summary

In summary, the principal consequences of increased pore water pressure and soil softening on ground response at the WLA site were: (1) greatly reduced predicted peaks in the response spectra between periods of 0.3 sec and 0.6 sec; (2) greater duration of ground shaking (extended essentially from 20 sec to 50 sec); and (3) greater energy or response values at long periods (greater than 0.7 sec) due to the development of ground oscillation.

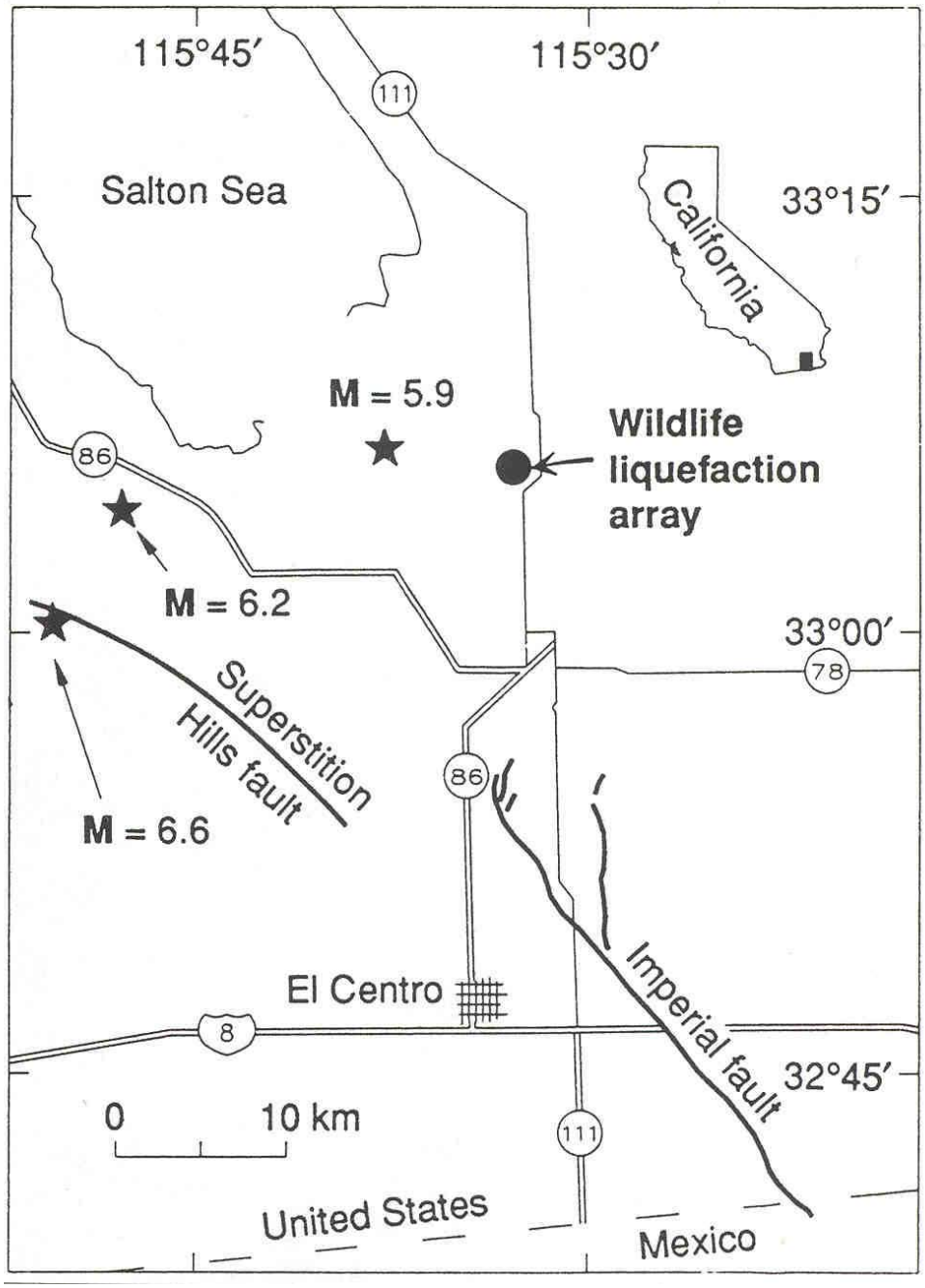

Figure 3.1. Map of Imperial Valley with marked location of WLA site and epicenters of earthquakes (after Holzer et al., 1989)

Table 3.1. Soil properties for sediment layers at the WLA site

Material Type	Layer Number	Thickness (m)	Unit Weight (kN/m^3)	G_{max} (MPa)	V_s (m/s)
Clayey Silt	1	0.5	15.7	23.1	120
	2	0.5	15.7	23.1	120
	:	:	:	:	:
	5	0.5	15.7	23.1	120
Silty Sand	6	0.5	17.3	25.4	120
	7	0.5	17.3	34.5	140
	:	:	:	:	:
	10	0.5	17.3	34.5	140
	11	0.5	17.3	21.3	110
	12	0.5	17.3	21.3	110
	13	0.5	17.3	63.6	190
	14	0.5	17.3	63.6	190
Silty Clay	15	0.5	20.4	75.2	190
	16	Infinite	20.4	75.2	190

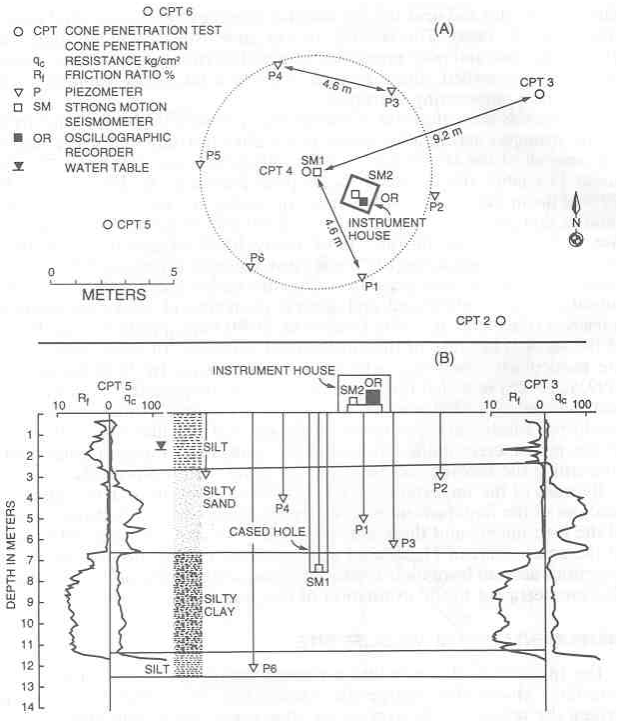

Figure 3.2. Site plan (a) and cross section (b) showing sediment layers and instrument locations at WLA (after Bennett et al., 1984)

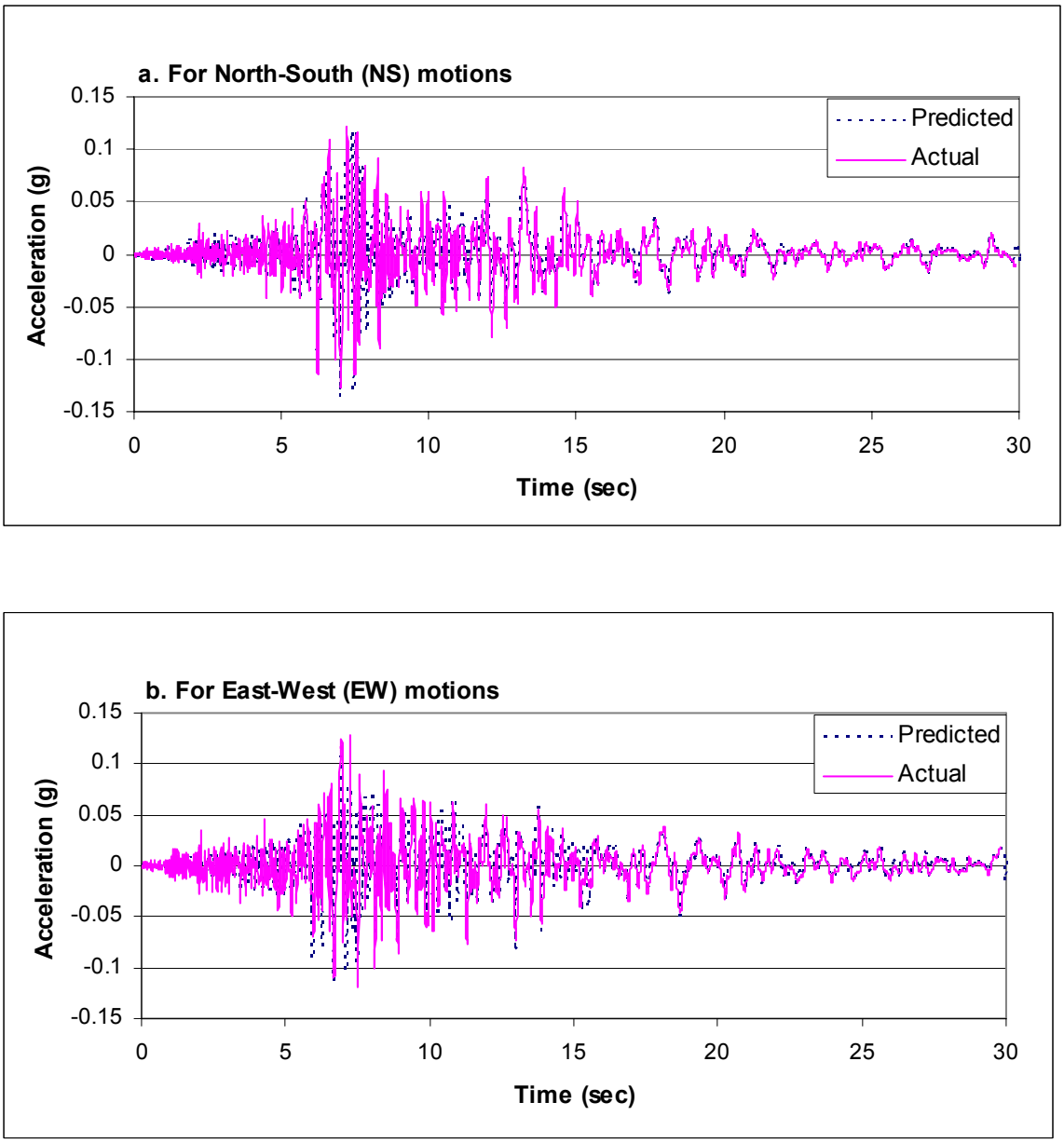

Figure 3.3. Predicted and actual acceleration time histories for WLA site during 1987 Elmore Ranch earthquake (M=6.2)

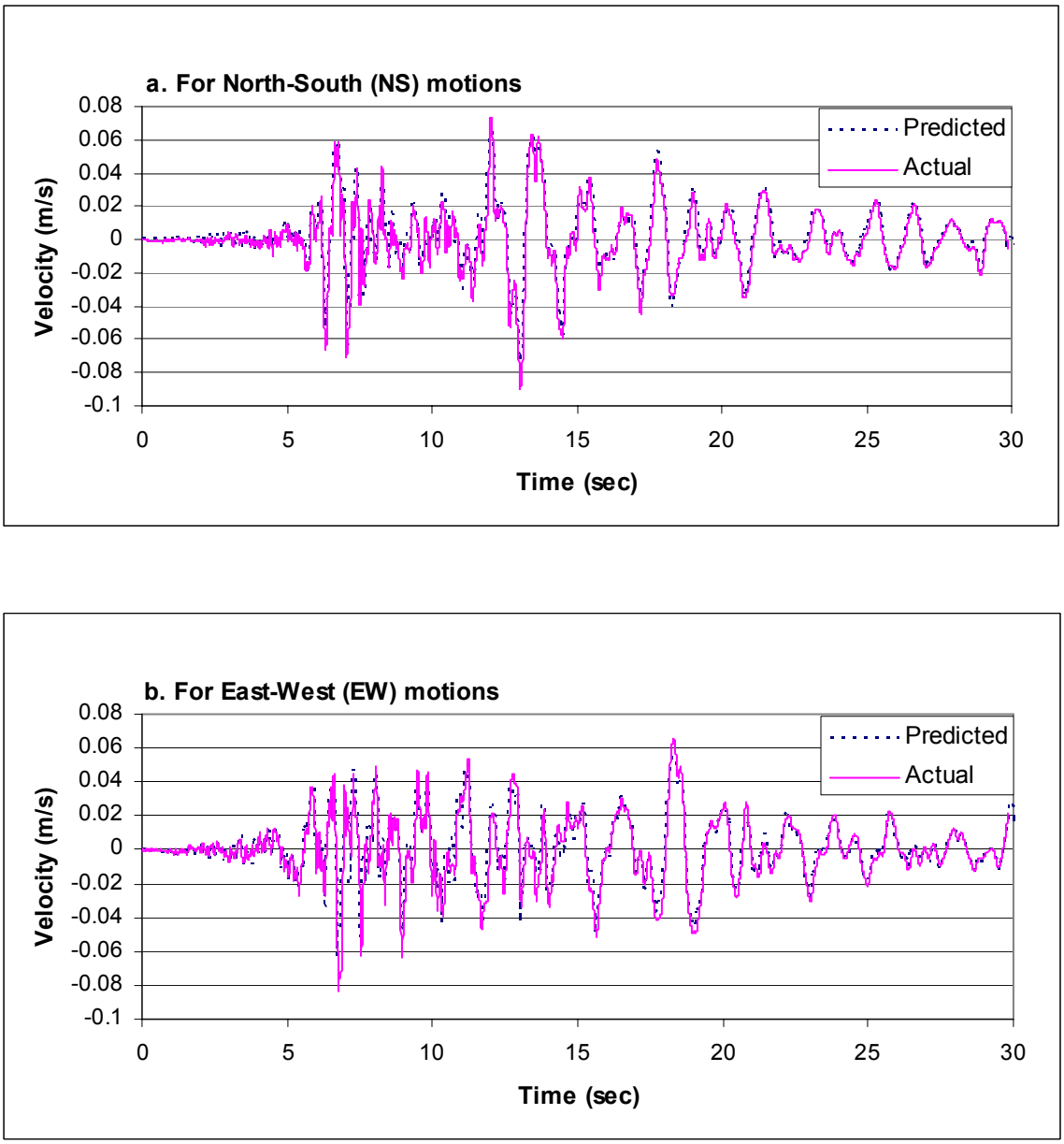

Figure 3.4. Predicted and actual velocity time histories for WLA site during 1987 Elmore Ranch earthquake (M=6.2)

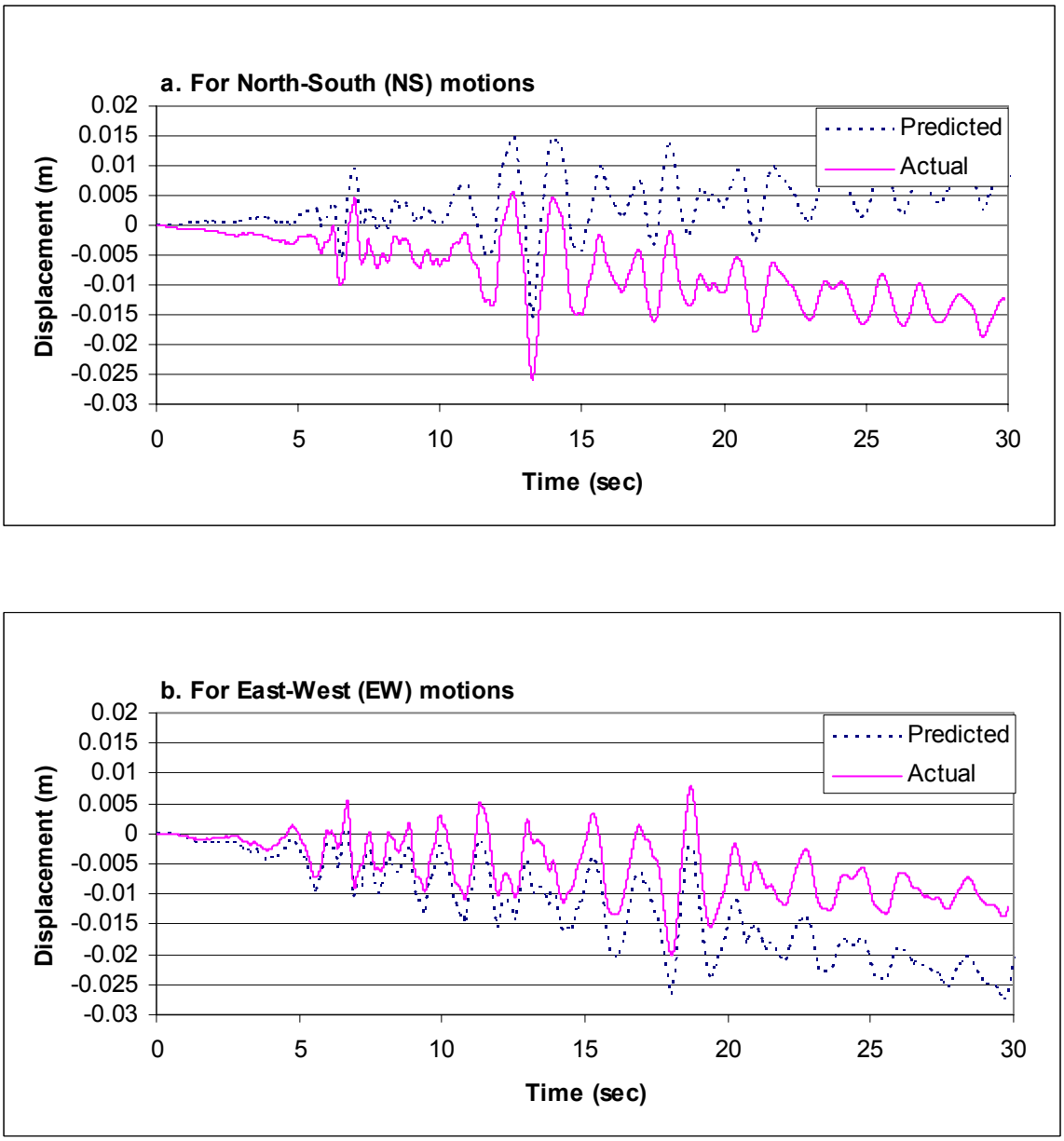

Figure 3.5. Predicted and actual displacement time histories for WLA site during 1987 Elmore Ranch earthquake (M=6.2)

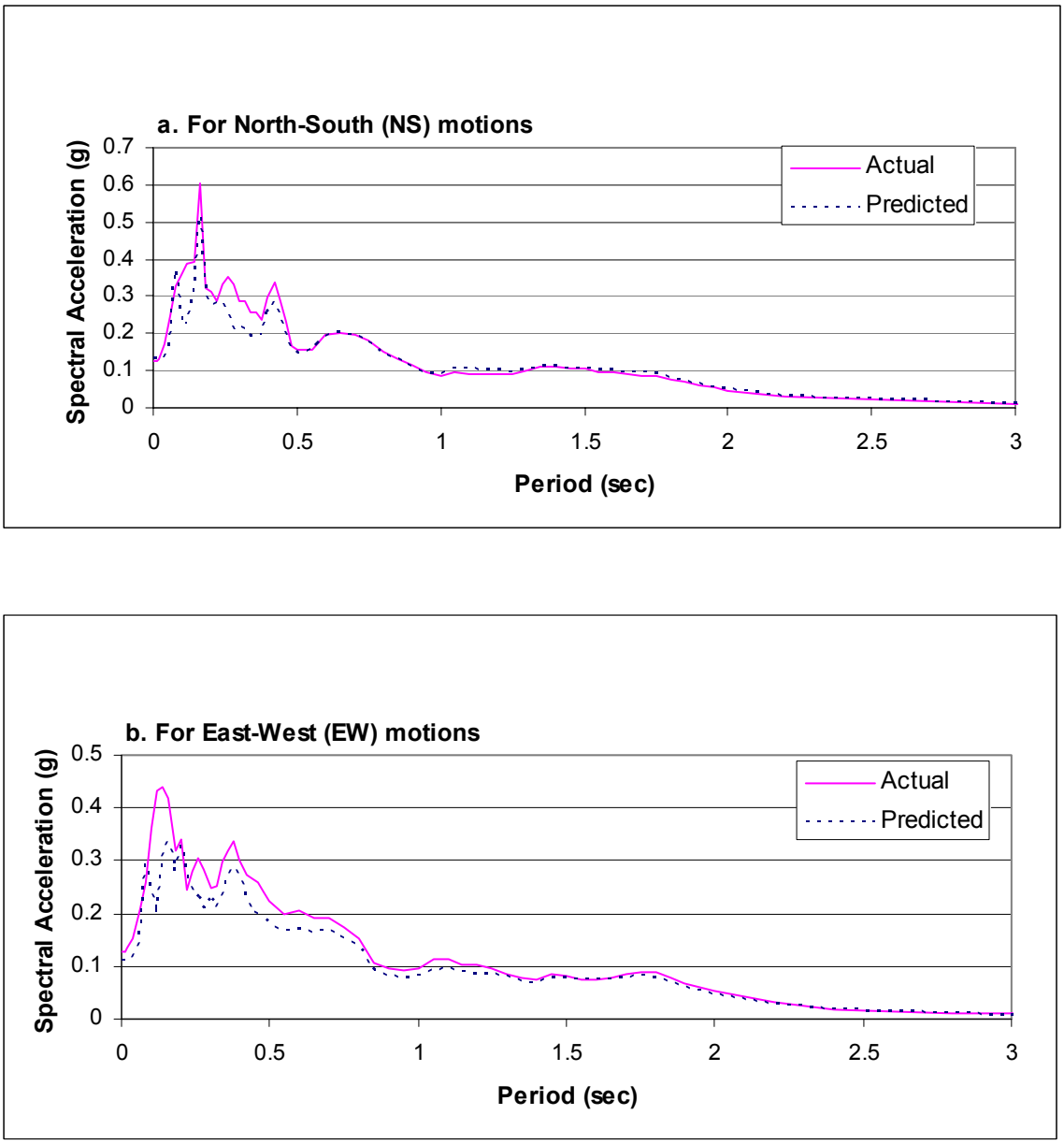

Figure 3.6. Predicted and actual response spectra for WLA site during 1987 Elmore Ranch earthquake (M=6.2)

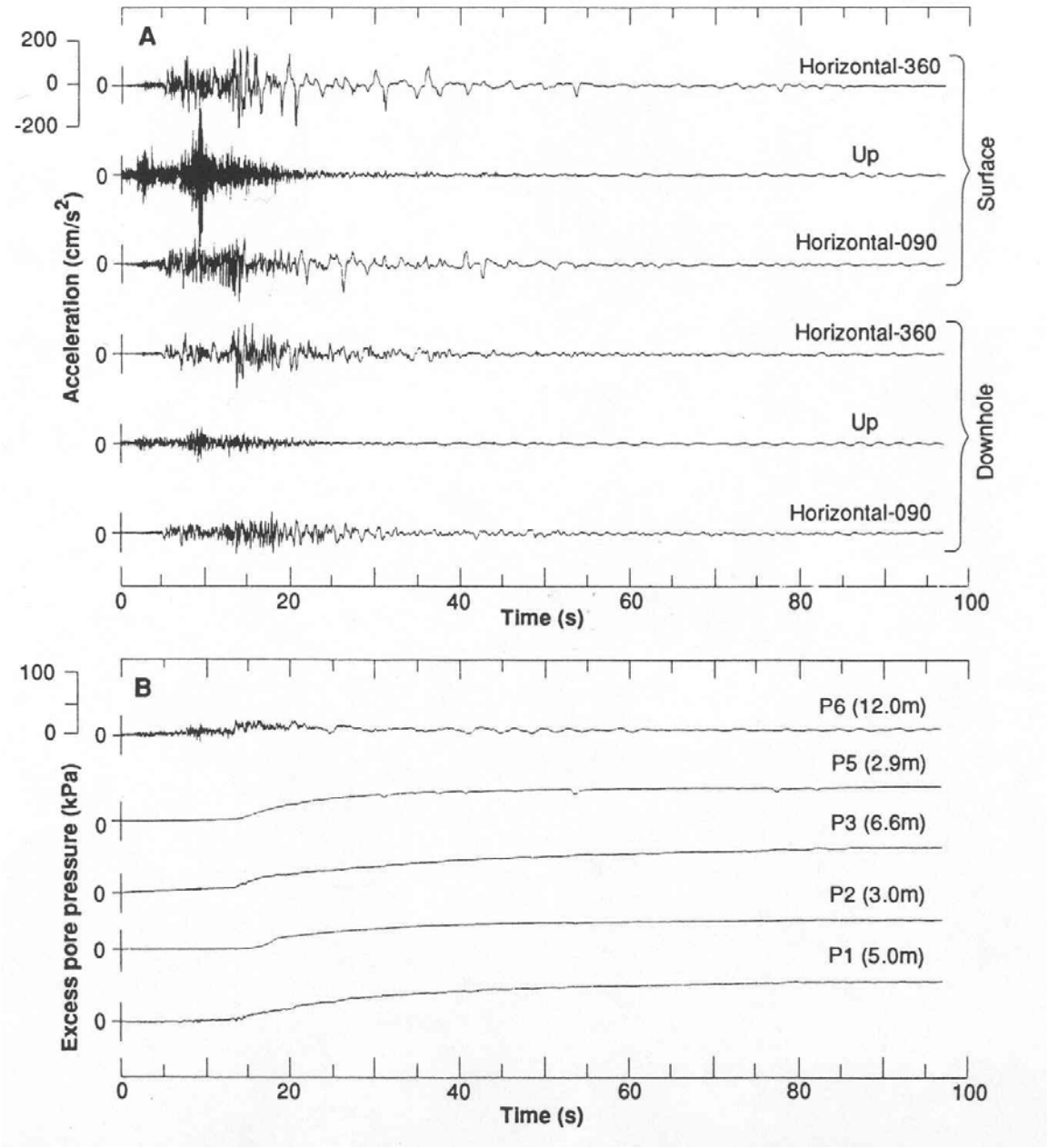

Figure3.7. Traces of recorded acceleration and pore water pressure from the WLA instruments during 1987 Superstition Hills earthquake (M=6.6) (Holzer et al. 1989)

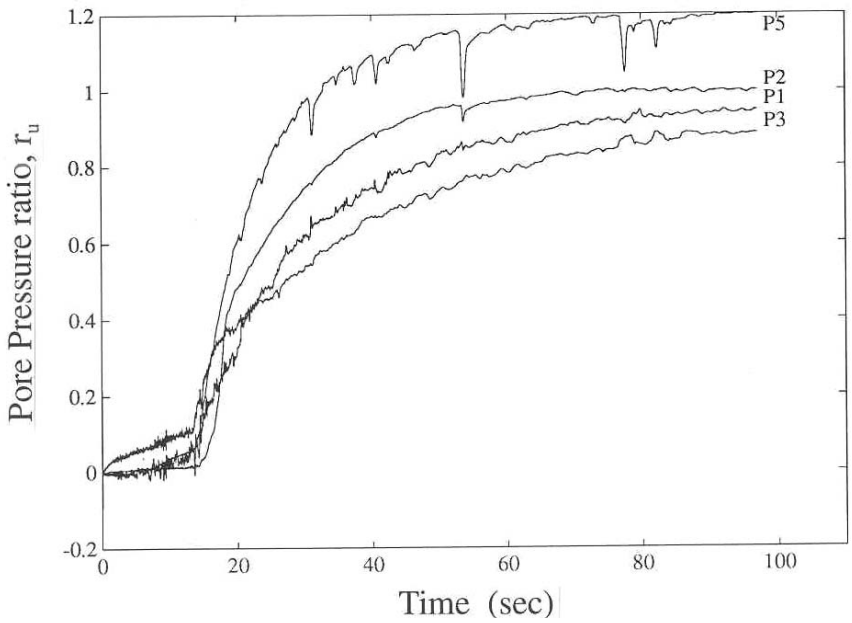

Figure 3.8. Pore water pressure ratio, r_u, versus time curves calculated from pore pressures recorded at WLA during 1987 Superstition Hills earthquake (M=6.6) (Dobry et al. 1989)

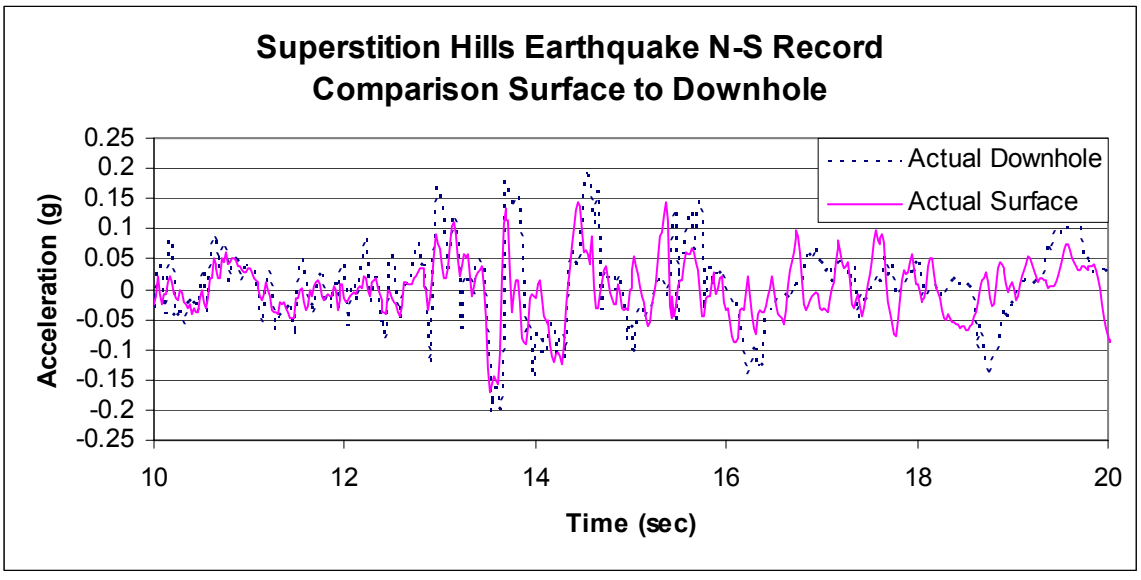

Figure 3.9. Actual surface and downhole acceleration time histories for WLA during 1987 Superstition Hills earthquake (M=6.6)

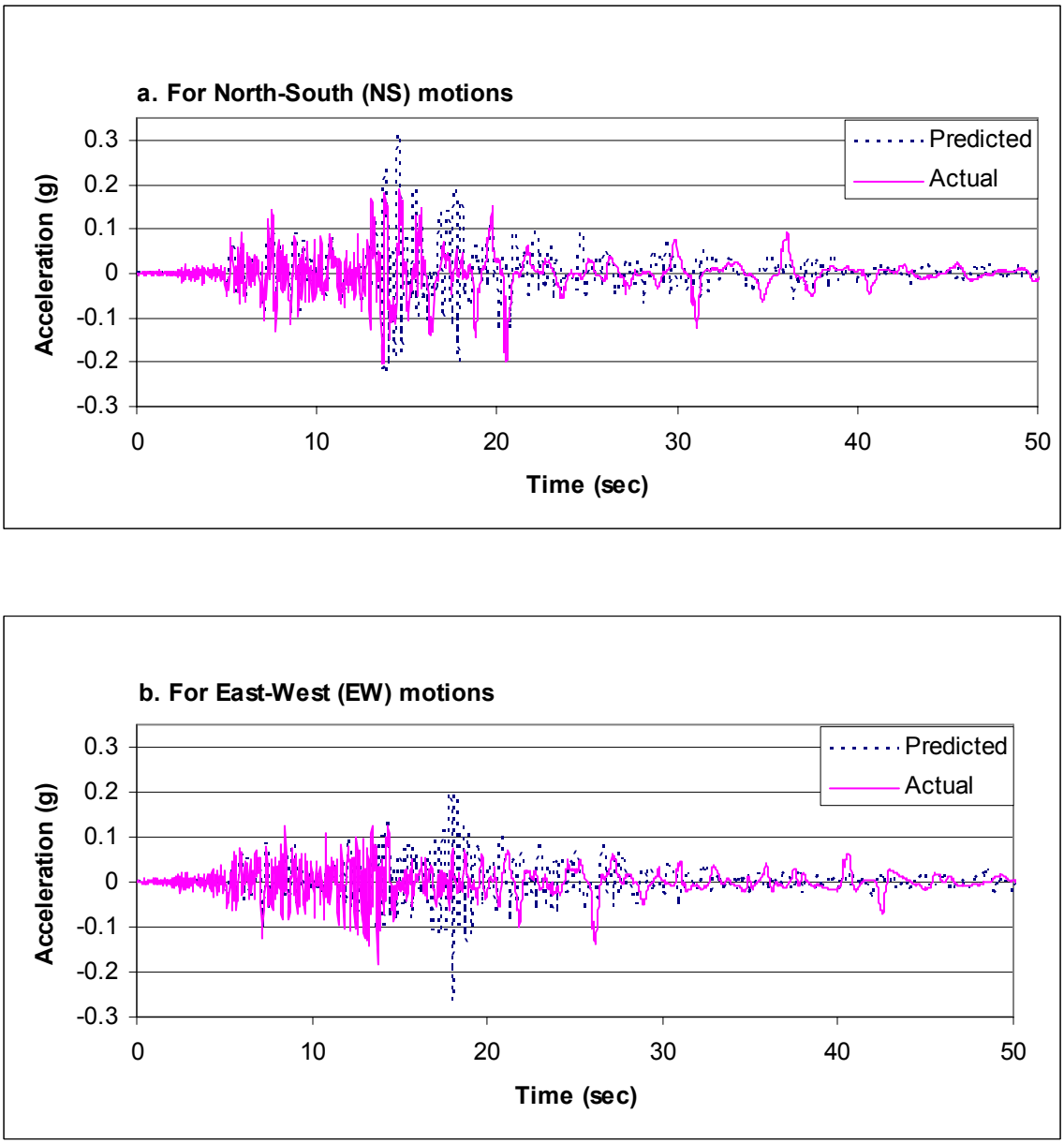

Figure 3.10. Predicted and actual acceleration time histories for WLA site during 1987 Superstition Hills earthquake (M=6.6)

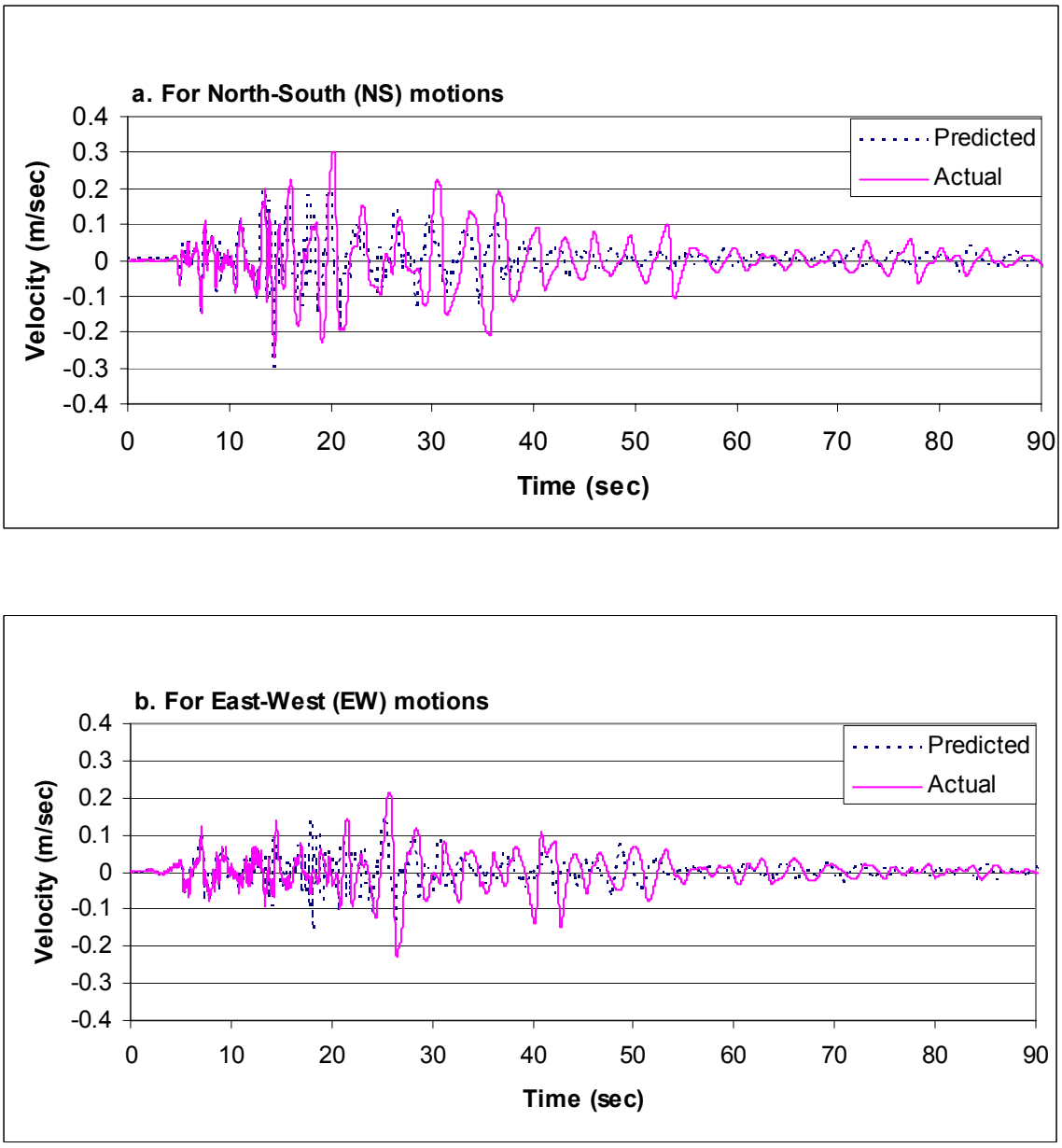

Figure 3.11. Predicted and actual velocity time histories for WLA site during 1987 Superstition Hills earthquake (M=6.6)

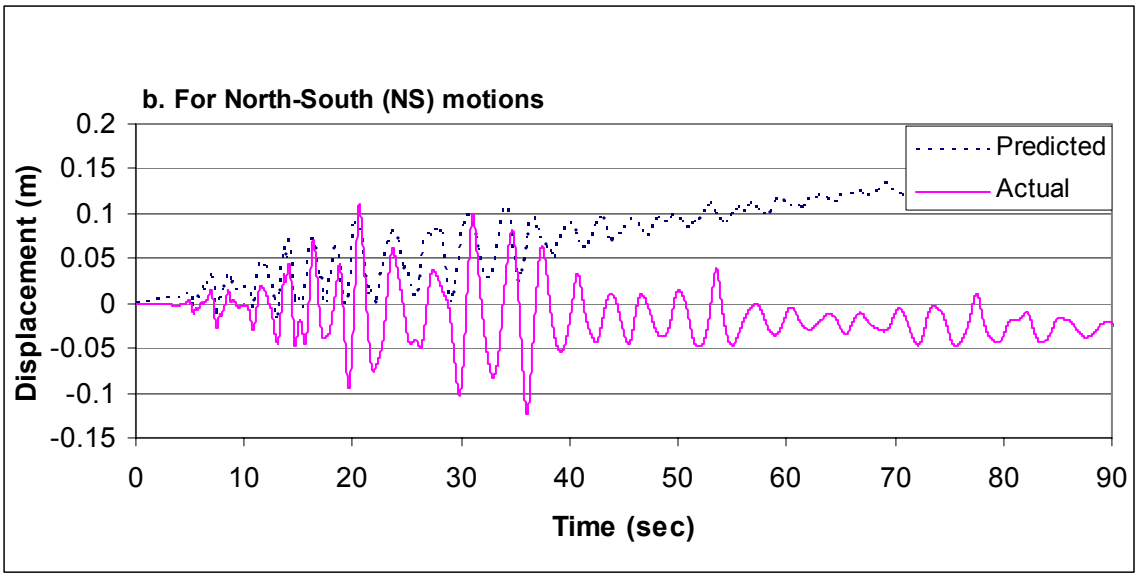

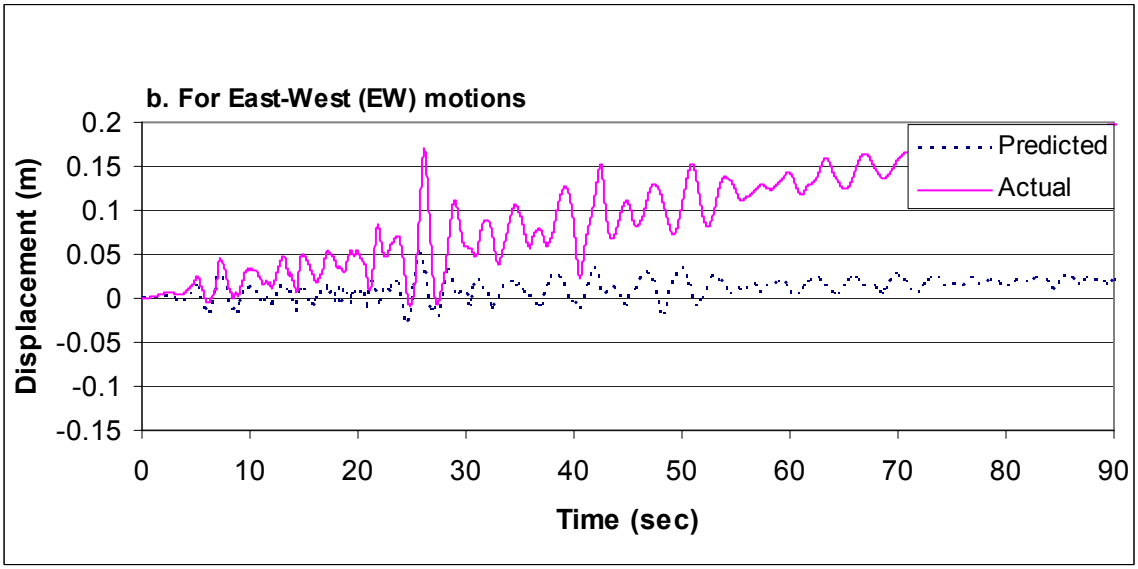

Figure 3.12. Predicted and actual displacement time histories for WLA site during 1987 Superstition Hills earthquake (M=6.6)

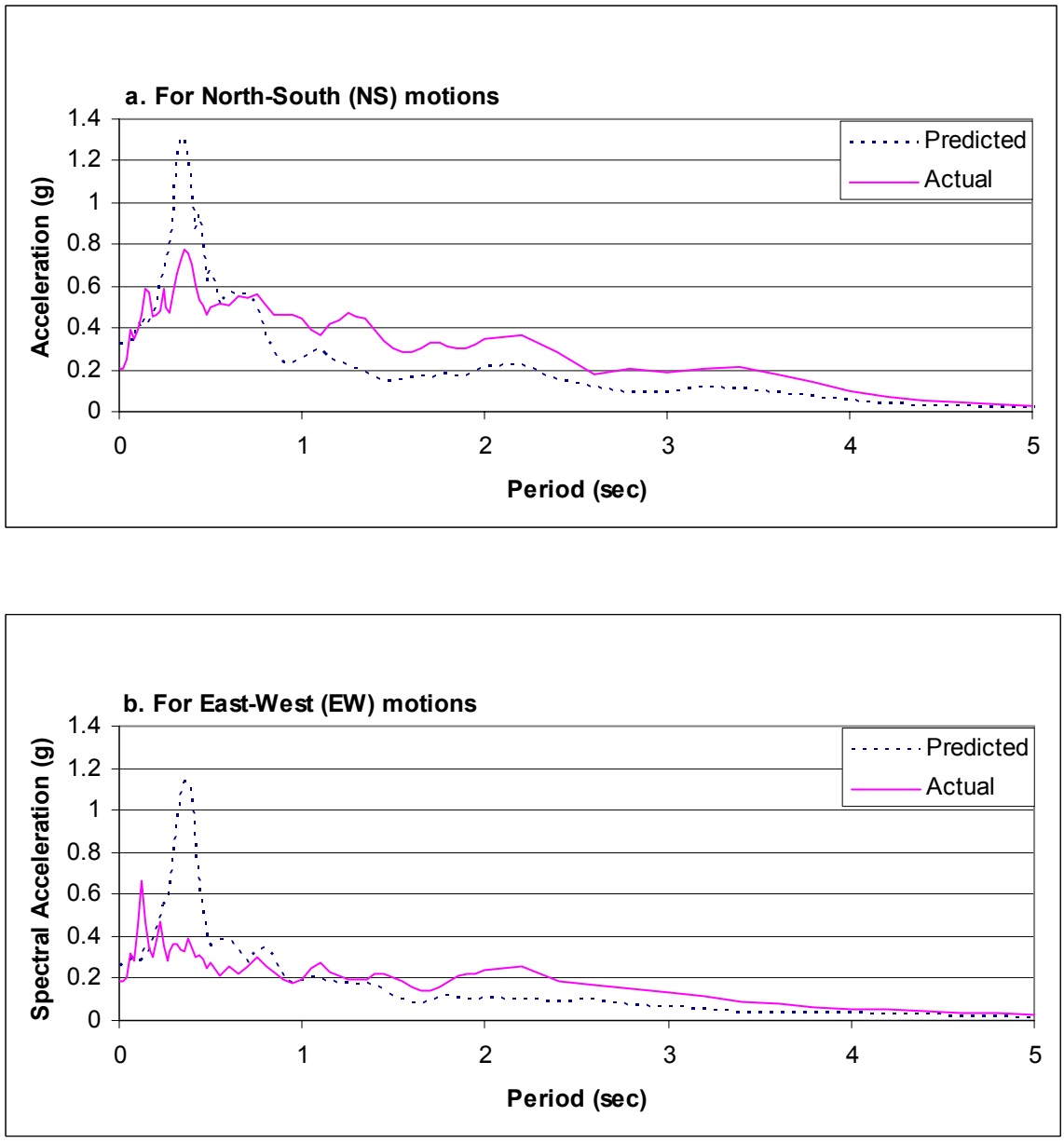

Figure 3.13. Predicted and actual response spectra for WLA site during 1987 Superstition Hills earthquake (M=6.6)

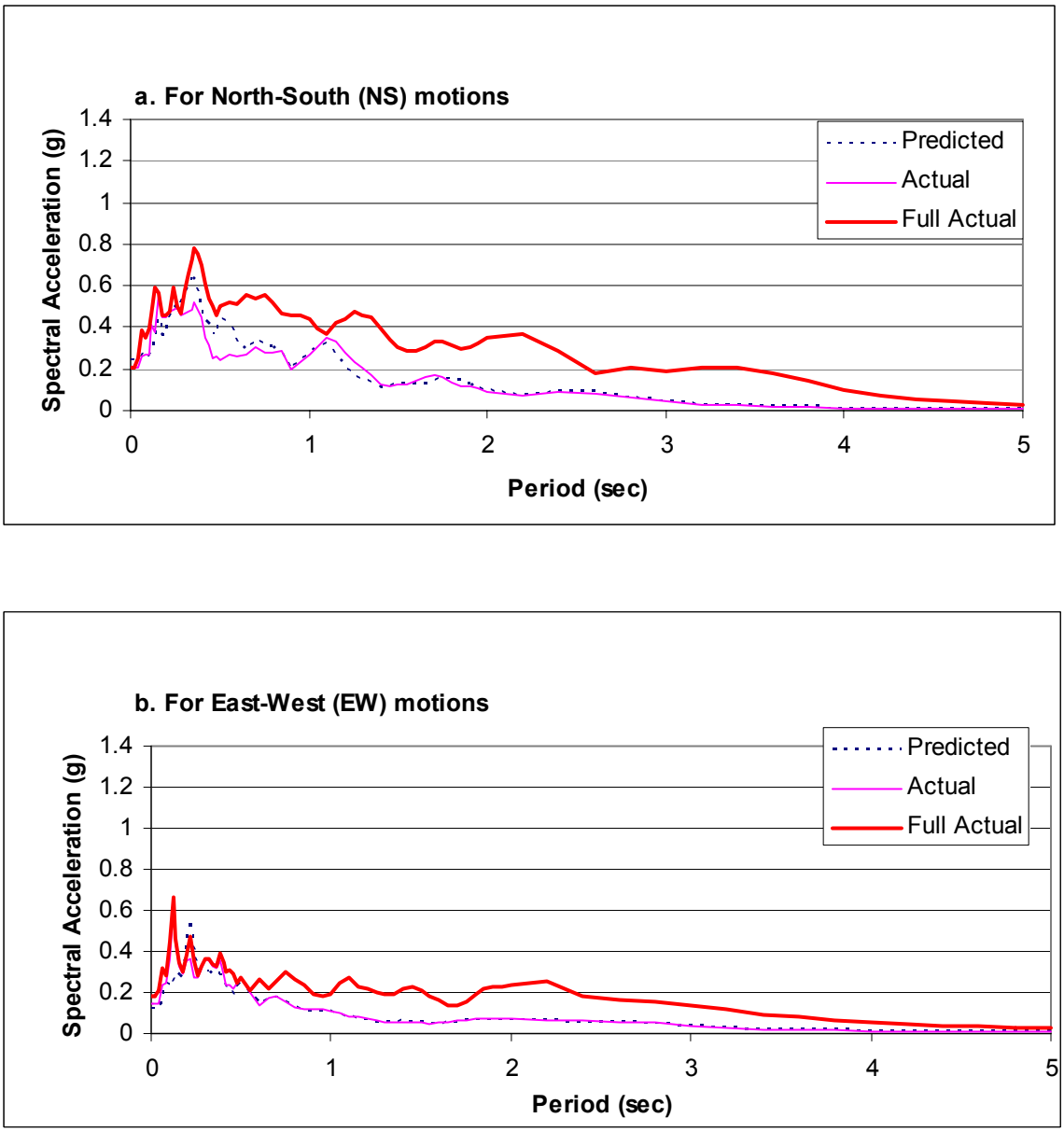

Figure 3.14. Predicted and actual response spectra calculated from the first 13.6 sec of acceleration record for WLA site during 1987 Superstition Hills earthquake (M=6.6)

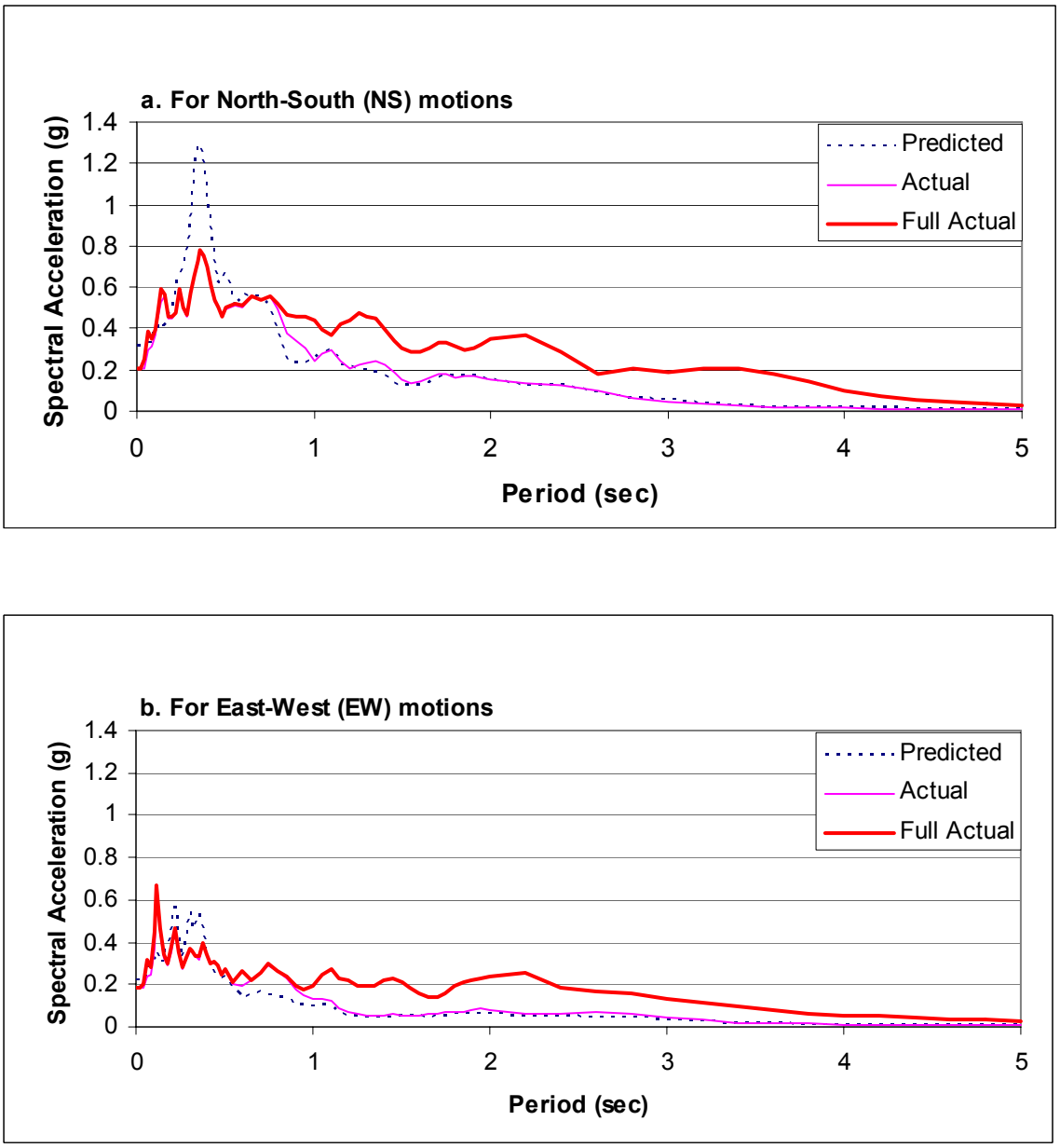

Figure 3.15. Predicted and actual response spectra calculated from the first 15 sec of acceleration record for WLA site during 1987 Superstition Hills earthquake (M=6.6)

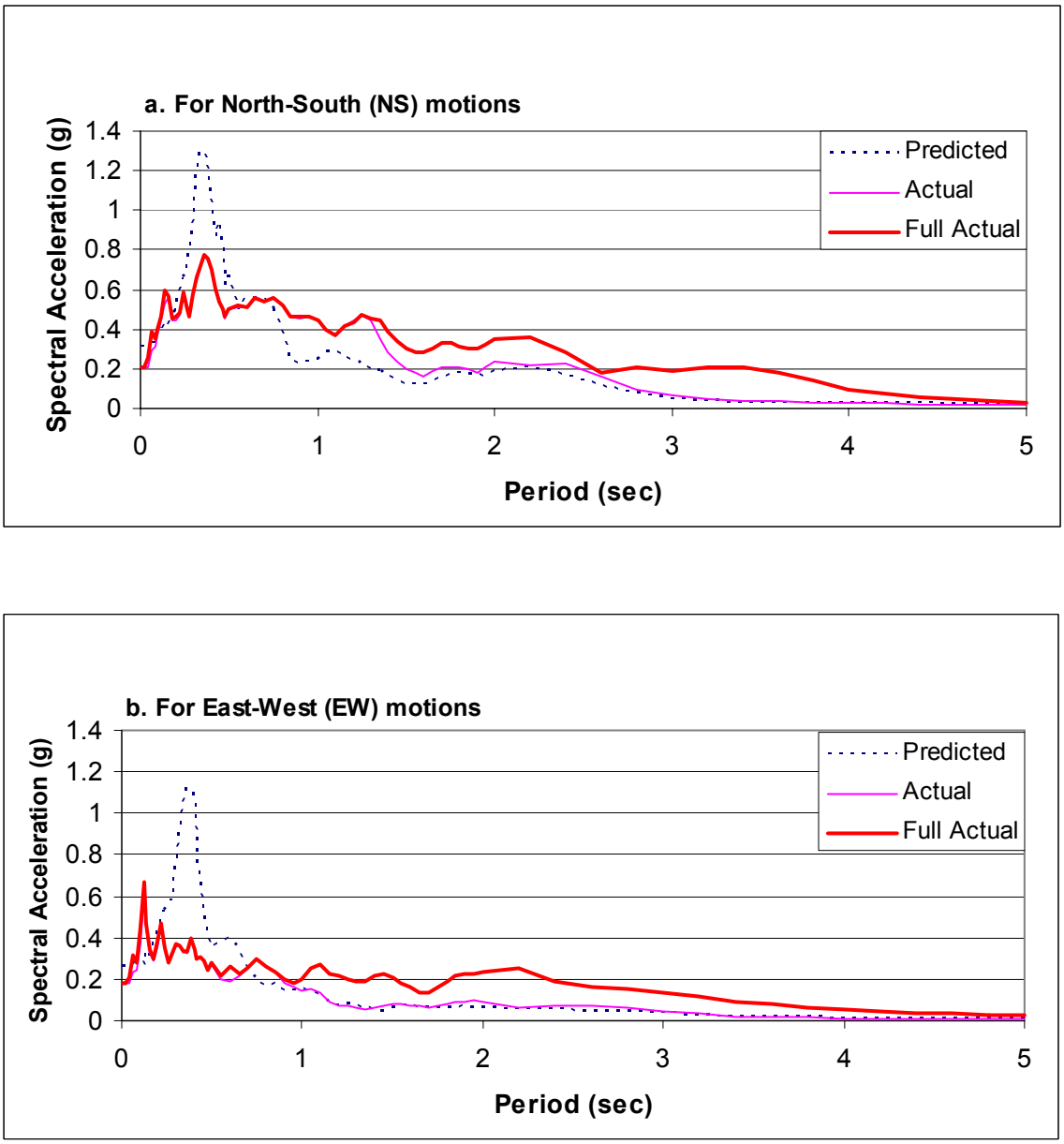

Figure 3.16. Predicted and actual response spectra calculated from the first 20 sec of acceleration record for WLA site during 1987 Superstition Hills earthquake (M=6.6)

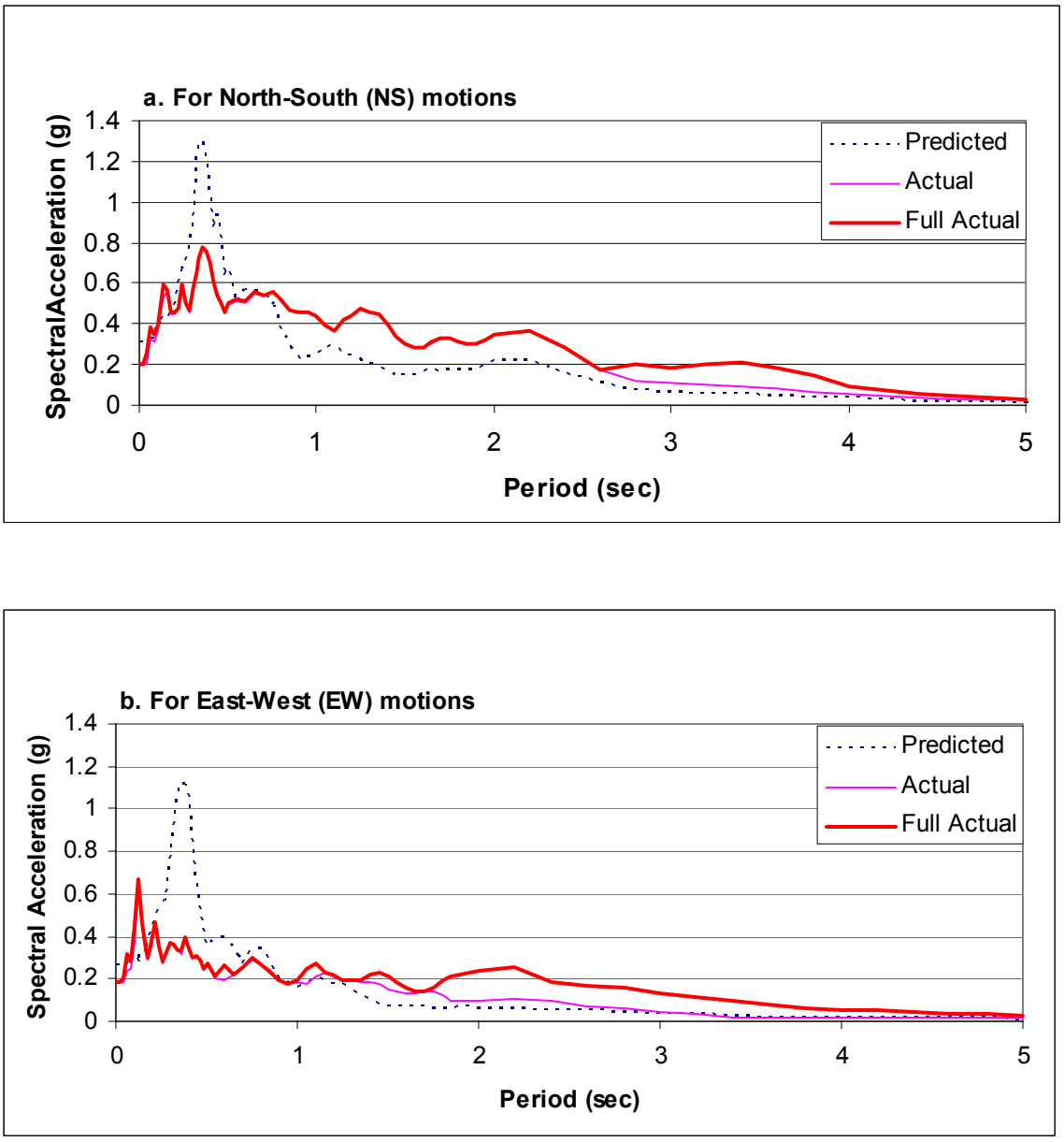

Figure 3.17. Predicted and actual response spectra calculated from the first 25 sec of acceleration record for WLA site during 1987 Superstition Hills earthquake (M=6.6)

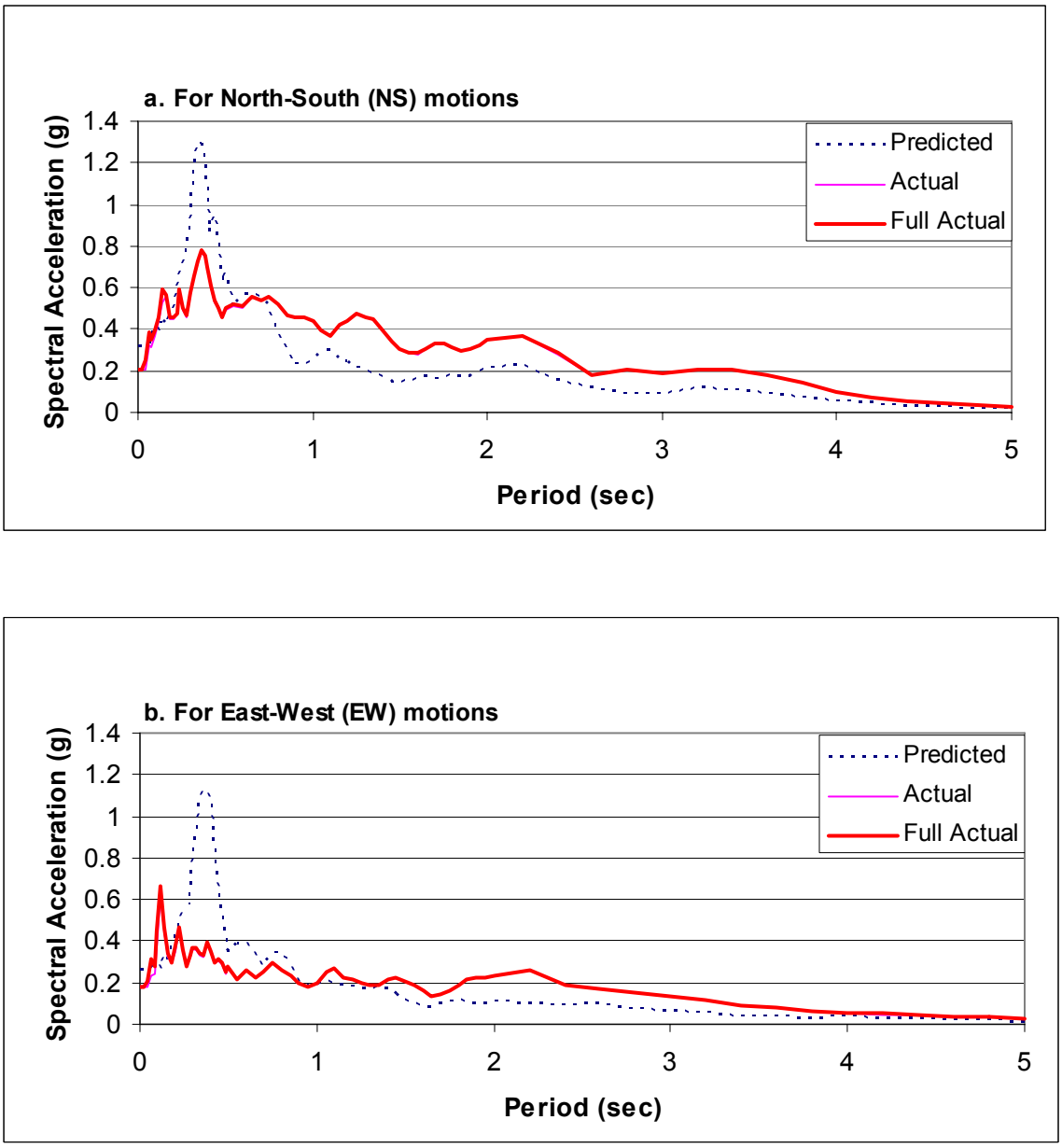

Figure 3.18. Predicted and actual response spectra calculated from the first 50 sec of acceleration record for WLA site during 1987 Superstition Hills earthquake (M=6.6)

SECTION 4

Port Island, Japan

Site History, Stratigraphy, and Instrumentation

Japan has experienced many large and devastating earthquakes due to its nearness to major tectonic plate boundaries. These large earthquakes have also generated widespread liquefaction in susceptible deposits, which are usually in lowland flat to gently sloping areas where much Japanese development has occurred. For example, much of the city of Kobe, Japan, is constructed on such a lowland with additional land reclaimed from the sea by filling parts of Osaka Bay. In particular, two large islands, Port and Rokko, were constructed over the past 40 years by barging granular soil excavated from nearby mountains and dumping the soil into the walled island areas. By this process these two islands and many shoreline areas were filled and developed into port facilities and industrial, commercial, and residential areas. At only a few localities were post-fill compactive procedures applied to make the granular soil denser to prevent liquefaction. Thus during the 1995 Kobe earthquake, liquefaction was widespread and devastating in much of the filled area.

After construction of the northern part of Port Island was complete in August 1991, an array of downhole accelerometers was installed near the northwest corner of the Island (Elgamal et al., 1996). This array consists of four three-component accelerometers, one at ground surface and others at depths of 16, 32, and 83 meters. A cross section showing the layout of instruments and site stratigraphy is diagrammed in Figure 4.1. No piezometers were installed at this site.

The Port Island downhole instrument array (PIDA) stratigraphic profile consists of an upper 4 m of compacted fill (above sea level) underlain by 15 m of loose (non-compacted) fill which is primarily composed of sand and gravel size particles that originated as decomposed Granite. The reclaimed fill is underlain by 8 m of alluvial clay, which in turn is underlain by a 34-m thick layer of alternating layers of dense sand and stiff clay. A deeper consolidated diluvial clay layer, more than 20 m thick., underlies the sand and clay sequence The water table is about 4 m below ground surface (Elgamal et al., 1996). Typical soil properties for each sediment layer are listed in Table 4.1. This list includes properties and parameters used in the response analysis using the program PROSHAKE for this site.

1995 Hyogoken-Nanbu Earthquake

The January 17, 1995, Hyogoken-Nanbu, Kobe earthquake (M=7.2) shook the Port Island area with peak horizontal accelerations in excess of 0.5 g measured at the PIDA site (Taniguchi, 1995; Elgamal et al., 1996). During this shaking, many susceptible areas liquefied, including the uncompacted fill within the PIDA soil profile. Liquefaction at this site generated large sand boils and accompanying ground settlements of 0.5 m to 0.75 m, and lateral ground displacements near the walled free face at the margin of the island (Bardet et al., 1995; EERC, 1995).

Reproductions of NS acceleration time history records from the surface and 16-m depth accelerometers, plotted on Figure 4.2, provide further evidence that liquefaction occurred within the uncompacted fill. These records are approximately congruent until 7 sec after triggering when an acceleration pulse with a peak acceleration of about 0.22 g passed through the site. From 7 sec onward, the period of the accelerations in the surface

record began to lengthen and surface motions attenuated with respect to the record from 16 m depth. Both of these behaviors are indicators that excess pore pressures began to develop about 7 sec after triggering and that uncompacted fill had fully softened after about 15 sec when compatibility is lost between the surface and at-depth traces.

Acceleration Time History Comparisons

Time histories of accelerations predicted at ground surface from the 16-m deep acceleration record using the program PROSHAKE along those measured at ground surface are plotted on Figure 4.3. Again, these time histories are noted as "predicted" and "actual," respectively, on the plot. These time histories indicate that the predicted and actual ground accelerations were nearly congruent until 7 sec in the record, when the first 0.2 g or greater acceleration pulse propagated though the site. At that juncture, the predominant period of the actual ground motions began to lengthen compared to that predicted, indicating the onset of pore-pressure rise and sediment softening. From that point onward, the acceleration spikes in the actual record were greatly attenuated with respect to predicted spikes. Beyond about 15 sec, coherency is lost between predicted and actual ground motions, indicating large pore pressures and major softening had occurred by that time.

One major difference between the ground motions recorded at WLA during the Superstition Hills earthquake and those recorded at PIDA during the Kobe earthquake is in arriving peak accelerations. The measured peak values at ground surface at WLA and PIDA were 0.21 g (NS) and 0.35 g (NS) respectively. The predicted values at ground surface, however, were about 0.20 (NS) at WLA, but about 0.60 g (NS) at PIDA. Thus,

the incoming strong motions were much stronger at PIDA than at WLA. The stronger motions at PIDA had several pronounced effects that were not as evident at WLA. First, soil softening was initiated at PIDA by motions prior to the arrival of predicted peak ground acceleration; thus, that peak is greatly attenuated in the actual record measured at ground surface. Second, the stronger motions apparently softened the site more quickly than at WLA, leading to greater attenuation of the higher frequency components of ground motion in the actual record.

Velocity Time History Comparisons

Velocity time histories, generated by integrating the acceleration time histories, are plotted on Figure 4.4. The velocity time histories show even more clearly the lengthening of period that occurred in actual motions relative to those predicted from ground motions monitored at the 16-m depth. On this figure, initial indication of lengthening of the characteristic period began at about 7 sec after triggering. It was very evident by 8 sec and even greater lengthening occurred thereafter. After 8.3 sec, the higher frequency motions in the predicted velocities were not transmitted through the softening layer and are not evident in the actual motions recorded at ground surface. Longer period phases of the predicted velocities, however, are generally reflected in the actual motions, indicating some resonance between incoming motions and the site response.

Displacement Time History Comparisons

Actual and predicted displacement time histories are compared in Figure 4.5. Interestingly, the actual and predicted displacements are roughly similar, both in frequency and in amplitude. This unexpected similarity indicates that there was indeed

resonance between the softened site and incoming long period motions. In this instance, both the actual and predicted motions died off quickly and similarly after strong ground accelerations ceased about 20 sec after triggering. Large amplitude ground oscillations did not persist after the cessation of strong motion at PIDA as they did at WLA following the Superstition Hills earthquake.

Total Acceleration Response Spectra

Elastic response spectra with 5 percent damping were calculated from both the predicted and actual ground motions at ground surface (Figure 4.6). Comparison of the actual and predicted spectra indicate that soil softening led to greatly decreased spectral response for periods less than 1.0 sec but had little effect on ground response for periods greater than 1.0 sec. Thus, soil softening at PIDA greatly diminished the capacity of the site to transmit short period motions ($T<1.0$ sec), but had little influence on longer period motions ($T>1.0$ sec). The slightly greater actual than predicted spectral response in both the NS and EW directions at periods between 1.6 and 2.3 sec indicates that the softened sediment slightly amplified ground motions in this period range. The congruence of spectra for periods greater than 2.3 sec, however, indicates that amplification of long period motions or ground oscillation did not occur.

Response Spectra for the First 8.3 Seconds of Ground Motion

To better decipher the influence of sediment softening with time on spectral response, spectra for various increments of time were computed for PIDA as they were for WLA. Response spectra computed from the predicted and actual ground motions for the first 8.3 sec of record are plotted on Figure 4.7. The predicted and actual spectra at this juncture are not greatly different, indicating that the increased pore-water pressures

and soil softening had little influence on the transmitted ground motions. However, most of the seismic energy was yet to propagate through the site.

Response Spectra for the First 10 Seconds of Ground Motion

Predicted and actual response spectra for the motions up to 10 sec are plotted on Figure 4.8. At 10 sec into the record, the incremental and final actual spectra are congruent for periods up to 1.1 sec. This indicates that nearly all major ground motions with periods less than 1.1 sec passed through the site in the first 10 sec. For periods less than 1.1 sec, predicted spectral values are mostly greater than the actual spectra, indicating that significant sediment softening and attenuation of motions occurred during the interval between 8 sec and 10 sec. At periods greater than 1.1 sec in the EW spectra, the incremental and final actual are not greatly different, indicating that all of the major seismic energy pulses in the EW direction passed through the site in the first 10 sec. A large amount of seismic energy, propagating in waves with periods greater than 1.1 sec, came after 10 sec in the NS direction. Differences between incremental spectra for the first 8.3 sec and 10 sec, both actual and predicted, indicate that a large amount of seismic energy in the 0.5 sec to 1.5 sec period range passed through the site in this 1.7 sec time interval. Because the soil profile had significantly softened by that time, however, predicted spectral values are much greater than measured values, indicating that much of the seismic energy during that period was absorbed by the softened sediment.

Response Spectra for the First 14.5 Seconds of Ground Motions

By 14.5 sec, sufficient long period energy (periods between 1.3 sec to 5 sec) had passed though the site to yield final spectral values over this period range. In other words, by 14.5 sec, the approximate time of cessation of strong ground accelerations at

the site, spectral maximums had occurred at all periods.

The predicted response spectra for first 14.5 sec of record (Figure 4.9) contain major spectral peaks at periods between 0.1 and 0.6 sec that are absent in the actual spectra for both the 8.3 sec and 14.5 sec time increments. These missing peaks (marked by the letter A) indicate that considerable incoming energy in the 0.1 to 0.6 period range was absorbed and did not propagate through the softened liquefiable layer. The softening also caused lead to lengthening of the vibrational period in some ranges. For example, predicted spectral peaks in the 0.6 sec to 0.8 sec period range (Peaks B) apparently shifted to periods of about 1.2 sec (Peaks B') in the actual spectra. Peak C, at a period of 1.8 sec, in the predicted spectra again is missing in the actual spectra. This absence indicates that energy that arrived later in this period range was also absorbed within the softening layer.

We also note that at periods greater than 2.3 sec, the predicted spectral response is essentially congruent with the actual response, indicating that amplification of ground motions did not occur in this period range and also that long-period ground oscillation did not develop at PIDA. The following are possible reasons for the occurrence of amplification and long-period ground oscillation at the WLA but not at PIDA. (1) Late arriving, low-amplitude, long-period ground motions were approximately in phase with and apparently drove the long-period ground oscillations that developed at WLA. (2) Although some low-amplitude long-period motions propagated through the site until about 30 sec (Figure 4.5), they apparently did not cause resonance within the softened site that continued beyond 30 sec. Consequently, ground motions died out rather rapidly after strong ground motions ceased (between 15 and 25 sec). Three, thicker liquefied

layers such as the 15-m layer at PIDA may not be as susceptible to ground oscillation as thinner liquefied layers, such as the 4-m layer at WLA.

Inferred Pore Water Pressures at PIDA Site

Although pore pressures were not measured, the following inferences are made based on similarities in behavior between PIDA and that observed at WLA. The pore-water pressures apparently began to rise with the arrival of the 7.0 sec acceleration pulse and reached levels sufficient for severe softening ($r_u > 0.2$) by 10 sec. Predicted strong motion pulses, characterized by acceleration peaks grater than 0.1 g, did not propagate to ground surface after 20 sec, indicating that major softening ($r_u > 0.5$) or liquefaction had occurred by that time.

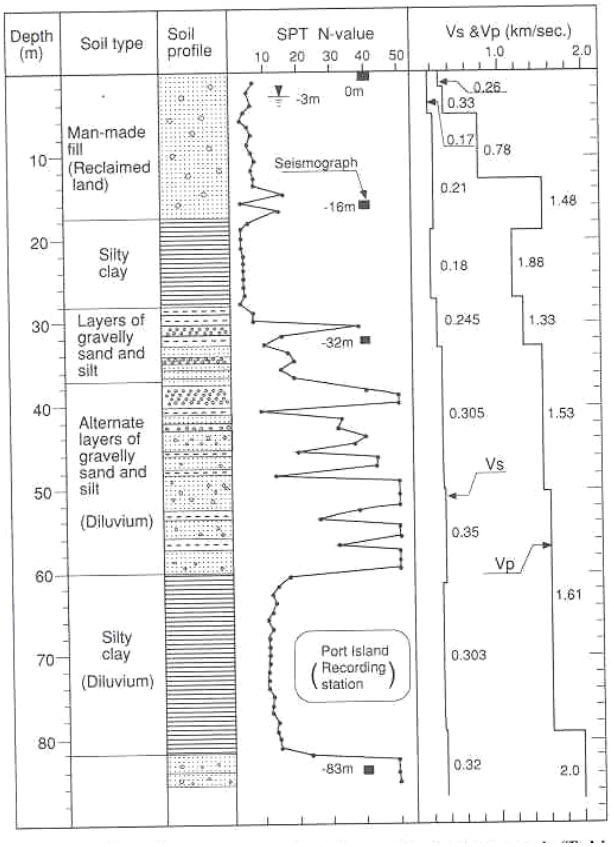

Figure 4.1. Site stratigraphy (a) and cross section (b) showing sediment layers and instrument locations at PIDA (after Ishihara et al., 1996)

Table 4.1. Soil properties for sediment layers at the PIDA site

Material Type	Layer Number	Thickness (m)	Unit Weight (kN/m^3)	G_{max} (MPa)	V_s (m/s)
Decomposed Granite Fill	1	1.3	20.6	60.7	170
	2	1.3	20.6	60.7	170
	:	:	:	:	:
	8	1.3	20.6	60.7	170
Sand with Gravel	9	1.5	20.6	92.6	210
	10	1.5	20.6	92.6	210
	:	:	:	:	:
	14	1.5	20.6	92.6	210
	15	5.0	14.2	47	180
	16	3.0	14.2	47	180
Sand With Clay	17	5.0	18.2	106.6	240
	18	able	18.2	106.6	300

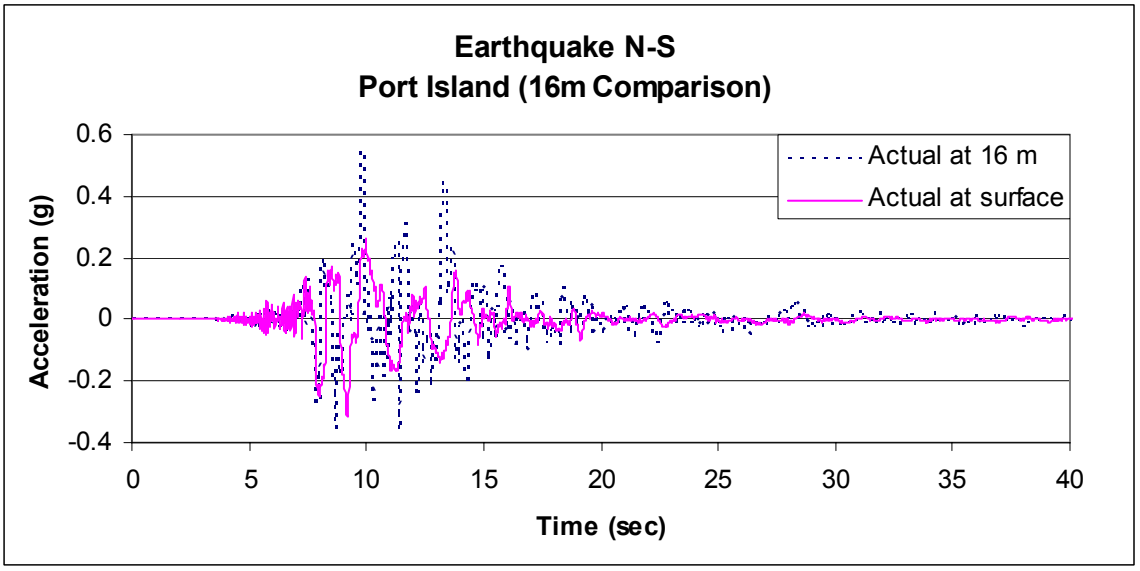

Figure 4.2. Actual surface and 16 m downhole NS acceleration time histories for PIDA site during 1995 Kobe earthquake (M=7.2)

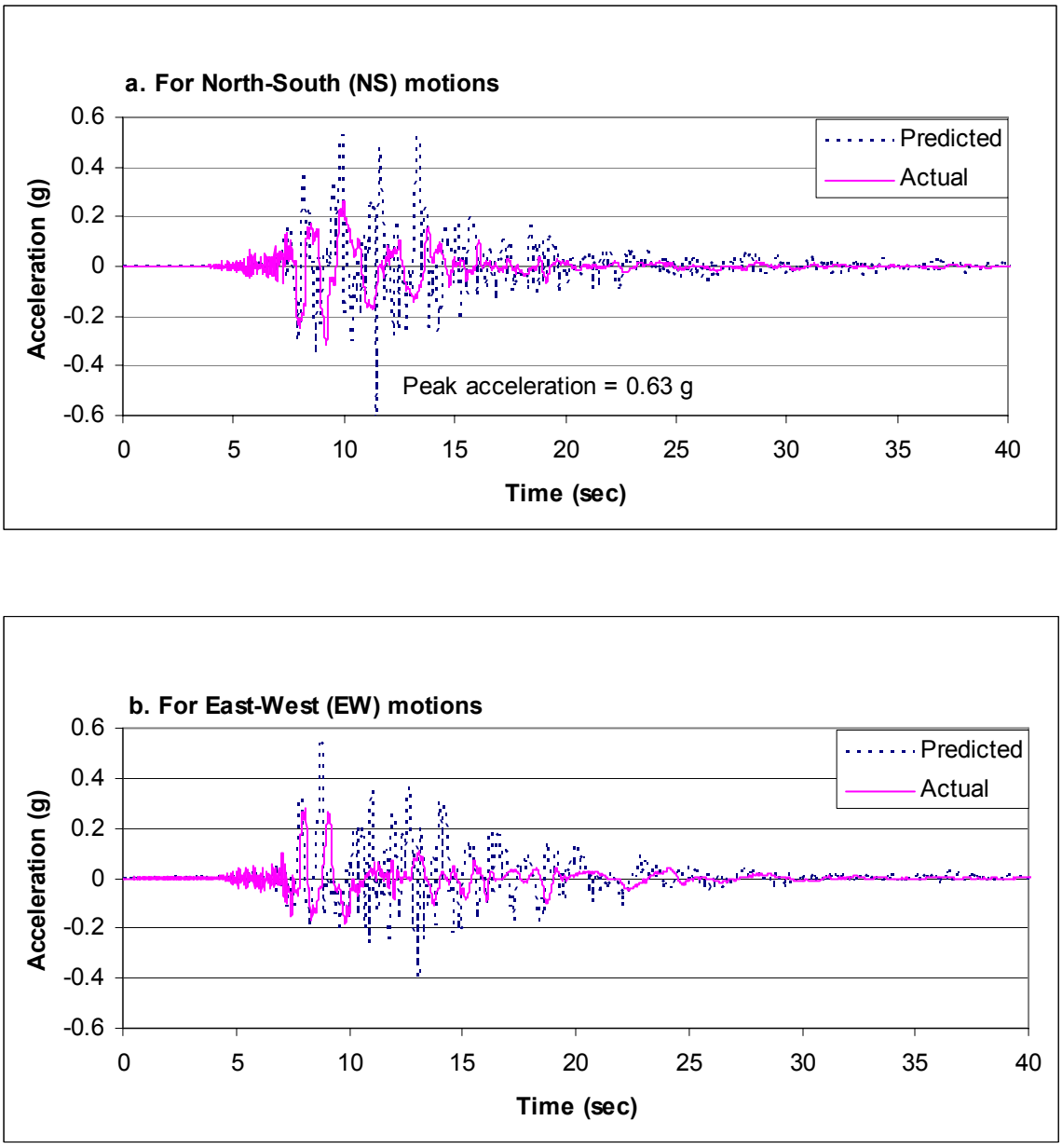

Figure 4.3. Predicted and actual acceleration time histories for PIDA site during 1995 Kobe earthquake (M=7.2)

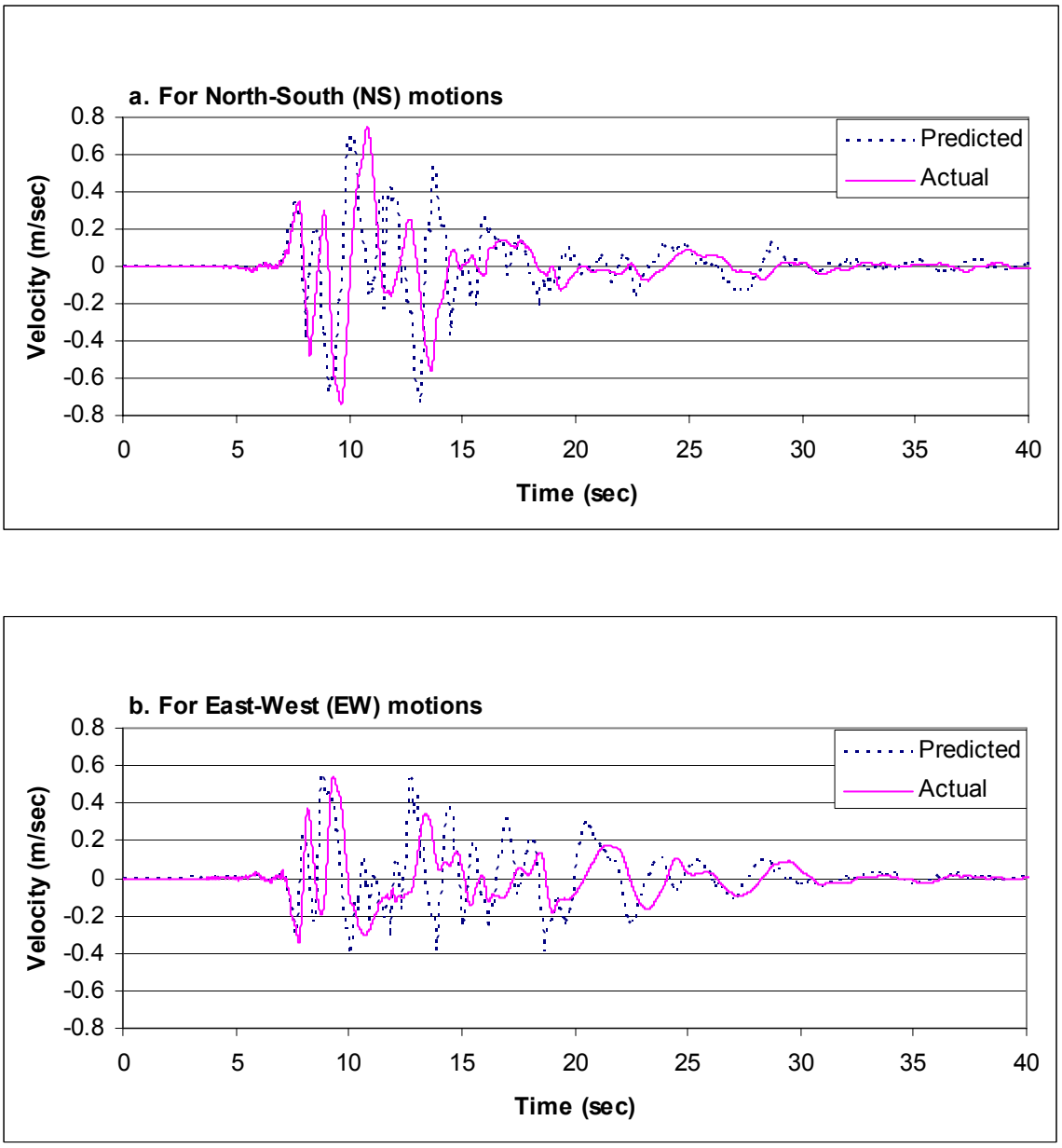

Figure 4.4. Predicted and actual velocity time histories for PIDA site during 1995 Kobe earthquake (M=7.2)

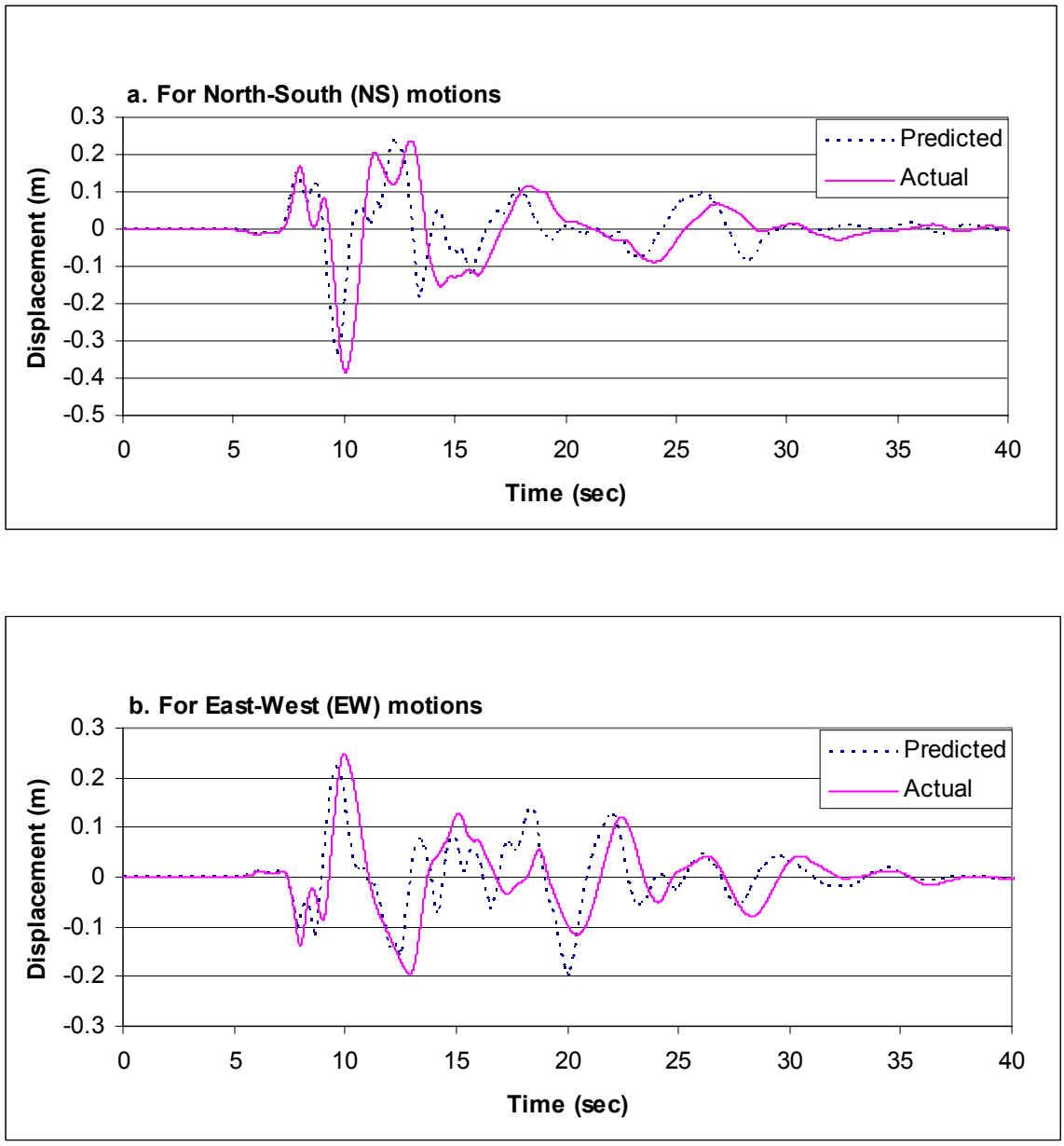

Figure 4.5. Predicted and actual displacement time histories for PIDA site during 1995 Kobe earthquake (M=7.2)

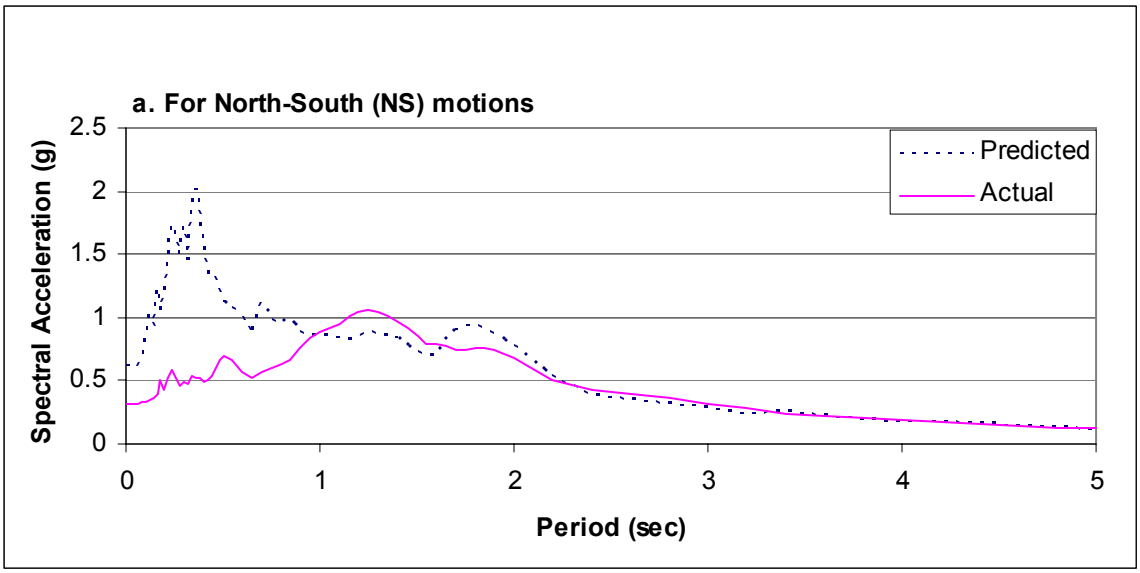

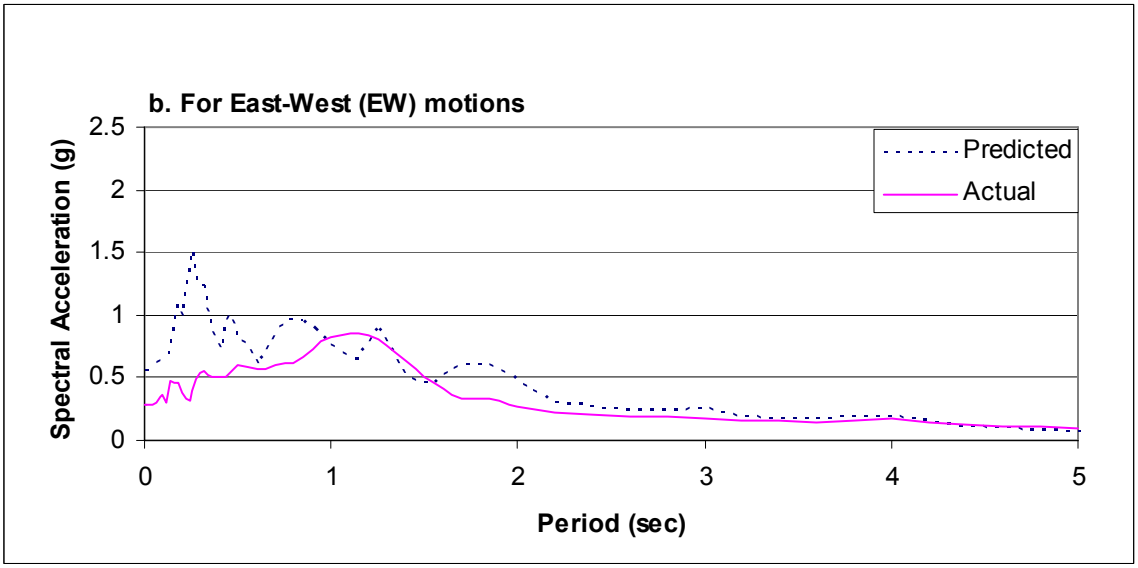

Figure 4.6. Predicted and actual response spectra for PIDA site during 1995 Kobe earthquake (M=7.2)

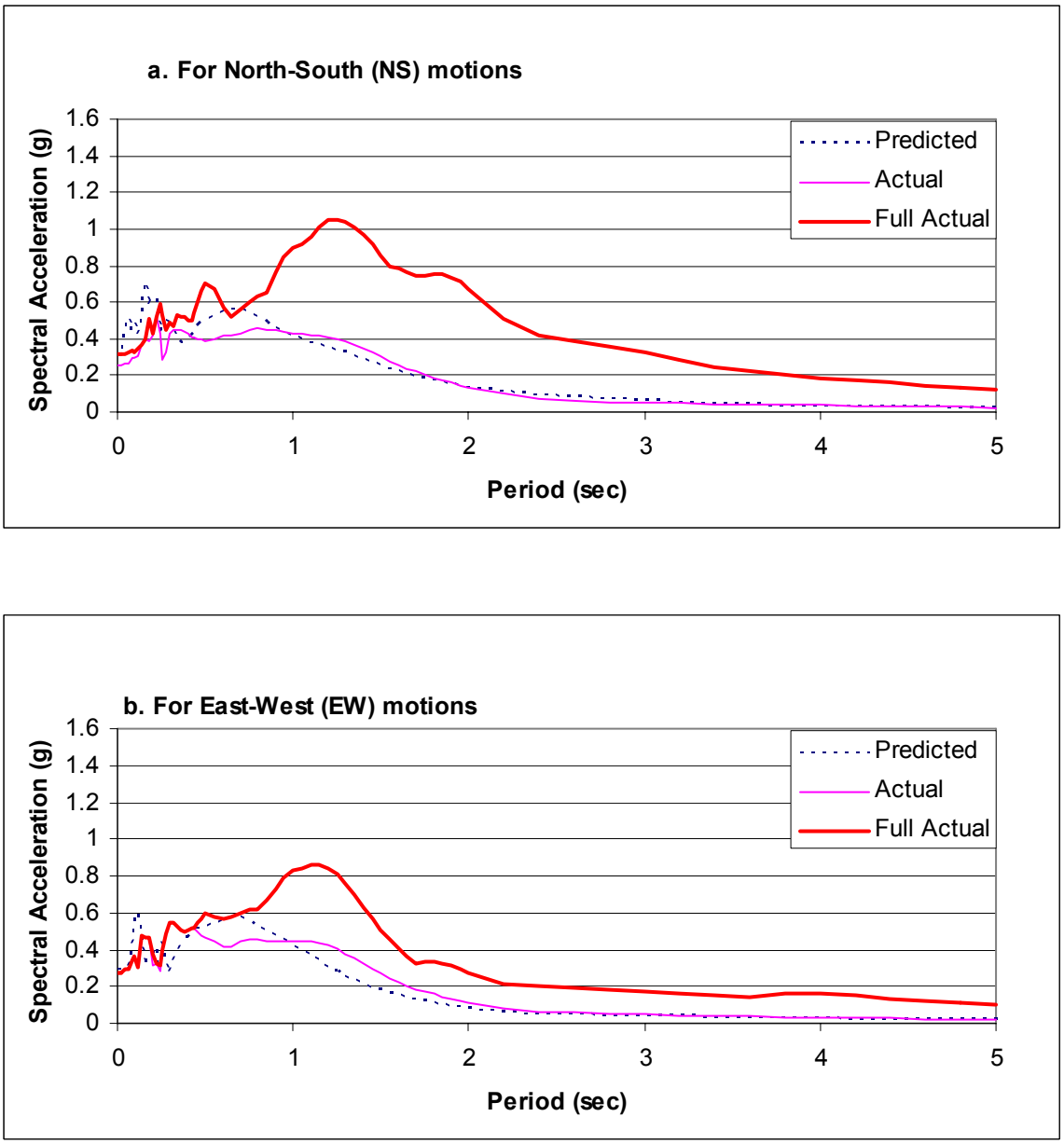

Figure 4.7. Predicted and actual response spectra calculated from the first 8.3 sec of acceleration record for PIDA site during 1995 Kobe earthquake (M=7.2)

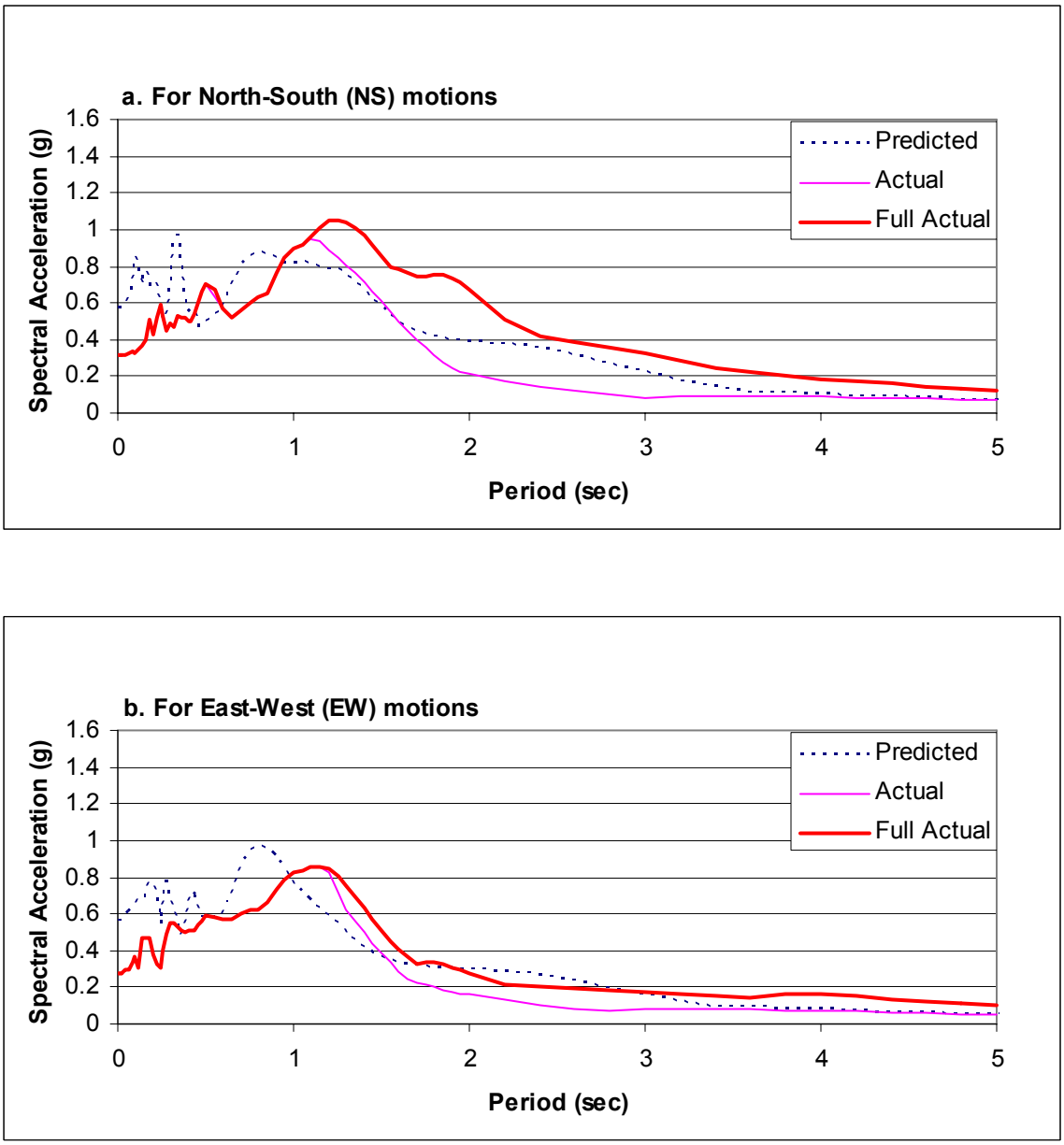

Figure 4.8. Predicted and actual response spectra calculated from the first 10 sec of acceleration record for PIDA site during 1995 Kobe earthquake (M=7.2)

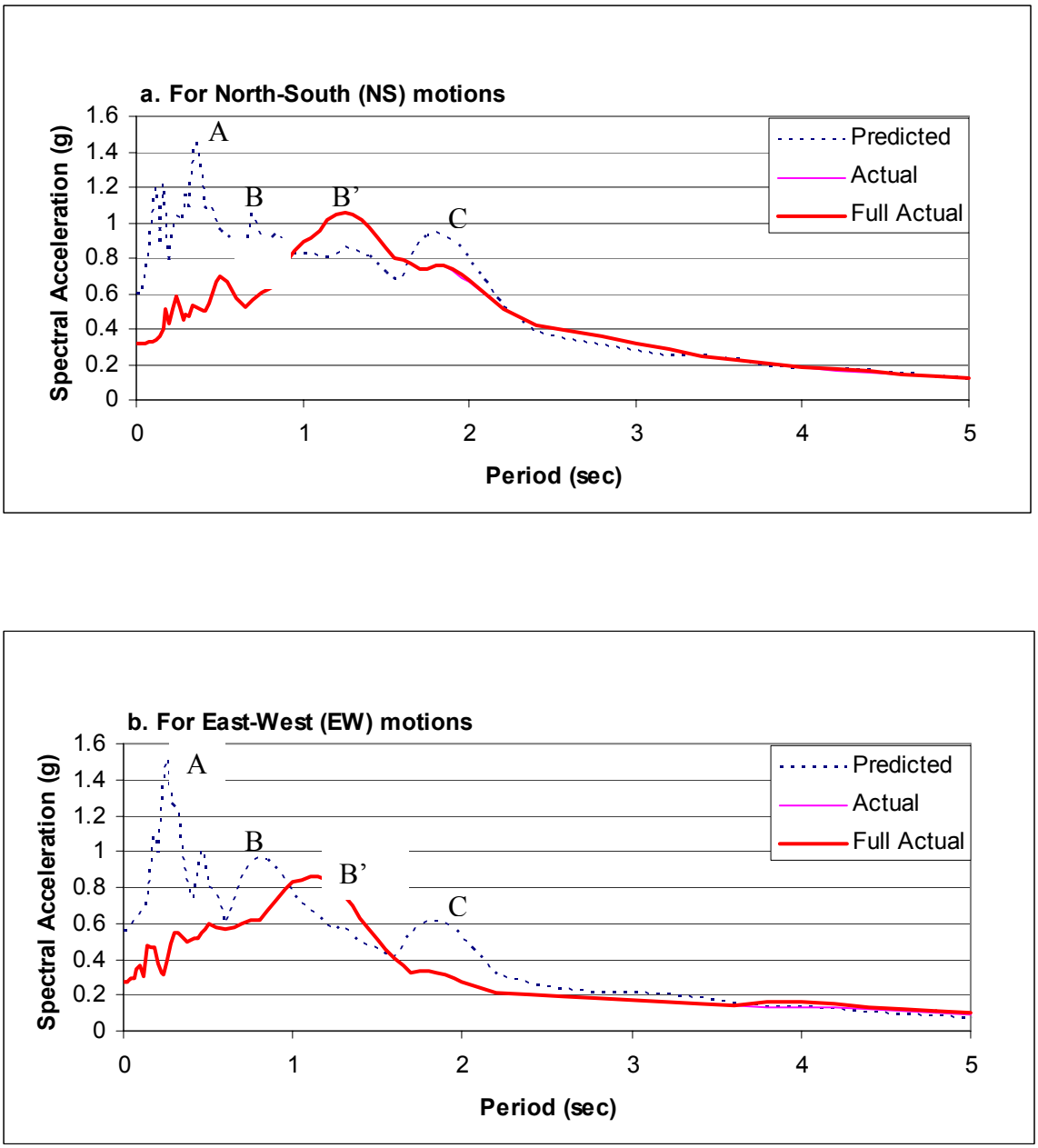

Figure 4.9. Predicted and actual response spectra calculated from the first 14.5 sec of acceleration record for PIDA site during 1995 Kobe earthquake (M=7.2)

SECTION 5

Treasure Island (TI) Site, Loma Prieta, California Earthquake

On October 17, 1989 an earthquake (M=6.8) shook Northern California generating liquefaction in several parts of the Monterey and San Francisco Bay areas. Of particular interest to this study were two instrumented sites in the San Francisco Bay area which were underlain by sediment that apparently softened and liquefied during the earthquake. The two sites were Treasure Island (TI) in San Francisco Bay and Alameda Naval Air Station (ANAS) on Alameda Island east of Oakland and near the eastern margin of San Francisco Bay (Figure 5.1). The records from these sites were analyzed using procedures similar to those used for the WLA, and PIDA sites, except that downhole accelerometers were not installed at sites. To compensate for the lack of downhole instruments, acceleration time histories recorded on a nearby bedrock site (Yerba Buena Island, YBI) were used to predict the ground motions that should have occurred at TI and ANAS in the absence of soil softening and liquefaction.

Site History

Treasure Island is a manmade, 160-hectare island that is located immediately northwest of Yerba Buena Island in the San Francisco Bay. At the time of the earthquake, Treasure Island was used as a US Navy base. That base, however, was decommissioned a few years after the earthquake. The island was constructed using the hydraulic fill process with materials excavated locally from the bottom of San Francisco Bay. The materials used to fill the island were primarily shoal sands excavated using hydraulic and clamshell dredging techniques. The island is underlain by a shallow-water sand bar and a soft, silty clay sediment, locally termed younger San Francisco Bay mud.

A perimeter rock dike was built in two to four stages on a bed of coarse sand placed over bay mud. This dike acted as a retaining system for the sandy sediment that was sluiced into the impoundment area. (Rollins, 1994). The fill is composed of granular materials that are uncompacted, uncemented, and saturated. These types of materials are generally highly susceptible to liquefaction.

The 1989 Loma Prieta earthquake generated surface effects of liquefaction at several localities on the island. These effects included sand boils and ground fissures, differential settlements, minor lateral spreads, and dike deformation. None of these liquefaction features, however, were noted within 100 m of the instrumented site, which is in an open field behind the island fire station.

TI Site Sediment Profile

The TI sediment profile (Figure 5.2) consists of four types of soils: fill, native shoal sand, recent bay sedimentary deposits (young bay mud), and older bay sedimentary deposits (older bay mud) (Rollins et al., 1994). The materials and depths vary from one side of the island to the other. However, for our analysis we used a sediment profile that was established near the strong motion instrument site. This sediment profile consists of 11.6 m of sandy fill which is underlain by 17.4 m of younger bay mud which is underlain by 12 m of dense fine sand which, in turn, is underlain 38 m of older bay mud. Bedrock was confirmed at a depth of approximately 85 m. Typical soil properties for each sediment layer are listed in Table 5.1. This list includes the properties and parameters required for the PROSHAKE analysis of the seismic response of the site.

Instrumentation

The locations or the strong motion accelerometer sites on Treasure Island (TI) and the bedrock site on Yerba Buena Island (YBI) are marked on Figure 5.1. Both are three-component instruments that recorded two horizontal and one vertical trace of accelerations sensed at each site. Both are also located in small single-story structures. The YBI instrument is located approximately 2.4 km southeast of TI.

Development of Predicted Ground Surface Motions for TI Site

The TI site unlike WLA and PIDA did not have a downhole accelerometer beneath the liquefiable layer. Without this downhole record, the analysis procedure is more difficult. In this instance, the bedrock outcrop motion at YBI must be transferred to the soft soil site at TI. This transfer was accomplished by using the rock outcrop motion as an input into the PROSHAKE program. The program then deconvolved the outcrop motion to the depth of the bedrock and transferred that motion under the TI site. The deconvolved motion was then propagated upward through an unsoftened TI soil profile. Soil properties used in the soil profile were those measured long after the pore pressures generated during the Loma Prieta earthquake had dissipated. This procedure provides a reasonable, but somewhat more uncertain, estimate of ground motions than were made for the WLA and PIDA sites. Nevertheless, this procedure provides a useful estimate of motions that should have occurred in the absence of soil softening and liquefaction.

A second problem that must be solved is accounting for differences in travel times for seismic waves to reach each of the recording instruments (YBI and TI). Because the epicenter of the earthquake was about 95 km south of YBI and 98 km south of TI, the seismic waves arrived at YBI shortly before they reached TI. Because of this difference

in wave arrival times, the time-histories of motions recorded at YBI were shifted to a later time to correlate with the motions at TI. The procedure we used to determine this time shift was to overlay the recorded acceleration time histories for both NS and EW and then shift the YBI record until the first arriving peaks at both sites matched. The time-shifted and overlain acceleration traces are plotted on Figure 5.3. A time shift of 1.9 sec was applied to the YBI record to produce the match shown on that figure. As a further test of this time shift, velocity and displacement time histories were calculated by integrating the acceleration records. Traces on these time histories were overlain which further confirmed an optimal time shift of 1.9 sec. This time shift is applied to all of the records used in the following analyses.

Comparison of the acceleration time histories plotted on Figure 5.3 from YBI and TI demonstrates that equivalent peaks on the TI record are about 3 times greater than those on the YBI record. The greater motions at the softer TI site were due to local site amplification of ground motions, an observation that has been made by many previous investigators (Rollins et al., 1994).

Record Comparisons

Acceleration Time Histories

Acceleration time histories from the actual TI record and those predicted from the YBI record using the PROSHAKE analysis described above are plotted in Figures 5.4a and b for the NS and EW directions, respectively. Until 13 sec after instrumental triggering, the predicted acceleration record closely approximates the measured record for both the EW and NS components of motion. Beyond 13 sec, the characteristic

periods of motion on the actual record lengthen with respect to the characteristic periods of the predicted motions. This period shift is indicative of softening of sediment in the soil profile. Between 13 sec and 15 sec, amplitudes of the motions varied as some actual peaks were higher than the predicted values and vise versa for other peaks. Beyond 15 sec, the period of the actual motions is much longer than that of the predicted motions and the amplitudes of the actual acceleration peaks are much smaller. By 15 sec, however, all of the stronger acceleration pulses had passed through the site and only small, end-of-event accelerations were being propagated.

Velocity Time Histories

Actual and predicted velocity time histories, calculated by integrating acceleration time histories, are plotted on Figure 5.5a and b for the NS and EW directions, respectively. Again, until 13 sec, the predicted velocity traces closely approximate the actual traces for both the EW and NS components of motion. Beyond 13 sec, the velocity traces diverge both with respect to frequency and amplitude of predominant waves in the record. In this instance, the period of the actual waves lengthened as occurred in the acceleration record. The amplitudes, however, of the actual waves are generally greater than the predicted waves, which is opposite to the relationship noted in the acceleration diagram. The velocity waves are generally longer period than the acceleration waves, indicating the longer period motions were being amplified when shorter period motions were being attenuated.

Beyond 15 sec, longer period oscillations developed in the measured record than in the predicted record. These longer-period velocity oscillations are smoother (contain less high-frequency components of motion) and are characterized by slightly greater

amplitudes than the predicted velocities. The lack of higher frequency motions indicates that the sediment had softened sufficiently to inhibit transmission of higher frequency ground motions.

Displacement Time History

Displacement time histories, generated by double integrating the acceleration time histories, are compared for both actual and predicted records in Figures 5.6a and b for the NS and EW directions, respectively. Similar to the velocity traces, the predicted displacement traces are nearly congruent with the actual record until 13 sec after triggering. Beyond 13 sec, the actual displacements transition into smooth long-period oscillations. Beyond 13 sec, the amplitudes of actual displacements in the EW record are much greater than those in the NS motion, These displacements also appear to be in phase with the predicted displacements. The predicted displacements, which are amplified depictions of the incoming bedrock motion, apparently excited or drove these long-period oscillations and generated the larger displacements in the EW direction. The smaller actual displacements in the NS direction are not in phase with the predicted displacements, indicating that the incoming motions in that direction were not generative of ground oscillation. Although ground oscillations occurred in the EW direction after strong accelerations from the earthquake ceased, these oscillations attenuated quickly, so that by 35 sec after triggering the site returned to a quiescent state.

Inferred Pore Pressure Response

No piezometers were in place at the TI site for measurement of water pressures at the time of the Loma Prieta earthquake. However, by comparison with the WLA records, we are able to infer approximate relationships between excess pore water pressures and

ground motions. Because actual and predicted motions were essentially congruent until about 13 sec after triggering, we infer that small if any excess pore pressures had developed at that juncture and that pore pressure ratios, r_u, were near zero. A major difference between the TI site and the WLA and PIDA sites is that more than half of the duration of strong ground motions had passed through the TI site before pore pressures began to significantly rise at 13 sec. Thus, soil softening caused no attenuation of these earlier ground motions and had less effect on response spectra, as discussed in the following subsection.

Between 13 sec and 15 sec, the period of the actual motions greatly lengthened with respect to the predicted motions. Beyond 15 sec, the capacity of softened sediment in the liquefiable layer to transmit high-frequency motions was greatly impaired. Based on comparisons with the WLA records, we estimate that pore pressure ratios quickly rose to about 0.4 - 0.5 by 15 sec. By 20 sec, the actual (measured surface motions) were in long period oscillation vibrating independently of incoming high-frequency motions, indicating a liquefied subsurface layer and pore pressure ratios near 1.0.

Response Spectra from Complete Time Histories

Acceleration response spectra calculated from complete records for both actual and predicted motions from the TI site are plotted on Figure 5.7a and b for EW and NS directions, respectively. The actual and predicted response spectra for the EW direction agree rather well, except for a missing small peak at a period of about 0.3 sec, an apparent shift of energy from lesser actual than predicted response between 0.9 sec and 1.5 sec, and greater actual than predicted response for periods greater than 1.5 sec. Soil

softening and the generation of ground oscillation is the apparent cause of this shift of energy to longer periods.

In the NS direction, the actual spectra are much greater than the predicted spectra at all periods. We do not know the reason for this great difference, but some inferences are gained by examining the relationship between spectral response and the time of arrival of the seismic energy.

Response Spectra for first 10 Sec of Record

Predicted and actual response spectra for the first 10 sec of record, well before excess pore water pressures began to rise, are plotted on Figure 5.8. At that time, a relatively small amount of seismic energy had propagated through the site and the 10 sec response spectra are only a fraction of their final values. The actual and predicted spectra, however, are approximately comparable, with some difference likely due to small timing errors we may have introduced in our procedure for applying a time correction.

Response Spectra for first 13 Sec of Record

Response spectra calculated for the first 13.0 sec of record are plotted on Figures 5.9. At that juncture, the actual and predicted spectra in the EW direction are roughly equivalent for periods less than 0.9 sec, except for a missing small peak at about 0.3 sec. The actual spectrum for the first 13 sec of record is also congruent with the final spectrum for periods less than 1.3 sec. This indicates that all of the maximums of energy pulses in this period range had passed through the site by this juncture, which is also the time at which pore water pressures apparently began to rise as noted above. Much of the difference between the actual and spectra for periods greater than 0.9 sec may be due to

small errors in correcting the time delay in the acceleration records between the YBI and TI sites. These differences largely disappear at the next time increment (14 sec); and therefore are not discussed here further.

For the NS direction, the actual and predicted response spectra are greatly different at the 13 sec juncture, with spectral values being much greater in the actual spectrum for nearly all periods. Also, the actual spectrum for the first 13 sec is nearly congruent with the final spectrum for periods less than 1.0 sec and not greatly different for periods greater than 0.9 sec. This congruence indicates that most of the seismic energy had propagated through the site in the EW direction by 13 sec and that a great amount or a burst of energy occurred in the 3.0 sec interval between 10 sec and 13 sec. Again this burst of energy passed through the site before pore water pressures rose significantly. We were unable to determine the reason for the measured spectral accelerations being greater than the predicted across a wide spectrum of periods. This greater measured response may have been due to some resonance phenomenon associated with the sudden burst of energy just as pore pressures were about to or beginning to rise or, for an unknown reason, the motions recorded on YBI in the NS direction during that interval are anonymously deficient in seismic energy. Because the actual seismic energy was distributed over a wide range of periods, we believe that the latter is a more plausible explanation.

Response Spectra for the first 14 Sec of Record

Response spectra calculated for the first 14 sec of record are almost identical with the final spectra, both for the predicted and actual responses (Figure 5.10). Again, this congruency indicates that the major seismic energy pulses had propagated through the

site by this time. At 14 sec, the predicted and actual response spectra approximately match for periods less than 0.9 sec in the EW spectra. For periods greater than 0.9 sec, predicted spectra are greater for periods between 0.9 and 1.5 sec. Conversely, actual response spectra for periods after 15 sec are greater than the predicted values. These differences are consistent with transfer of seismic energy from the 0.9 sec – 1.5 sec range to the 1.5 sec or greater range due to soil softening and the generation of ground oscillation. In the NS direction, the responses also were nearly complete, but were greatly different as explained in the previous paragraph.

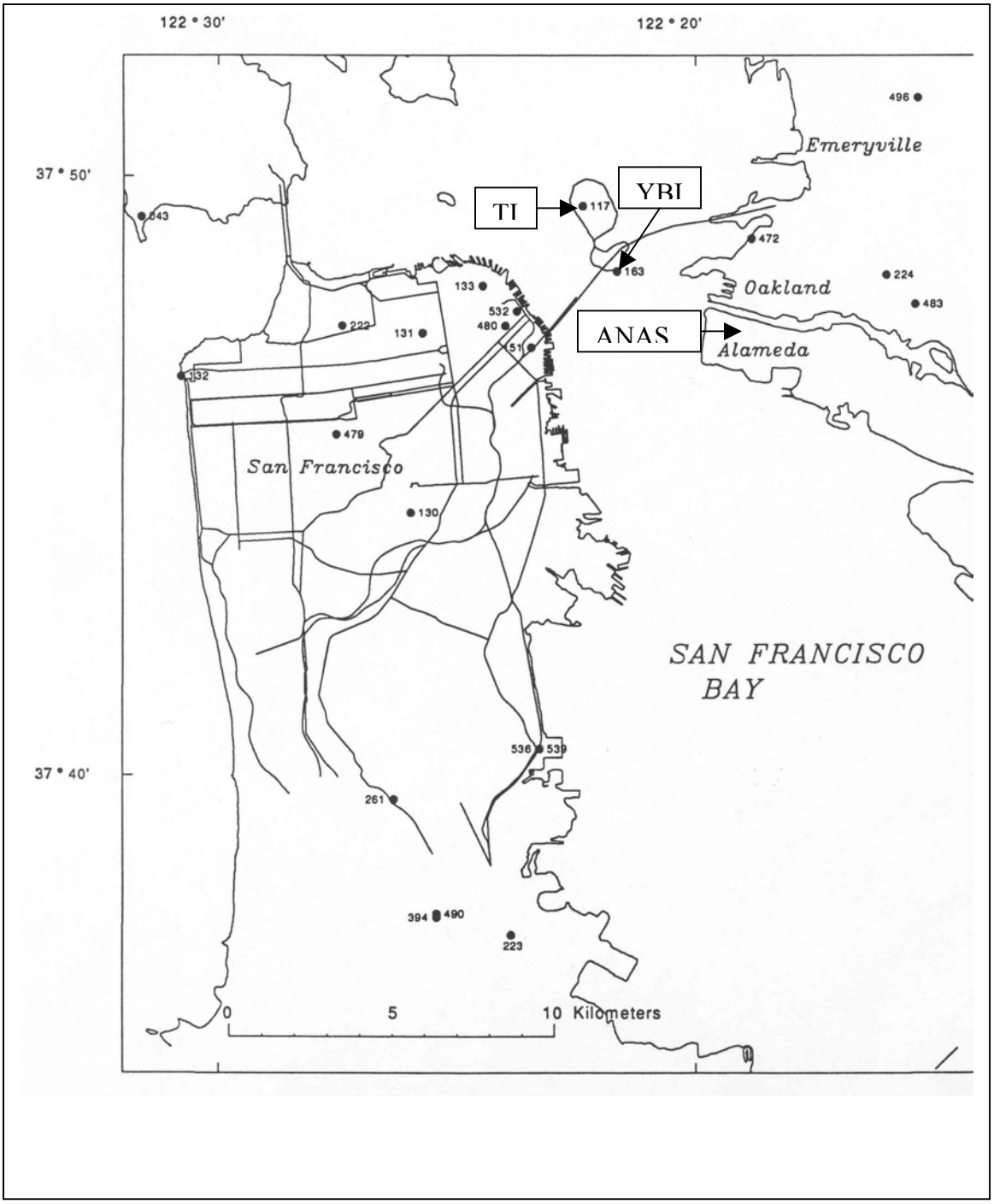

Figure 5.1. Map of San Francisco Bay area showing locations of TI and ANAS sites (after Brady and Shakal, 1994)

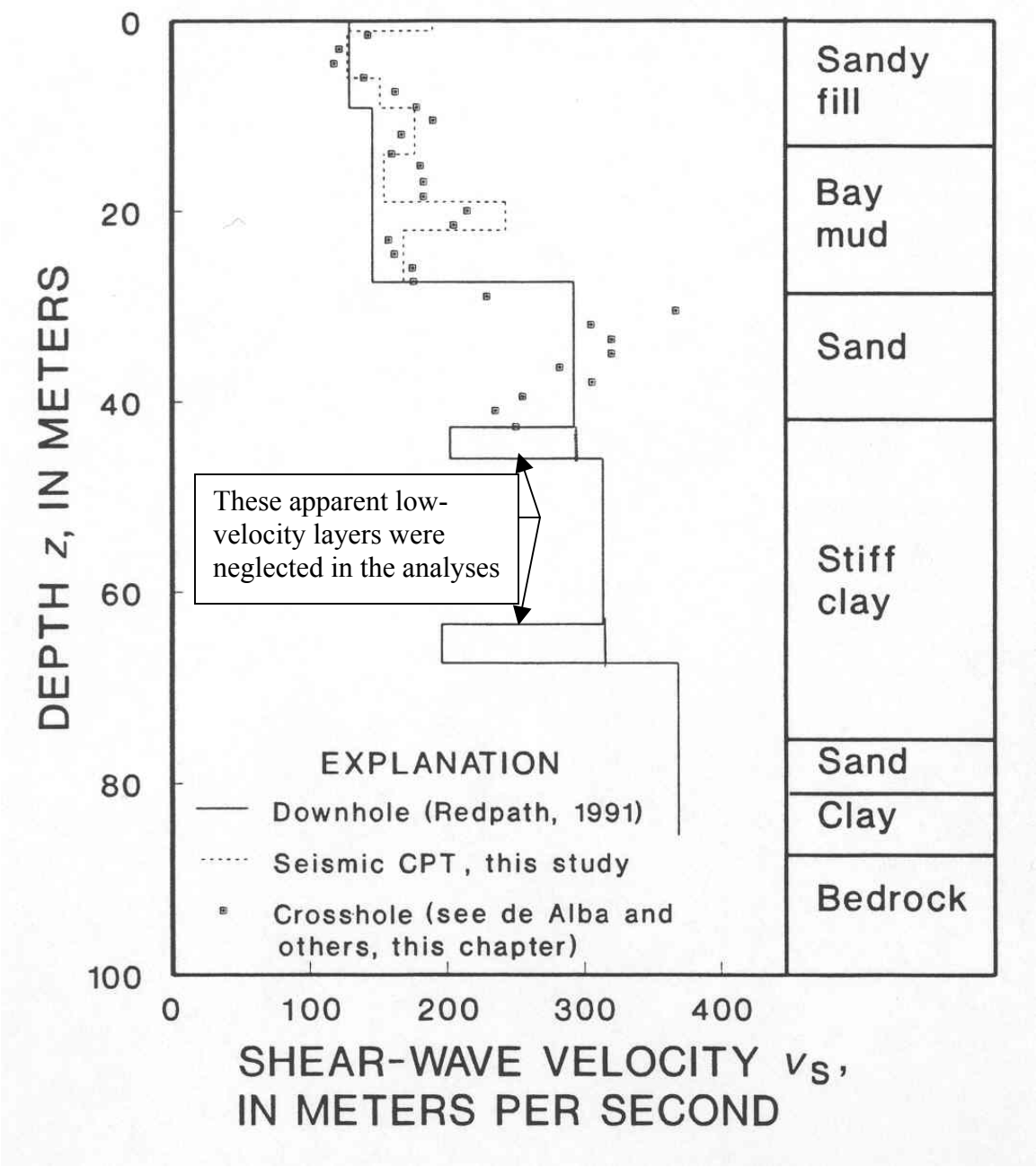

Figure 5.2. Site cross section showing sediment layers at TI (after Rollins et al., 1994)

Table 5.1. Soil properties for sediment layers at the TI site

Material Type	Layer Number	Thickness (m)	Unit Weight (kN/m^3)	G_{max} (MPa)	V_s (m/s)
Sand Fill	1	0.9	18.9	461.7	490.1
	2	5	18.1	30.2	128
	3	3	18.1	42.6	152.1
	4	2.7	18.9	60.3	177.1
Young Bay Mud	5	2.3	15.7	50.2	177.1
	6	4.9	15.7	38.6	155.1
	7	3	17.3	104	242.9
	8	7	17.3	50.2	168.9
Fine Dense Sand	9	12.2	18.1	157.7	292.6
Old Bay Mud	10	4.9	18.1	157.7	292.6
	11	21.3	19.6	197.3	313.9
	12	7.3	19.6	272.4	368.8
	13	4.6	19.6	272.4	368.8
Sand	14	7.6	19.6	272.4	368.8
Old Bay Mud	15	Infinite	22	3333.5	1219.2

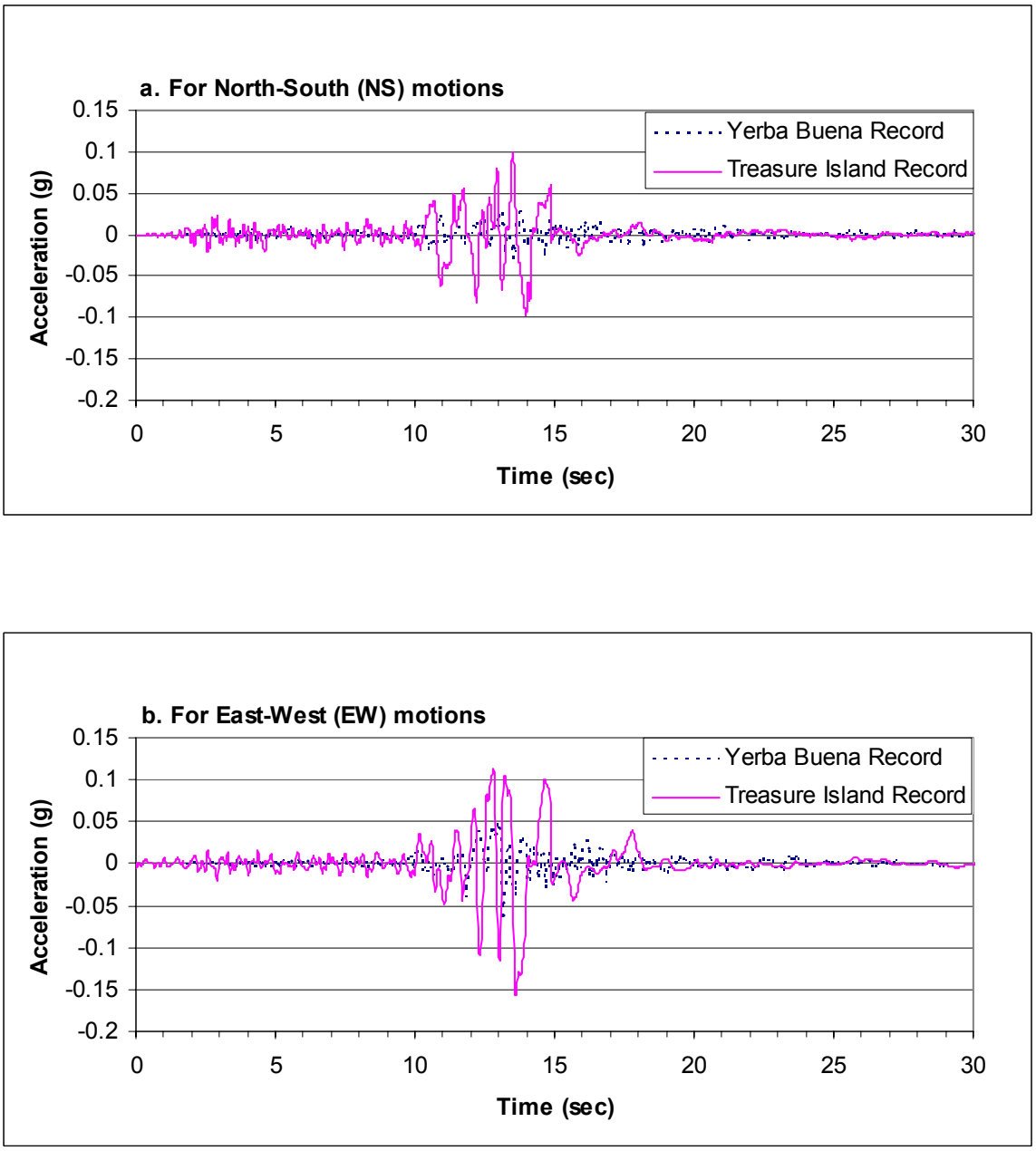

Figure 5.3. Actual surface acceleration time histories for TI and YBI sites during 1989 Loma Prieta earthquake (M=6.8)

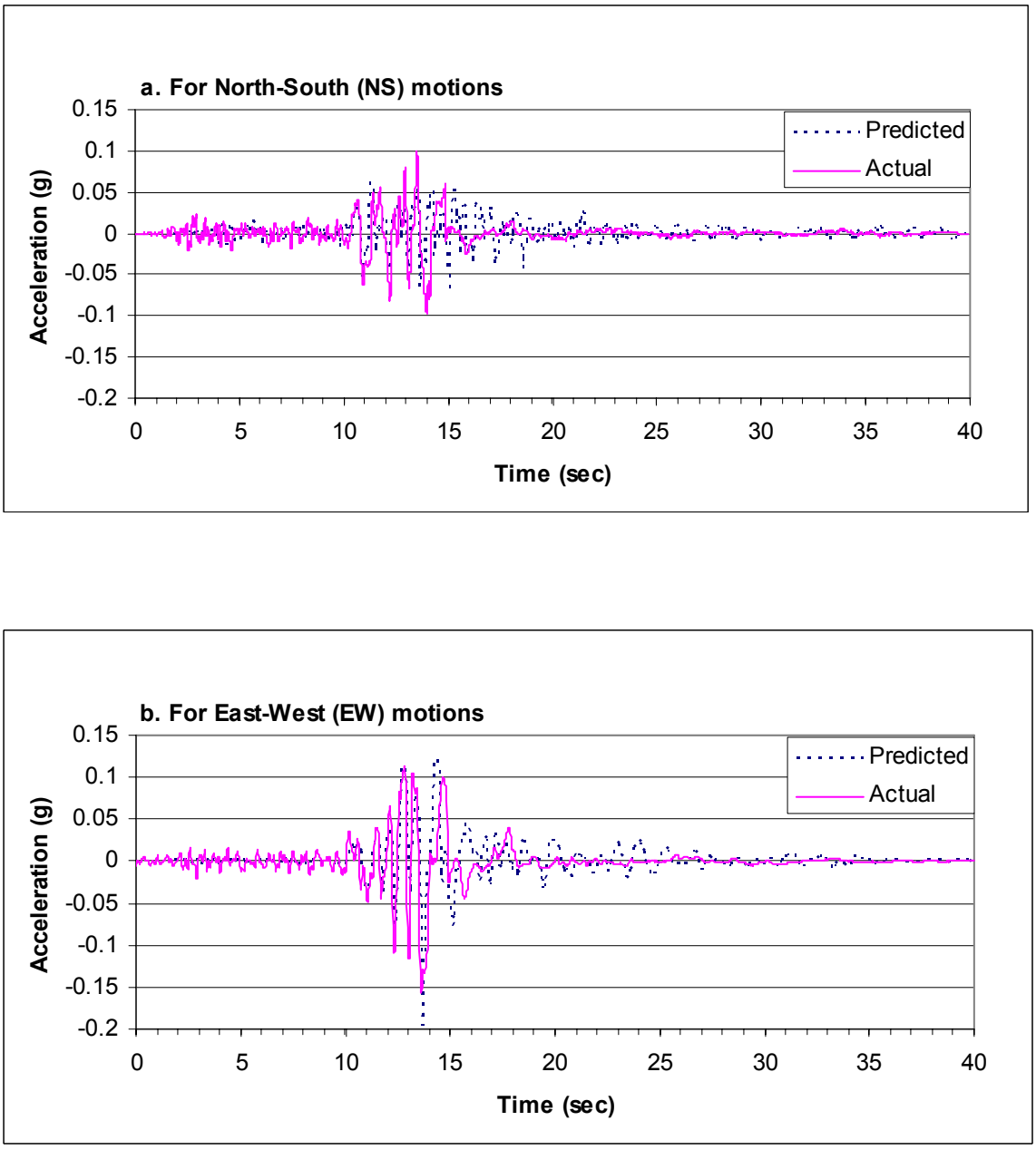

Figure 5.4. Predicted and actual acceleration time histories for TI site during 1989 Loma Prieta earthquake (M=6.8)

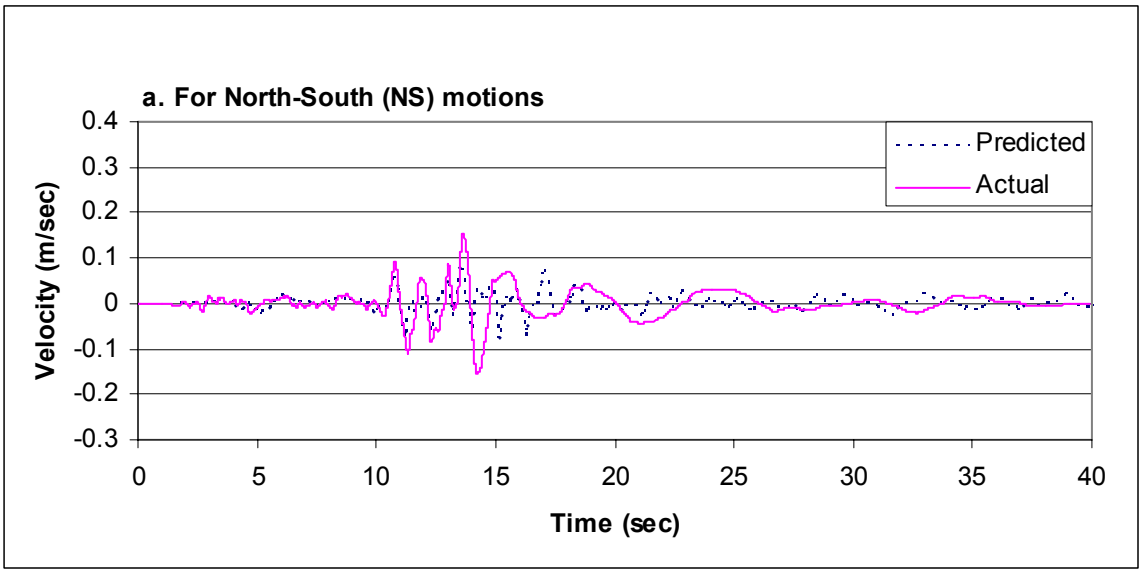

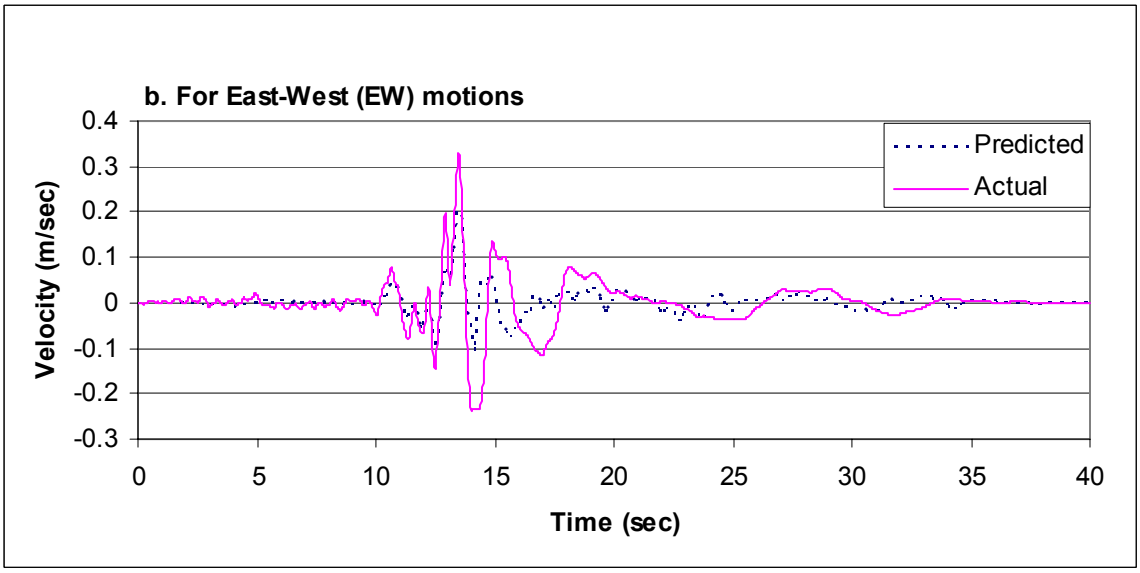

Figure 5.5. Predicted and actual velocity time histories for TI site during 1989 Loma Prieta earthquake (M=6.8)

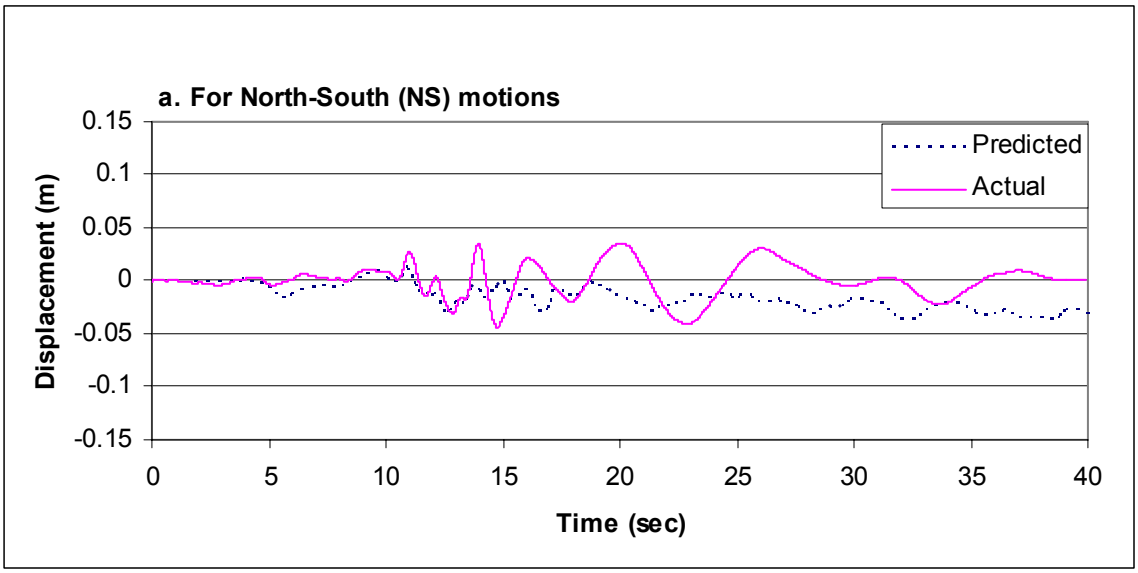

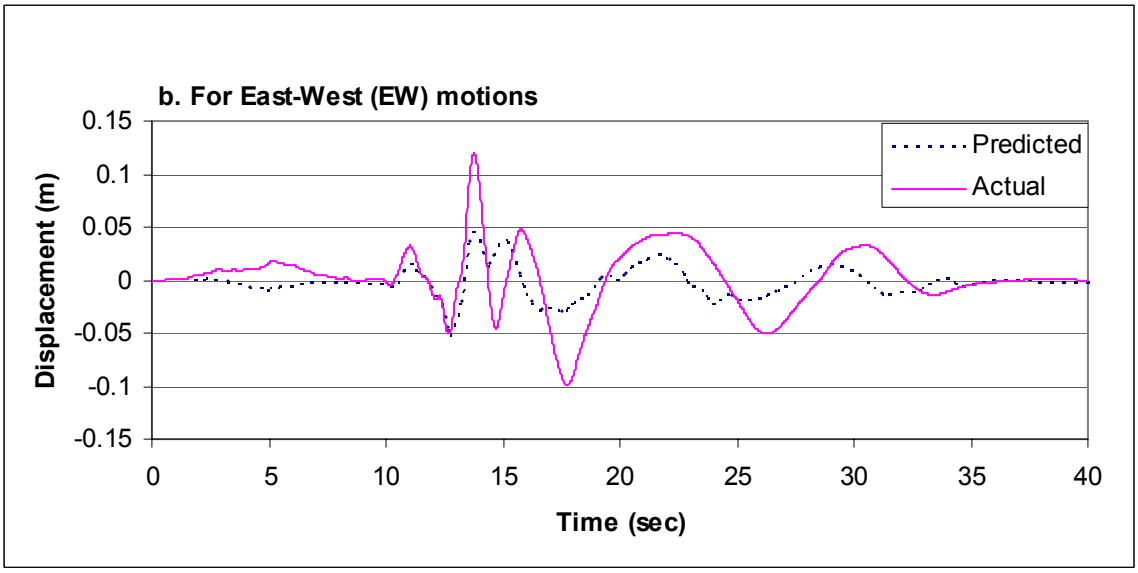

Figure 5.6. Predicted and actual displacement time histories for TI site during 1989 Loma Prieta earthquake (M=6.8)

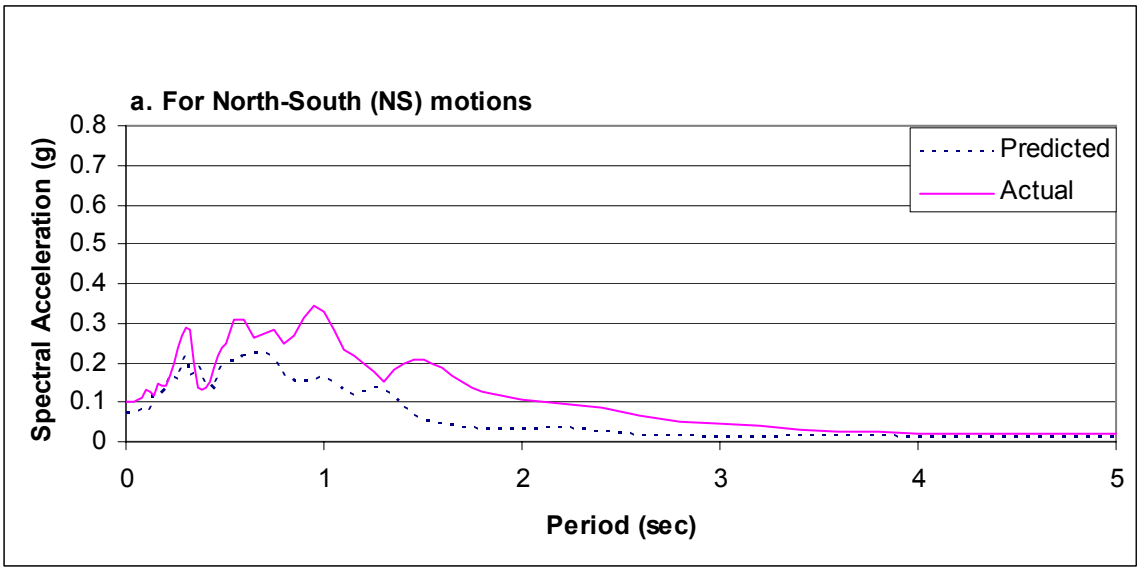

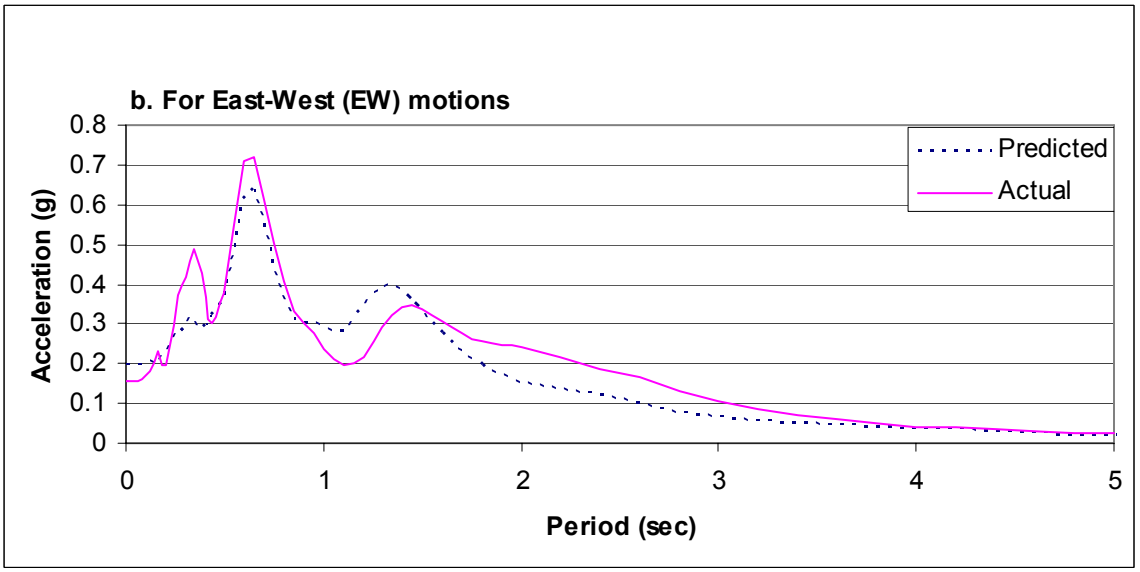

Figure 5.7. Predicted and actual response spectra for TI site during 1989 Loma Prieta earthquake (M=6.8)

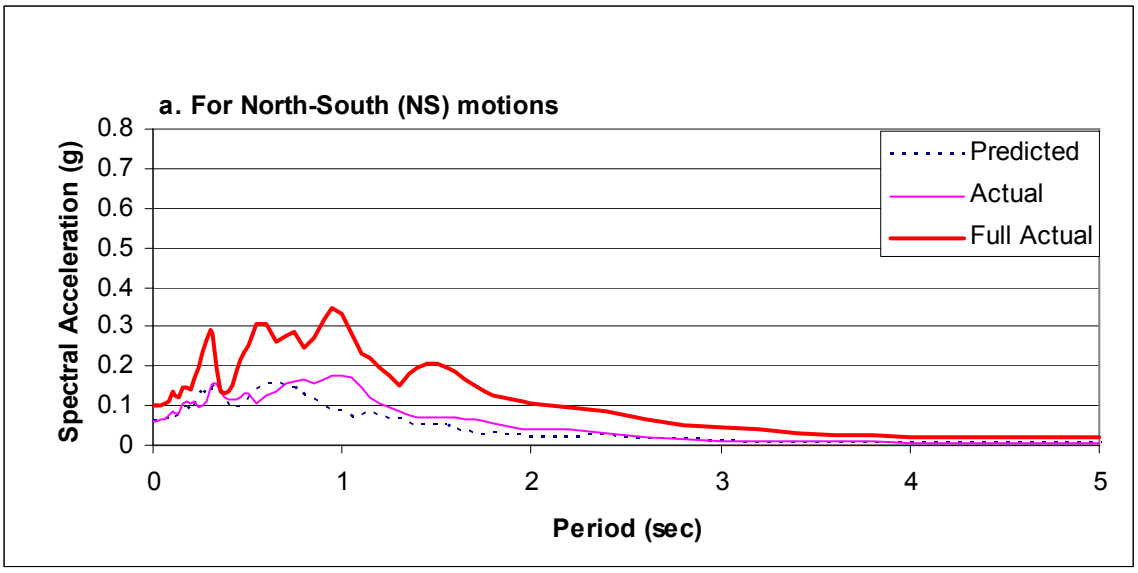

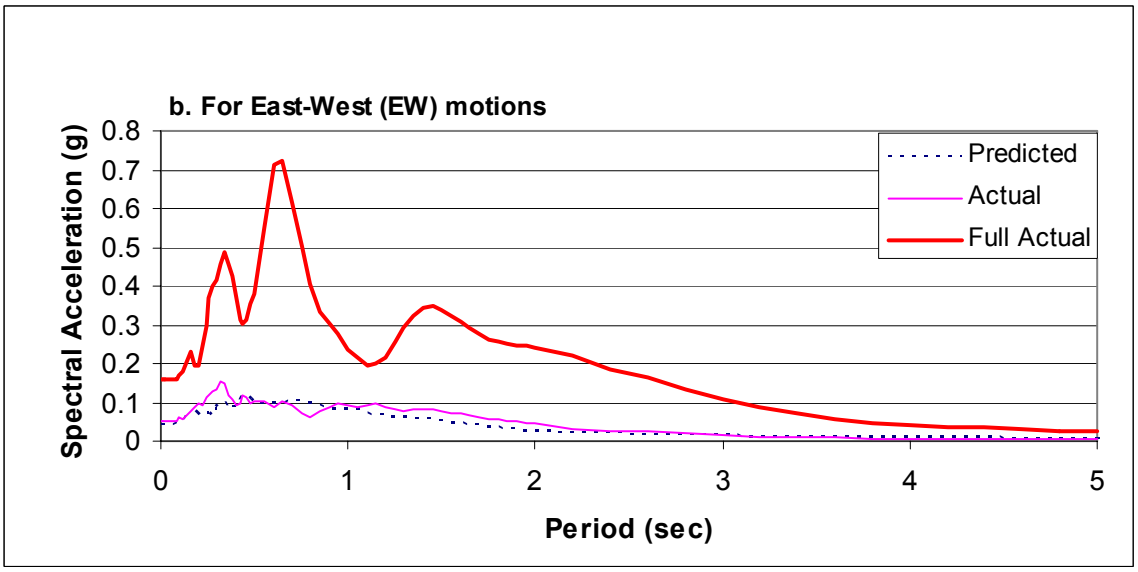

Figure 5.8. Predicted and actual response spectra calculated from the first 10 sec of acceleration record for TI site during 1989 Loma Prieta earthquake (M=6.8)

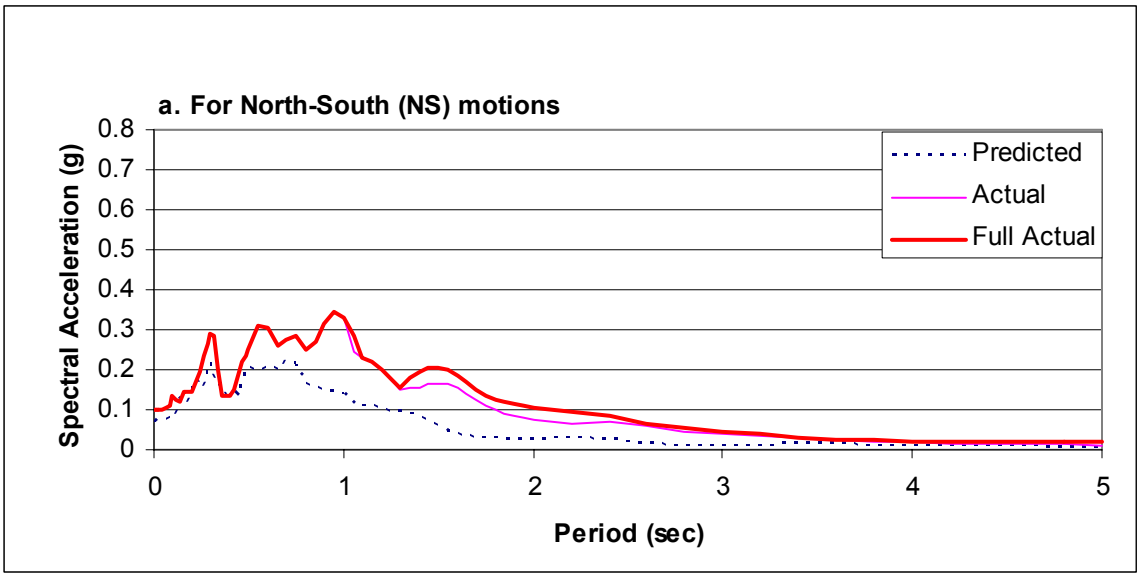

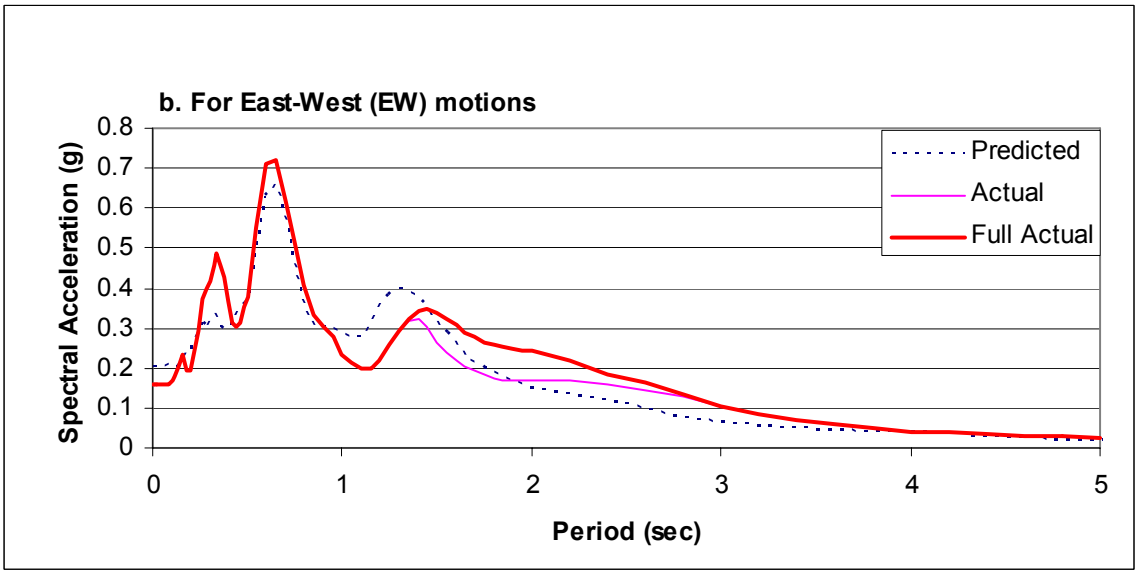

Figure 5.9. Predicted and actual response spectra calculated from the first 13 sec of acceleration record for TI site during 1989 Loma Prieta earthquake (M=6.8)

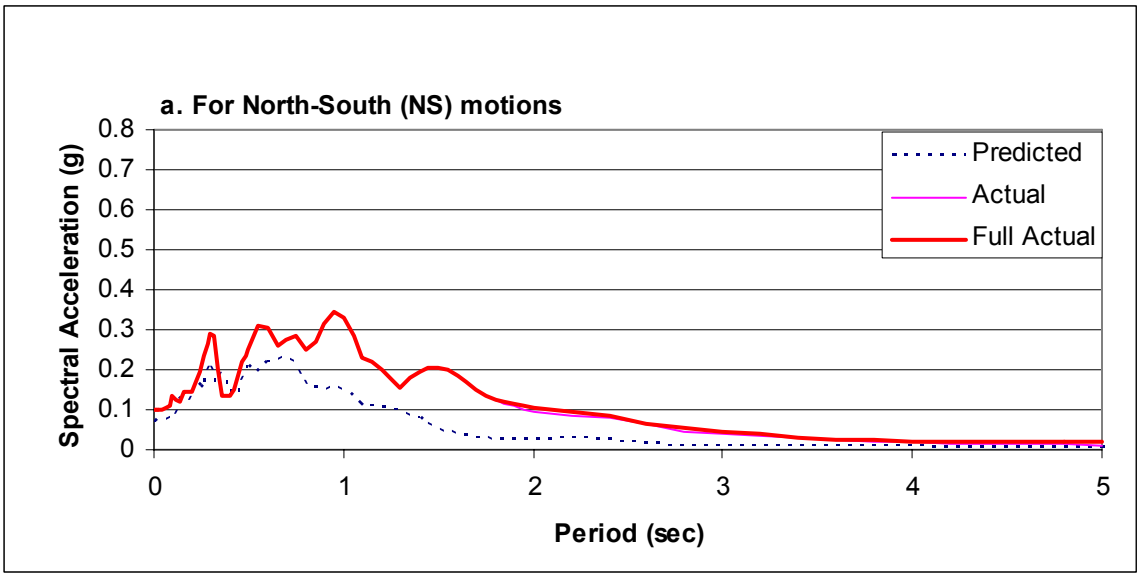

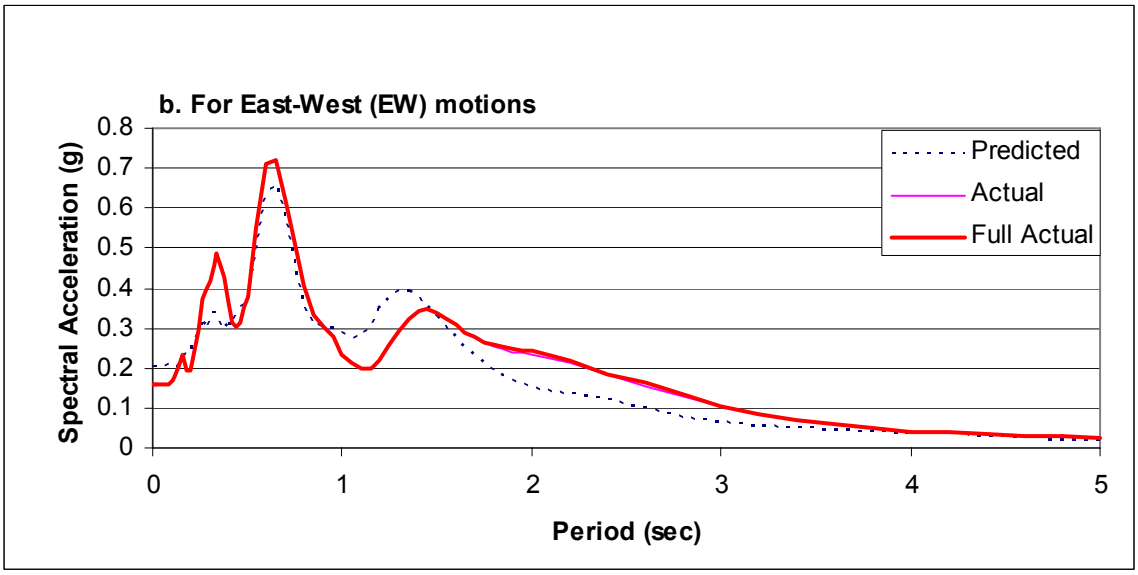

Figure 5.10. Predicted and actual response spectra calculated from the first 14 sec of acceleration record for TI site during 1989 Loma Prieta earthquake (M=6.8)

SECTION 6

Alameda Naval Air Station (ANAS) Site, 1989 Loam Prieta Earthquake

Site History, Stratigraphy, and Instrumentation

The Alameda Naval Air Station (ANAS) site is located on a filled area that forms a northwestward extension of Alameda Island, east of Oakland, California. The instrument station ANAS is located 7.2 km southeast of TI and 5.3 km southeast of YBI instruments. That part of the island was constructed between 1939 and 1940 using hydraulic procedures. The fill was dredged from nearby exposures of the Merritt Sand formation beneath San Francisco Bay. The fill was placed behind the rockfill seawalls which enclose an area of about 10 km^2 (Carlisle, Rollins 1994). Similar to Treasure Island, the fill beneath ANAS is uncompacted and susceptible to liquefaction. Evidence of liquefaction at the ANAS site following the Loma Prieta earthquake included sand boils and ground settlement. Differential settlement was particularly noted around nearby pile-supported buildings

The analysis we performed for the ANAS site is similar to that for the TI site in that we used the rock outcrop motion recorded at YBI as an input motion. That motion was then deconvolved to a base level, transferred under the ANAS site, and then propagated upward through an unsoftened soil profile. The soil properties for the analysis were determined several years after the earthquake from a test borehole drilled to bedrock just east of the ANAS accelerometer (Carlisle and Rollins 1994). The soil column consists of 4.8 m of loose sandy fill, underlain by a 9.0 m of younger bay mud, which is underlain by 13.5 m of dense Merritt sand, which is in turn underlain by 113 m

of stiff clay with sporadic gravelly sand layers (Figure 6.1). Soil properties for each sediment layer, including those used in our analyses, are listed in Table 6.2.

Record Comparisons

Acceleration Time Histories

Acceleration time histories from the recorded or actual ANAS motions and surface motions predicted from the YBI record using the PROSHAKE procedure are plotted in Figures 6.2a and b for the NS and EW directions respectively. Until about 11 sec after instrumental triggering, the predicted acceleration records rather closely approximate the measured record for both the EW and NS components of motion. Immediately after 11 sec, large acceleration peaks occurred in the actual records that were much larger than those predicted. These peaks were as large as 0.26 g and 1.4 g in the NS and EW directions respectively. The arrival of these large peaks apparently initiated the generation of excess pore water pressure, leading to longer periods in the actual accelerations. Between 11 sec and 15 sec, the amplitudes of acceleration peaks in the actual motions were generally much larger than equivalent peaks in the predicted motions, indicating that the site during those few seconds was in resonance with and amplified the incoming motions.

Velocity Time Histories

Actual and predicted velocity time histories, developed by integrating the acceleration time histories with respect to time, are plotted on Figure 6.3a and b for the NS and EW directions respectively. Again, until about 11 sec, the predicted velocity plots rather closely follow the actual record for both the EW and NS directions. Beyond

11 sec, the actual and predicted velocities diverge with the actual velocities lengthening in period. Between 11 and 15 sec, the amplitudes of the actual motions are much greater than the predicted amplitudes, a relationship that is consistent with the records from TI.

Beyond 15 sec, longer period oscillations developed in the actual record that are smoother (less high-frequency motion) and generally characterized by slightly greater amplitudes than oscillations in the predicted record. The lack of higher frequency motions in this segment of the actual record indicates that the sediment had softened sufficiently to prevent transmission of higher frequency ground motions. The velocity response indicates that long period oscillations were initiated at about 12 sec, particularly in the EW record.

Displacement Time History

Displacement time histories, generated by double integrating the acceleration time histories, are compared for both actual and predicted records in Figures 6.4a and b for the NS and EW directions respectively. Similar to the velocity traces, the predicted displacement traces are nearly congruent with the actual record until 11 sec after triggering. Beyond 11 sec, the traces diverge with the actual displacements transitioning into long-period oscillations that are roughly in phase with longer-period components of the predicted motions. In contrast to the long-period actual displacements that developed at TI, which were smaller than the predicted displacements and rather quickly attenuated, the actual displacement oscillations at ANAS were larger than the predicted values and continued until at least 30 sec after triggering. Thus, much more ground oscillation developed at ANAS than at TI, but not as much in either amplitude or duration as that which occurred at WLA.

Inferred Pore Pressure Response

No piezometers were in place at the ANAS site to measure pore water pressures during the Loma Prieta earthquake. By comparison with the WLA records, however, we are able to infer some approximate relationships between excess pore water pressures and the ground motions recorded at ANAS. Because actual and predicted motions were essentially congruent until about 11 sec after triggering, we infer that little if any excess pore pressures had developed at that juncture and that pore pressure ratios, r_u, were near zero.

Between 11 sec and 15 sec, the period of the actual motions greatly lengthened with respect to the predicted motions. Beyond 15 sec, the capability of softened sediment in the liquefiable layer to transmit high-frequency motions was greatly impaired. Based on a comparison with the WLA records, we estimate that pore pressure ratios quickly rose from near zero at 11 sec to as much as 0.5 by 15 sec. By 20 sec, the actual (measured surface motions) were in long period oscillation vibrating independently of incoming high-frequency motions, indicating a liquefied subsurface layer and pore pressure ratios near 1.0.

Response Spectra from Complete Time Histories

Acceleration response spectra calculated from complete records for both actual and predicted motions from the ANAS site are plotted on Figure 6.5a and b for NS and EW directions respectively. As at TI, the actual and predicted response spectra for the EW direction agree rather well. The primary difference is at periods between 2 sec and 4 sec where actual spectral values are greater than the predicted values. As will be shown later, that difference was due to transfer of energy into longer-period ground oscillations.

In the NS direction, the actual spectra are much greater than the predicted spectra at all periods. We do not know the reason for this great difference, but some inferences are gained by examining the relationship between spectral response and the time of arrival of the seismic energy.

Response Spectra for first 11 Sec of Record

Predicted and actual response spectra for the first 11 sec of record, up until excess pore water pressure apparently began to rise, are plotted on Figure 6.6. At that juncture, the predicted and actual spectra in the EW direction are roughly equivalent with only a major peak at about 0.4 sec in the actual EW spectrum missing in the predicted spectrum. This missing peak may be partly due to timing errors in our calculations, because much of that peak is filled in the spectra calculated for the first 12.5 sec of record (Figure 6.7). The breadth of the actual spectral acceleration peak in the NS record is greater than the predicted peak, but the height of the peaks are roughly equivalent. Thus for the first 11 sec of record, prior to the onset of pore pressure development, the actual and predicted spectra are roughly comparable.

Response Spectra from first 12.5 sec of record

Response spectra calculated for the first 12.5 sec of record are plotted on Figure 6.7. At that juncture, the actual and predicted spectra in the EW direction are roughly equivalent for periods less than 1.0 sec. The actual spectra for this increment of time (12.5 sec) and the final actual spectra are also congruent, indicating that nearly all of the seismic energy for periods less than 1 sec had passed through the site at this juncture. The rest of that energy at periods greater than 1.0 sec will propagate though the site over the next few seconds. Development of ground oscillation as a consequence of sediment

softening and liquefaction is the apparent reason for the delay in the arrival of this long period energy.

For the NS direction, the actual and predicted response spectra are greatly different at the 12.5 sec juncture, with spectral values at all periods, with the actual values being much greater than the predicted values. Also, the actual spectrum for the first 12.5 sec is nearly congruent with the final spectrum for periods less than 0.9 sec and not greatly different at periods greater than 0.9 sec. This congruence indicates, as in the EW direction, that most of the seismic energy propagated through the site by 12.5 sec, and that most of this energy passed though the site in the 1.5 sec interval between 11.0 and 12.5 sec. The reason for this sudden burst of energy between 11 sec and 12.5 sec is not clear, but a similar phenomenon occurred at TI as noted previously. As noted in the discussion of the TI records, we were unable to determine whether this larger actual response was due to some resonance phenomenon associated with the sudden rise of pore pressures and severe soil softening that began to occur at both sites during this short time interval, or whether, for an unknown reason, the motions recorded on YBI in the NS direction during that interval are anonymously deficient seismic energy. Because the actual seismic energy was distributed over a wide range of periods, we believe that the latter is a more plausible explanation.

Response Spectra for the First 15 Sec of Record

Response spectra calculated for the first 15 sec of record are almost identical with the final spectra, both for the predicted and actual responses (Figure 6.8). In the EW direction, the responses between the predicted and actual spectra are very close, except for periods between 2 sec and 4 sec where ground oscillation apparently caused greater

actual response than was predicted. In the NS direction also, the responses were nearly complete, but were greatly different as explained in the previous paragraph.

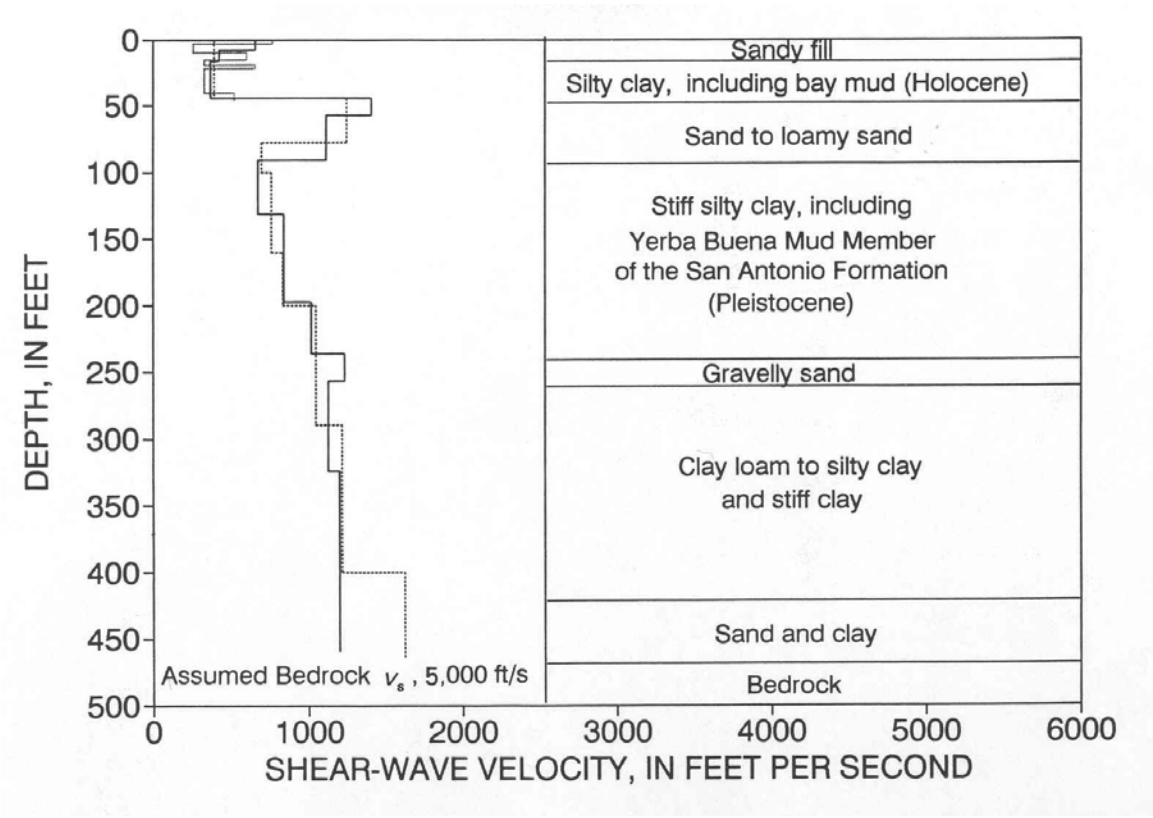

Figure 6.1. Site cross section showing sediment layers at ANAS (after Carlisle and Rollins, 1994)

Table 6.1. Soil properties for sediment layers at the ANAS site

Material Type	Layer Number	Thickness (m)	Unit Weight (kN/m^3)	G_{max} (MPa)	V_s (m/s)
Sand Fill	1	1.0	17.3	97	235
	2	1.0	17.3	11	80
	3	1.0	17.3	11	80
	4	1.6	18.9	66	185
	5	1.2	17.1	18	100
Clayey Silt	6	0.9	17.1	70	200
	7	1.4	17.1	18	100
	:	:	:	:	:
	10	1.4	17.1	18	100
	11	1.4	17.1	45	160
Clayey to Silty Sand	12	1.7	17.1	344	400
	13	1.9	17.1	344	400
	14	1.9	21.2	344	400
	15	1.9	21.2	344	400
	16	1.9	21.2	344	400
Silty Sand	17	2.0	21.2	120	235
	18	2.0	21.2	120	235
Stiff Silty Clay	19	3.0	20.4	115	235
	20	3.0	18.9	126	256
	:	:	:	:	:
	25	3.0	18.9	126	256
	26	3.0	18.9	151	280
	:	:	:	:	:
	29	3.0	18.9	151	280
	30	3.9	18.9	241	355
	31	3.9	18.9	241	355
	32	3.9	18.9	241	355
	33	1.2	21.2	271	355
Gravelly Sand	34	3.0	19.6	251	355
Clay Loam to Silty Clay	35	1.2	21.2	271	355
	36	5.2	19.6	251	355
	37	5.2	19.6	251	355
	38	4.2	19.6	335	409
	:	:	:	:	:
	45	4.2	19.6	335	409
	46	6.7	19.6	595	5448
	47	4.0	21.2	642	5448
	48	5.2	19.6	595	5448
	49	4.3	21.2	642	5448
Bed Rock	50	Infinite	22	7500	1829

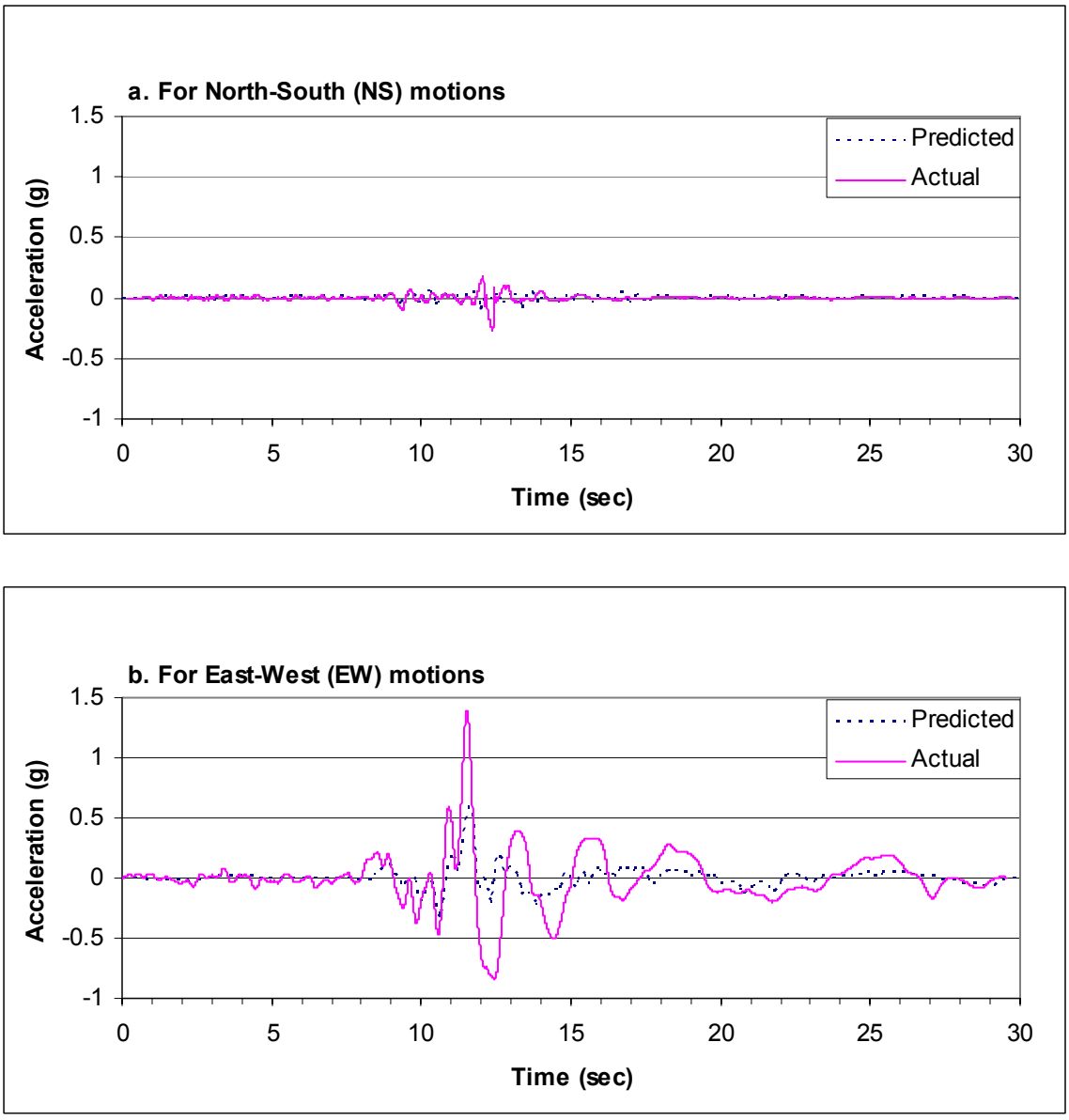

Figure 6.2. Predicted and actual acceleration time histories for ANAS site during 1989 Loma Prieta earthquake (M=6.8)

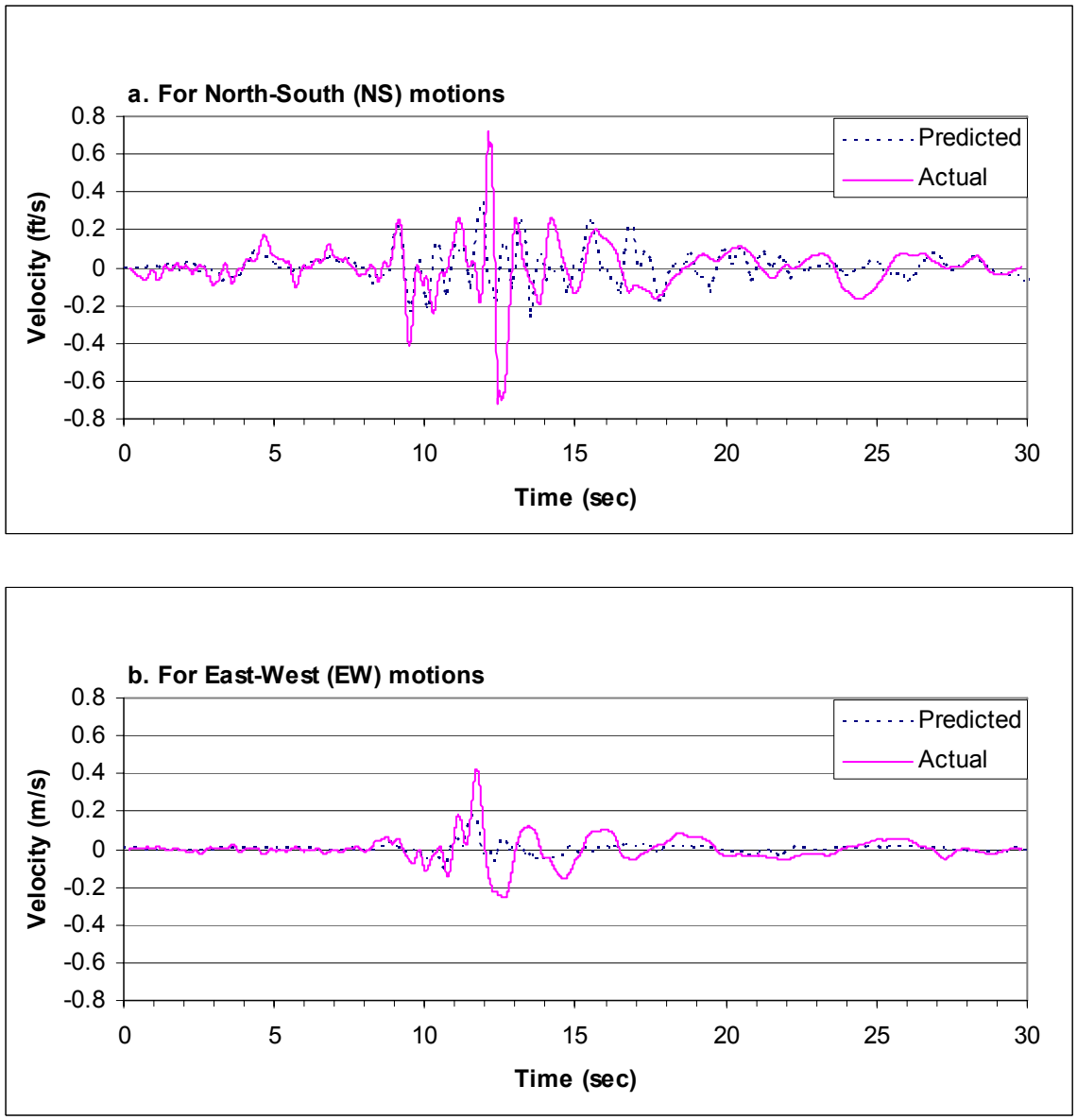

Figure 6.3. Predicted and actual velocity time histories for ANAS site during 1989 Loma Prieta earthquake (M=6.8)

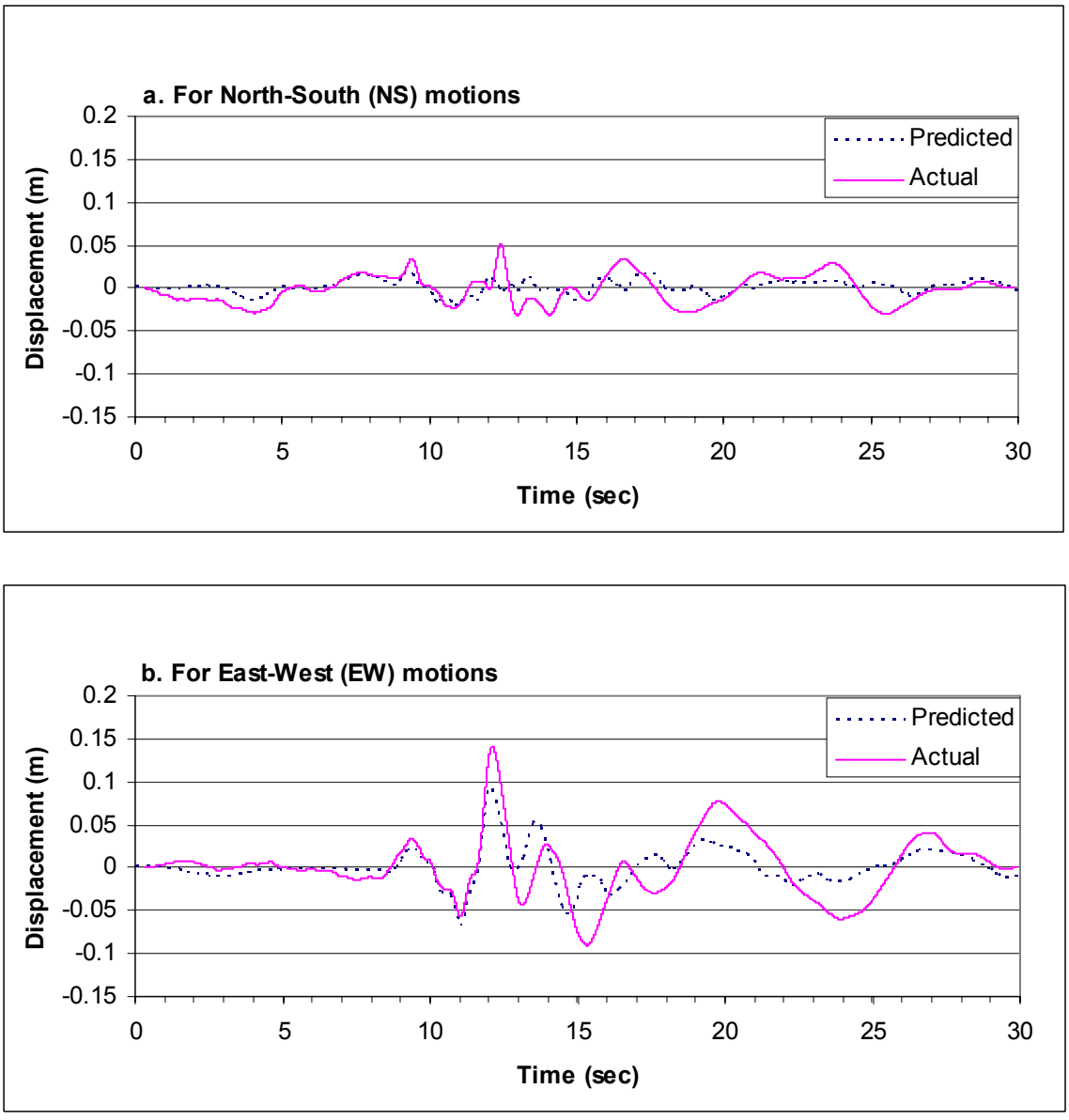

Figure 6.4. Predicted and actual displacement time histories for ANAS site during 1989 Loma Prieta earthquake (M=6.8)

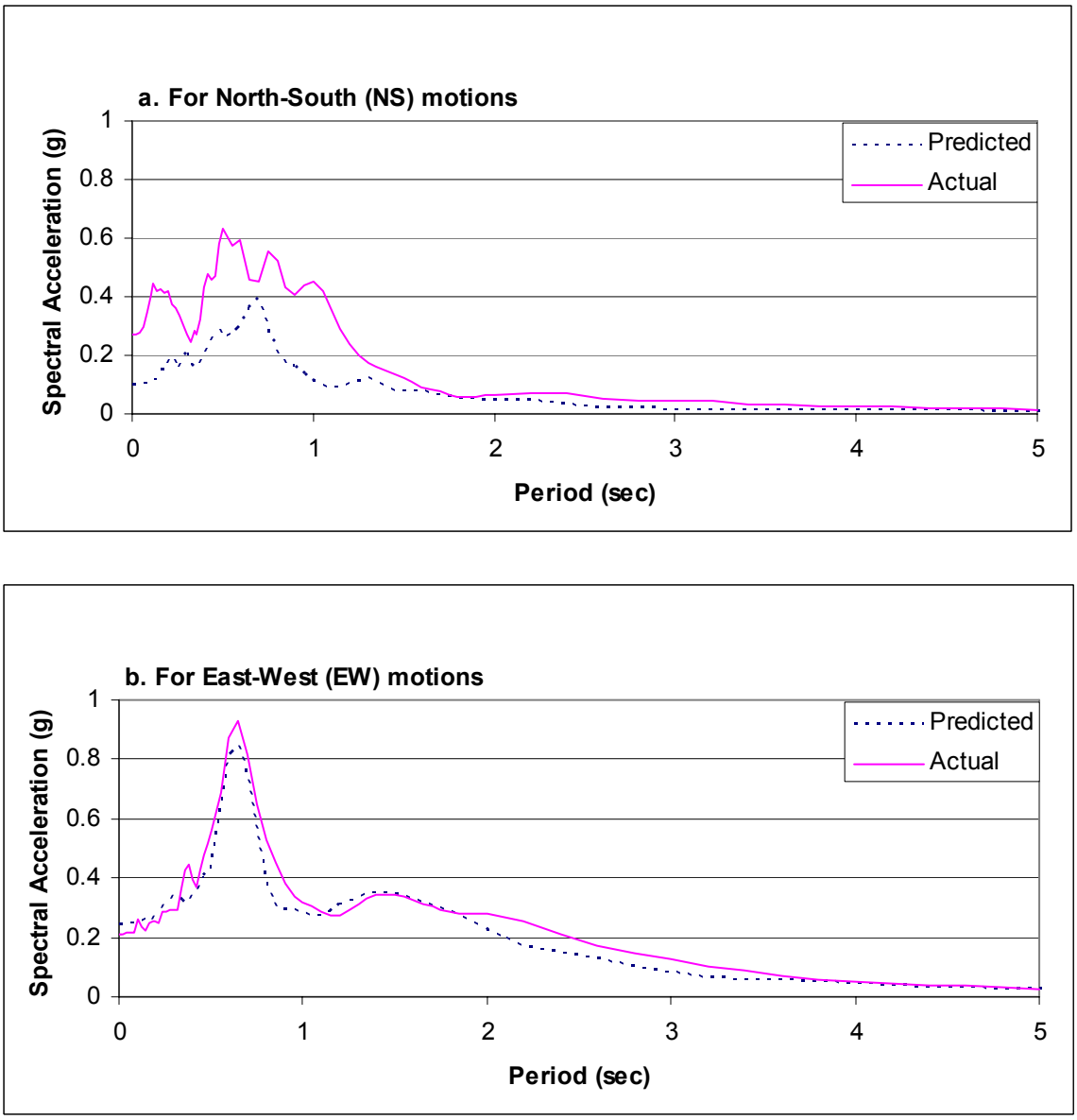

Figure 6.5. Predicted and actual response spectra for ANAS site during 1989 Loma Prieta earthquake (M=6.8)

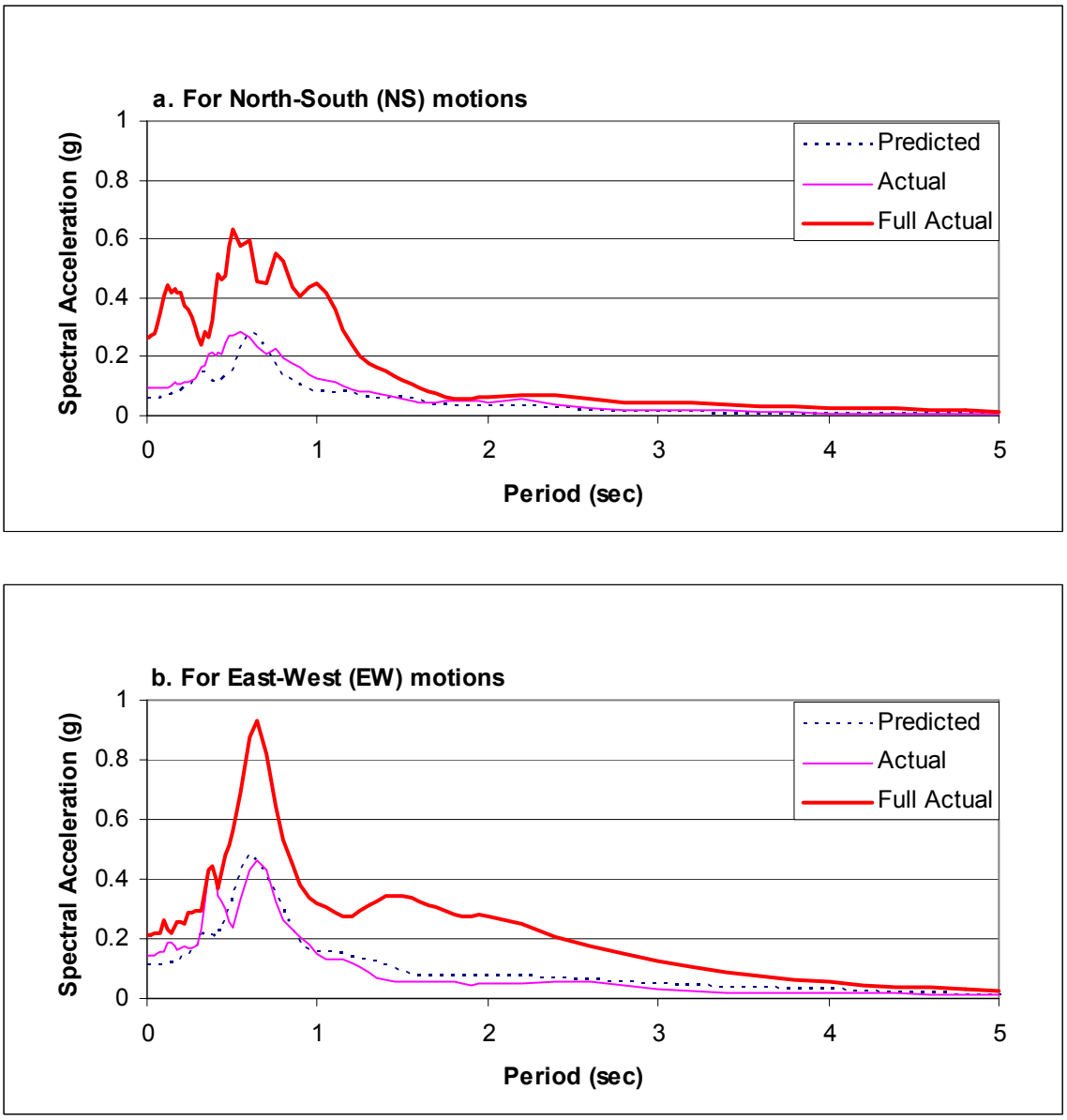

Figure 6.6. Predicted and actual response spectra calculated from the first 11 sec of acceleration record for ANAS site during 1989 Loma Prieta earthquake (M=6.8)

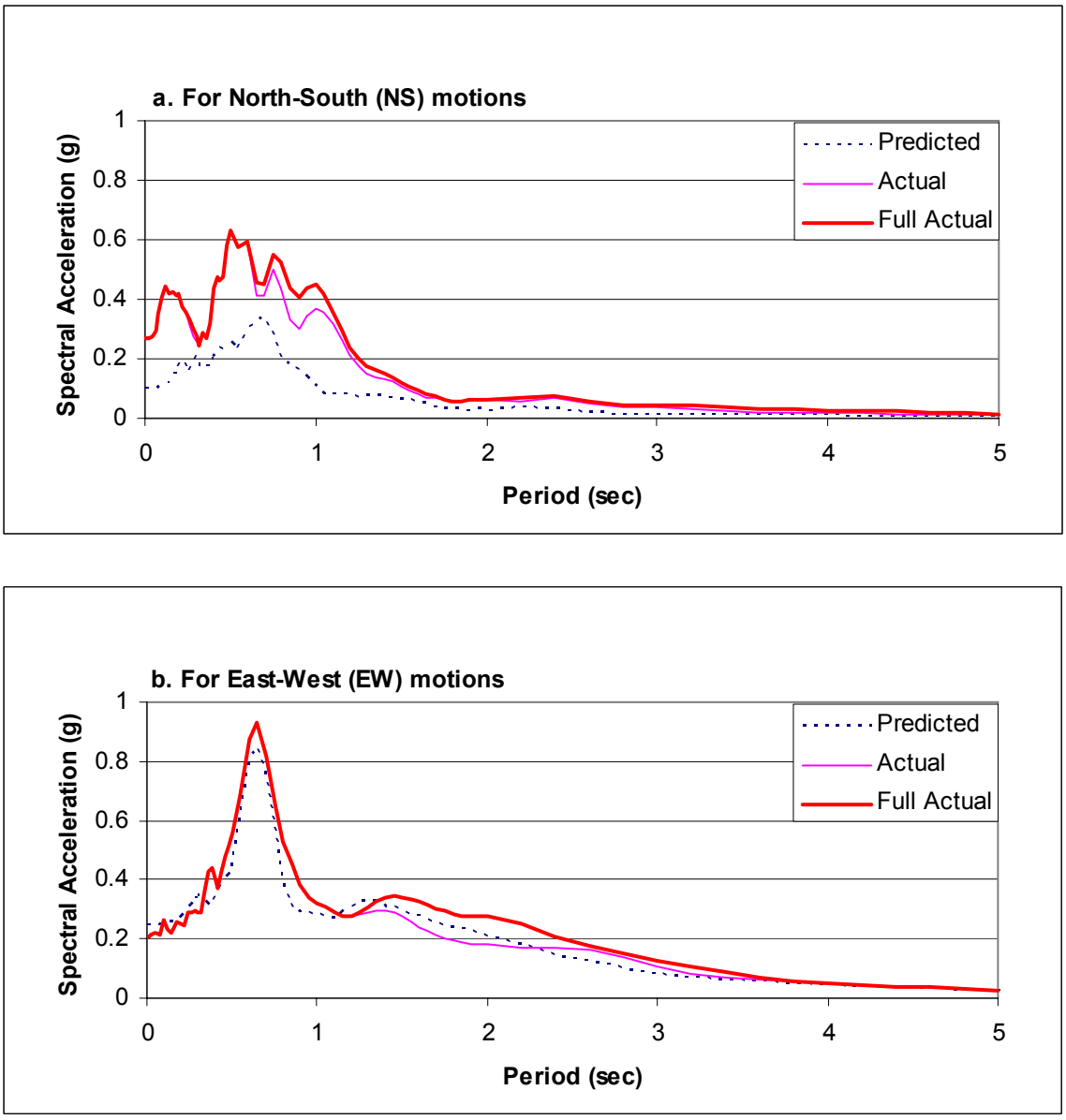

Figure 6.7. Predicted and actual response spectra calculated from the first 12.5 sec of acceleration record for ANAS site during 1989 Loma Prieta earthquake (M=6.8)

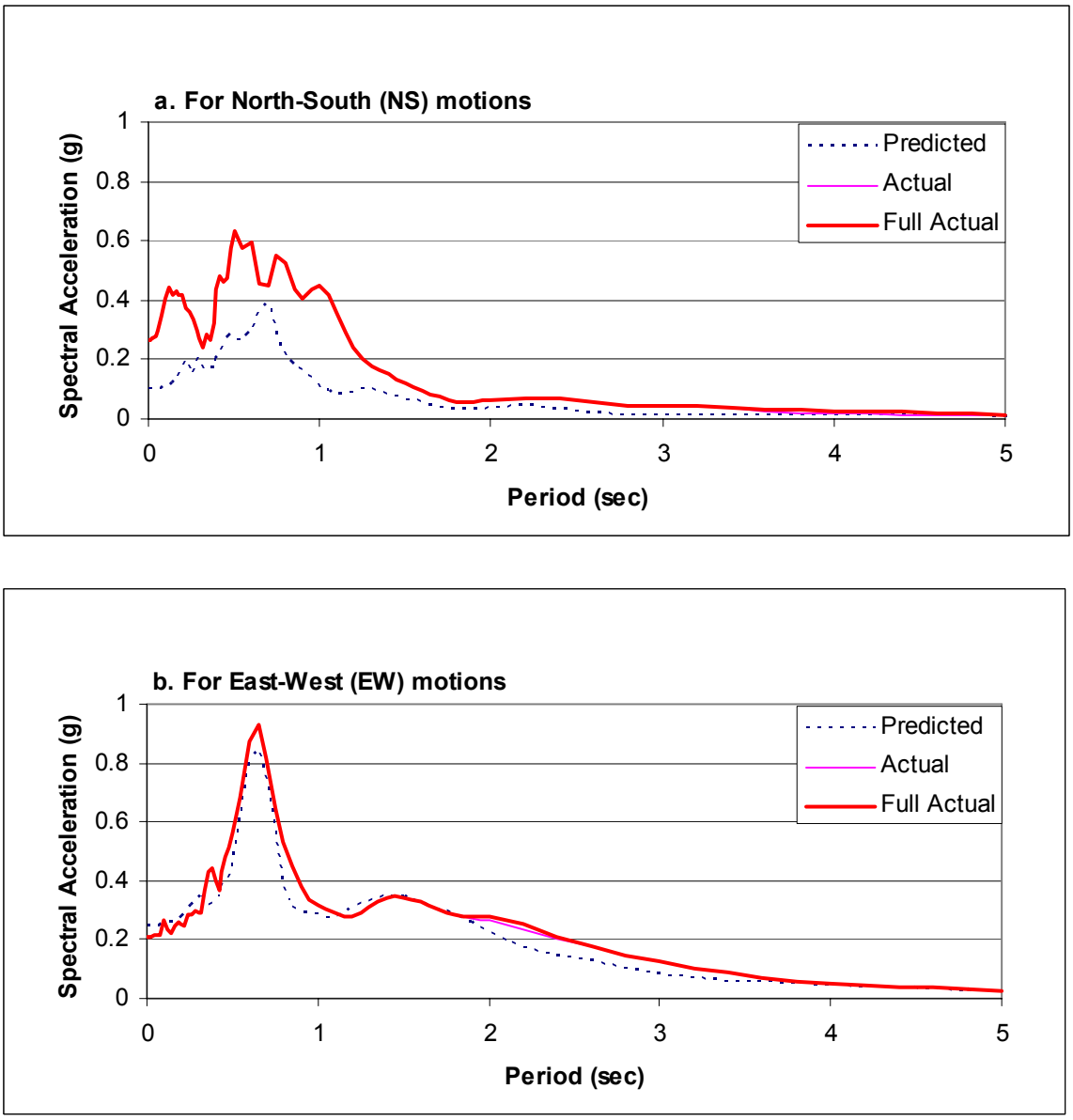

Figure 6.8. Predicted and actual response spectra calculated from the first 15 sec of acceleration record for ANAS site during 1989 Loma Prieta earthquake (M=6.8)

SECTION 7

1964 Niigata, Japan Earthquake

Site History, and Stratigraphy

On June 16, 1964**,** the Niigata, Japan area was shaken by a magnitude 7.5 earthquake (Hirono, 1968) that liquefied much of the flood plain and reclaimed areas surrounding the Shinano River (Figure 7.1). The seismic shaking caused wide spread damage to buildings, roads, bridges, and other engineered structures. Much of the damage was caused by liquefaction-induced loss of bearing strength and lateral spreads. The Kawagishi-Cho apartment complex in Niigata, Japan, experienced extensive damage due to loss of bearing strength, including tilting and overturning of 5-story buildings (Figure 7.2). This area, which includes a strong motion instrument site, is located on reclaimed land (loose sand) near the Shinano River (Kawasumi, 1968).

The Niigata plain on which the city is founded is underlain by three principle alluvial formations**:** upper, middle, and lower. The upper formation is composed of loose, grayish, and coarse to medium grained sand, intercalated with silt and clay. This upper formation extends from ground surface to a depth of approximately 15 m. The middle formation is a uniform bluish-gray fine sand that is well-rounded, well-sorted fine sand and contains marine shells. This formation extends to a depth of 40 m. The lower formation consists of thick, alternating layers of dark gray, fine sand and silt and extends to a depth of about 80 m. Gravelly and bedrock materials lie at depths greater than 80 m (Morimoto, 1968).

A profile showing shallow soil layers and properties at the Kawagishi-cho apartment complex or NJ site is reproduced in Figure 7.3. This profile indicates deposits

of very loose sand, with measured standard penetration blow counts less than 10, to a depth of 5 m. The very loose sand is underlain by an additional 5 m of loose sand with measured blow counts between 10 and 15. Blow counts are generally greater but more variable to a depth of 20 m than the base of the upper alluvial formation as noted above, with measured blow counts ranging from 10 to 30. Denser sediments with higher blow counts apparently lie below the base of the soil profile shown in Figure 7.3. This profile indicates that highly liquefiable (blow counts less than 15) extend to depths of at least 10 m, and possibly to 20 m, below the NJ site.

Acceleration Time Histories from Niigata, Japan (NJ) Site

The Niigata earthquake occurred in the infancy of modern strong motion monitoring and only one 3-component strong motion instrument had been placed within the heavily shaken area. That instrument was in the basement of an undamaged building in the Kawagishi-Cho apartment complex. No down hole accelerometers or piezometers were installed at this site nor were there any recordings of ground motion on nearby bedrock outcrops. Thus, our study of the Niigata earthquake consists of an analysis of the measured motions only from the NJ site.

The acceleration time histories records at the NJ site are plotted in Figure 7.4a and b for the NS and EW directions respectively. Using the time of instrumental triggering as a reference (0 sec), the first acceleration spike with amplitude greater than 0.05 g occurred at the 2 sec time mark; the peak recorded horizontal acceleration of 0.16 g occurred at the 9 sec time mark, and the last acceleration peak greater than 0.05 g in the main sequence of accelerations occurred at the 12 sec time mark. Thus, the duration of strong ground shaking was about 10 sec at the NJ site. However, by the time the peak

acceleration passed through the site at 9 sec, the subsurface sediment had markedly softened, as noted later, which likely modified and possibly reduced the peak acceleration compared to that which would have occurred in the absence of soil softening. Because there is no companion record from a downhole accelerometer or instrument on bedrock for reference, no estimates of unsoftened site response or peak acceleration could be developed for this site.

The character of the acceleration time history is similar to those at other sites where subsurface sediment softening and liquefaction occurred during seismic shaking. By comparing the accelerograms in Figure 7.4 with those from other sites, we make the following inference: detectable lengthening of the characteristic period in the NS and EW acceleration time histories began at about the 7 sec mark. Based on similar behavior at WLA, where pore pressures were recorded, we suggest that pore water pressures began to rise and soil softening initiated at the 7 sec mark. By 10 sec, the acceleration time histories were dominated by longer-period waves with characteristic periods of about 1.5 sec in the EW direction and 3.0 sec in the NS direction. Many higher frequency small spikes are superimposed on the longer wave motions, indicating that much high-frequency energy was still propagating through the softening sediment at that juncture. From 10 sec onward, the site was in near harmonic resonance or oscillation with the characteristic period of the waves continuing to increase with time. The wave amplitudes beyond 10 sec are variable but with a slowly decaying trend. At 20 sec the characteristic period was about 5 sec in both the EW and NS directions. At 40 sec the characteristic period was about 7sec in both directions. A shorter period harmonic wave, however, was superimposed in the longer-period EW waves between the 20 sec and 60 sec time marks.

At 60 sec the characteristic period was 8 to 10 sec in both directions with greatly diminished shorter period motions. The ground oscillation, particularly in the NS direction, appears to have continued well beyond the end of the acceleration record at 100 sec.

Velocity Time Histories

Integration of the recorded acceleration time histories with respect to time produced the velocity time histories plotted on Figure 7.5. Because velocity response is generally affected more by longer period motions than accelerations, the velocity histories in Figure 7.5 are characterized by less high-frequency and more long-period motion than the accelerograms in Figure 7.4. The velocity traces indicate that long-period harmonic waves began to form as early as 4 sec. These oscillations continued to increase in amplitude until 9 sec. At 9 sec, the largest motions from the earthquake passed through the site, causing large velocity pulses to develop over the next few seconds. These large pulses then transitioned into more regular oscillations with shorter-period subharmonic motions, particularly in the EW trace, for the duration of the 100-sec length of record. The characteristic periods of the velocity waves are roughly comparable to those noted for the acceleration waves at the various time increments noted in the previous section.

Displacement Time History

Displacement time histories for the NJ site were generated by integrating the velocity time histories with respect to time (Figure 7.6). This integration produced permanent displacements or drifts in the time histories, indicating that the acceleration records may not have been adequately corrected for drift during record processing.

Because the rate of drift is nearly constant with time, which is an unlikely occurrence, the drifts in the displacement traces on Figure 7.6 are most likely due to record processing rather than permanent displacement of the site. Some permanent displacement may have occurred at the site due to lateral spread, but rate of movement would not likely have been constant with time. No post earthquake field measurements are reported from which permanent displacements could be determined. The displacement traces on Figure 7.6 emphasize long-period components of ground motions even more than the velocity traces. These traces indicate that ground displacements at the site were dominated by rather smooth 6 sec time mark onward. As noted earlier, strong ground accelerations ceased at the 12 sec time mark. The traces in Figure 7.6, however, clearly show that ground oscillation continued well beyond that time mark with peak-to-peak ground displacements remaining rather steady at 0.6 m to 1.2 m for the next 90 sec. These displacements continued to generate cyclic shear deformations in the subsurface sediment over this extended period. Cyclic shear deformations are the primary mechanism that generates increased pore water pressures. Thus, pore water pressures likely continued to increase after the cessation of strong ground motions until they reached their maximum pore water pressure ratios, r_u, of 1.0. During this extended interval of ground oscillation, the characteristic period of the waves increased with time from approximately 6 sec at the 12 sec time mark to approximately 8-12 sec at the 60 sec time mark. These characteristic periods are comparable for those determined from the acceleration and velocity time histories as noted above.

Inferred Excess Pore Water Pressures

Based on the characteristics of the acceleration, velocity and displacement time histories noted above, and comparison with similar traces from the WLA site where pore water pressures were measured, we deduced the following estimates of pore pressure development at the NJ site. Significant excess pore water pressure most likely did not develop prior to the 7 sec time mark when the characteristic period of the recorded acceleration waves began to lengthen. However, the period lengthening that began at 7 sec is an indicator that excess pore pressures and soil softening began to develop at that time. The arrival of the most intense ground motions, including the peak acceleration at about 9 sec, apparently generated large increases in pore water pressure during the 9-10 sec interval, leading to the large and long-period ground oscillations that characterized the ground response thereafter. This softened site response indicates an r_u of at least 0.5 by the 10 sec time mark. The primary sequence of strong ground motions was complete by the 12 sec time mark with r_u apparently still much less than 1.0, as indicated by the higher frequency motions superimposed on the longer period oscillations in the acceleration record. Pore pressures apparently continued to rise after the cessation of strong ground motions as indicated by the continued lengthening of the characteristic period of oscillations and the decay of the higher frequency motions. By the 60 sec time mark, the site was oscillating in near steady state with little high-frequency motion evident in the acceleration traces. This response indicates that the site was fully liquefied ($r_u = 1.0$) at that juncture. As indicated, a rather slow attenuation of the amplitudes of the ground oscillations, oscillation and a liquefied condition must have continued well beyond the end of the record at the 100 sec time mark.

Comparison of Response Spectra

Response spectra calculated from the full (100 sec) acceleration record from the NJ site are plotted on Figure 7.7. These spectra contain short period peaks (periods between 0.1 sec and 0.6 sec) which are typical of spectra from earthquake shaking of stiff granular sites without sediment softening. These spectra also contain broad peaks at periods greater than 1 sec which are not typical of spectra from stiff sites. By examining development of spectra for various time increments, as we have done for other sites, relationships between peak development and soil softening can be deciphered.

Spectra for the first 5 sec of the acceleration record (up to the 5 sec time mark) are plotted in Figure 7.8 along with the full spectra for reference. The 5 sec time mark passed before pore water pressures began to rise, as noted above. By 5 sec, sufficient short period energy had propagated through the site to fill in all of the peaks in the full spectra for periods less than 0.3 sec. Conversely, little energy for spectral periods greater than 1.0 sec had propagated through the site.

Spectra from the first 8 sec of record, after pore pressure began to rise but prior to the arrival of the peak acceleration, are plotted on Figure 7.9. These spectra change little from the 5 sec spectra, indicating that no new and stronger ground motion pulses propagated through the site between the 5 sec and 8 sec time marks.

Spectra from the first 10 sec of record, after the peak acceleration pulse and the time at which r_u had risen to about 0.5, are plotted in Figure 7.10. Sufficient energy propagated through the site in the 2 sec interval (between 8 sec and 10sec) to fill in the final spectra for periods less than 1.0 sec in the NS spectra and 1.7 sec in the EW spectra. Spectral values also rose greatly during this time interval for periods greater than 1.0 and

1.7, respectively. This increase filling indicates that most of the seismic energy for periods greater than about 0.3 sec passed through the site during this 2 sec interval. By the 10 sec time mark, ground oscillation had developed at the site and the only increased spectral values generated after that time were at periods greater than 1.0 sec.

Response spectra for the first 12 sec of record are plotted on Figure 7.11. By that juncture, the final spectral values were reached except for some gaps at very long periods (>4.0 sec). Thus, by the end of the strong motion sequence, at 12 sec, the response spectra were essentially complete for both short and long period motions. Although long period oscillation continued at the site for at least another 90 sec, the motions associated with these oscillations were not great enough to generate increased spectral values, except for periods greater than 4.0 sec. These gaps eventually filled after 40 sec of shaking. Thus, the long sequence of oscillations after 12 sec of record caused no significant increase in spectral response. This long sequence of motions, however, added greatly to the duration of ground shaking and likely to the damage induced.

This analysis of times at which motions propagated through the site generating various peaks in the response spectra indicates that the short period peaks (<0.7 sec) developed before the 8.0 sec time mark, while the site was relatively stiff. The broader peaks at periods greater than 0.7 sec filled in as the site softened, leading to longer period response. Without the softening induced by increased pore water pressures and liquefaction, the spectra peaks at periods greater than 0.7 sec would likely have been greatly reduced if developed at all.

Figure 7.1. Map of Shinano River area Niigata, Japan, showing Kawagishi-Cho where strong-motion instrument was located (After Hamada, et al., 1986)

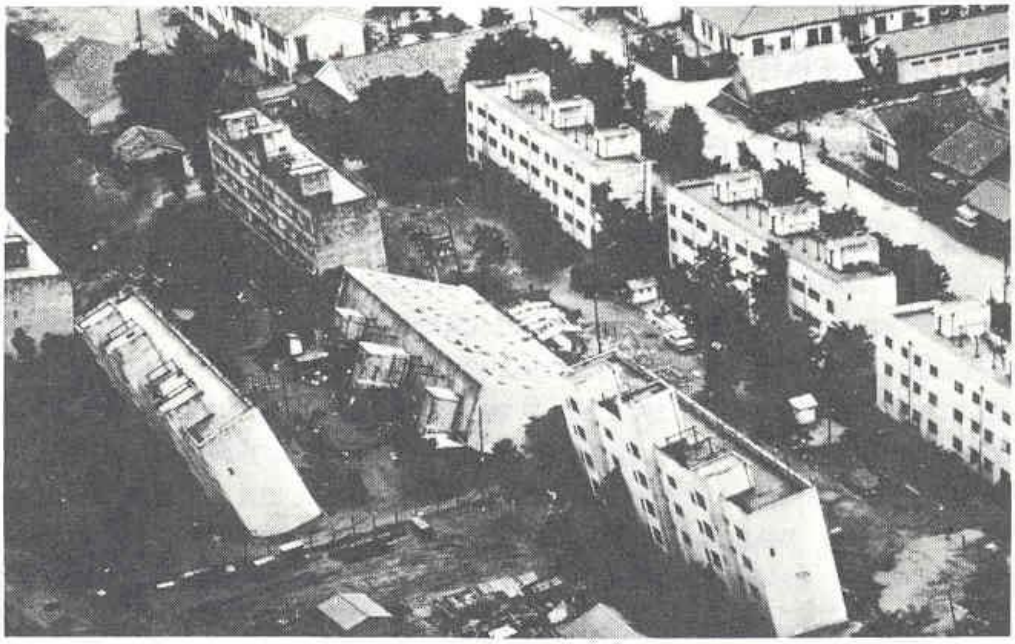

Figure 7.2. Kawagishi-Cho apartment complex Niigata, Japan, after 1964 Niigata, Japan earthquake (M=7.5)

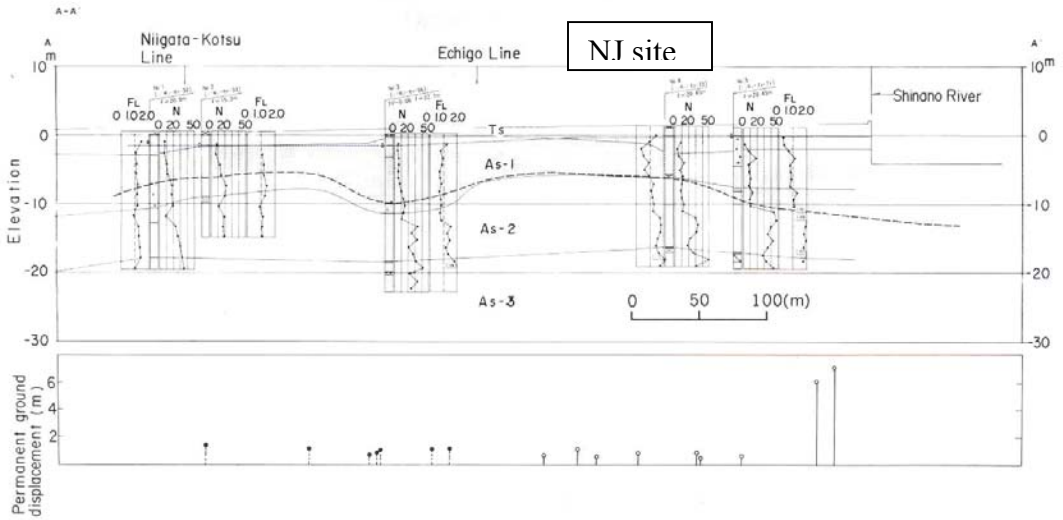

(a) Section A–A′

Figure 7.3. Site cross section showing sediment layers at Kawagishi-Cho apartment complex (NJ site) (modified from Hamada, et al., 1986)

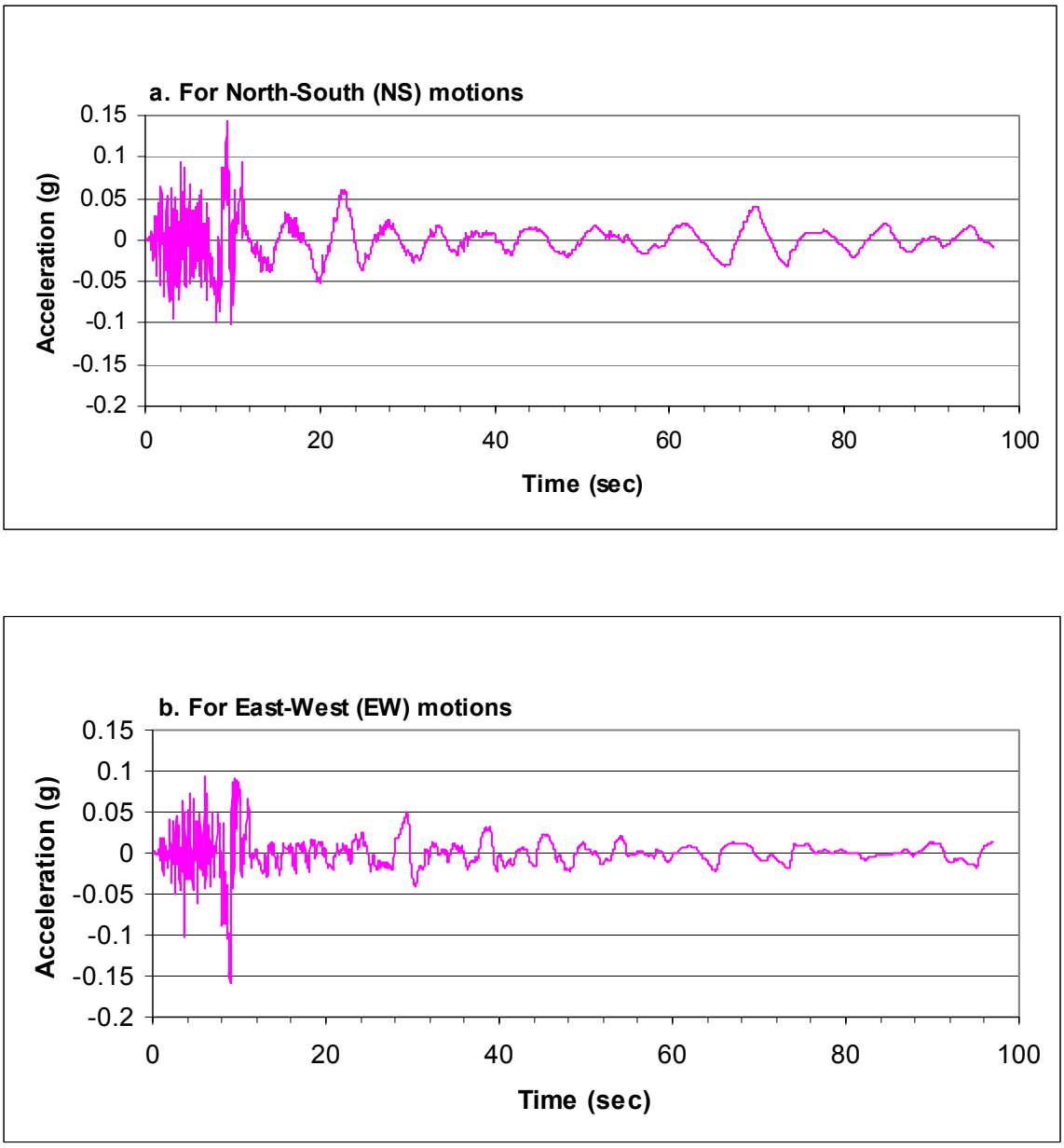

Figure 7.4. Actual acceleration time histories for NJ site during 1964 Niigata, Japan earthquake (M=7.5)

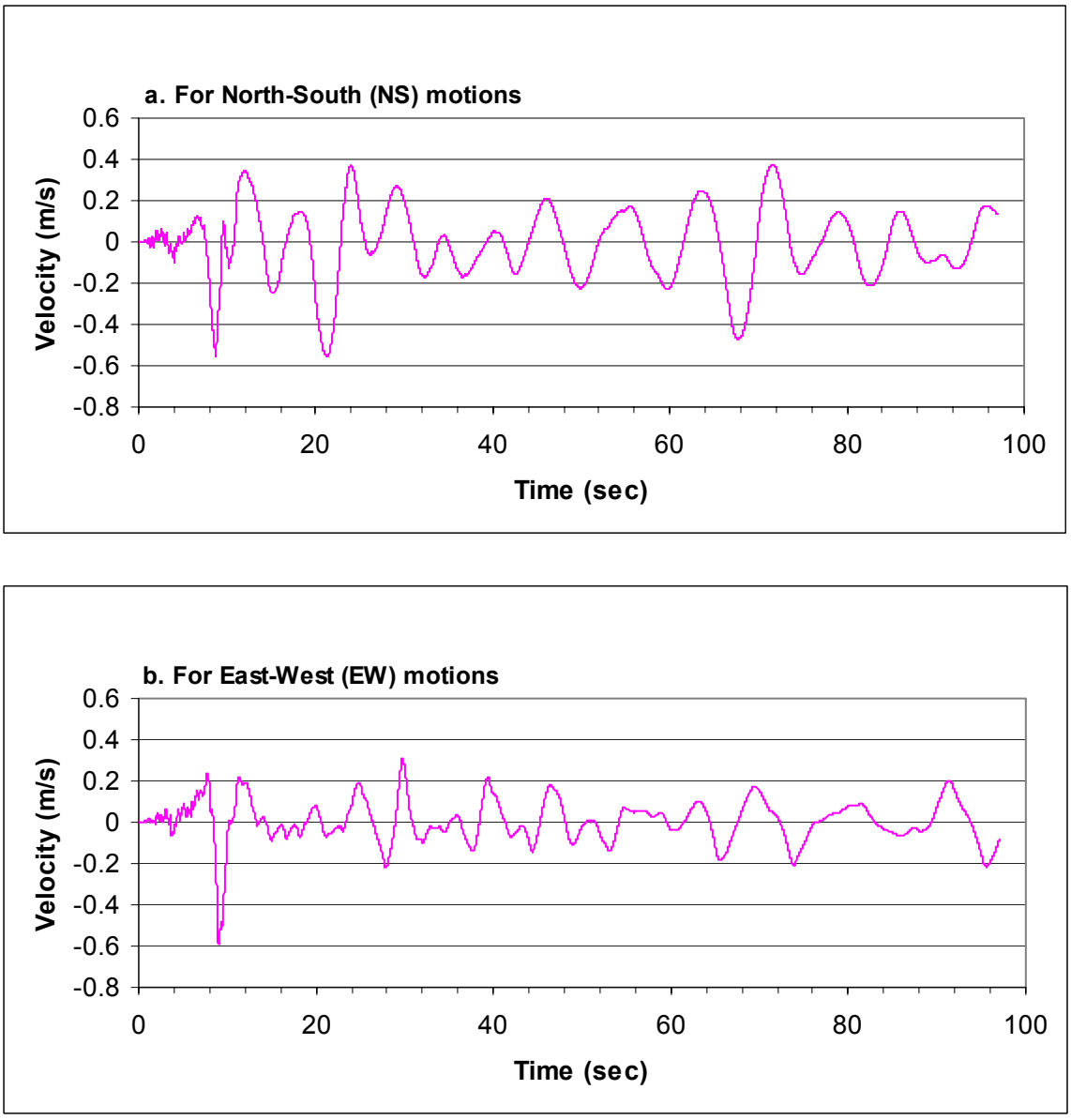

Figure 7.5. Actual velocity time histories for NJ site during 1964 Niigata, Japan earthquake (M=7.5)

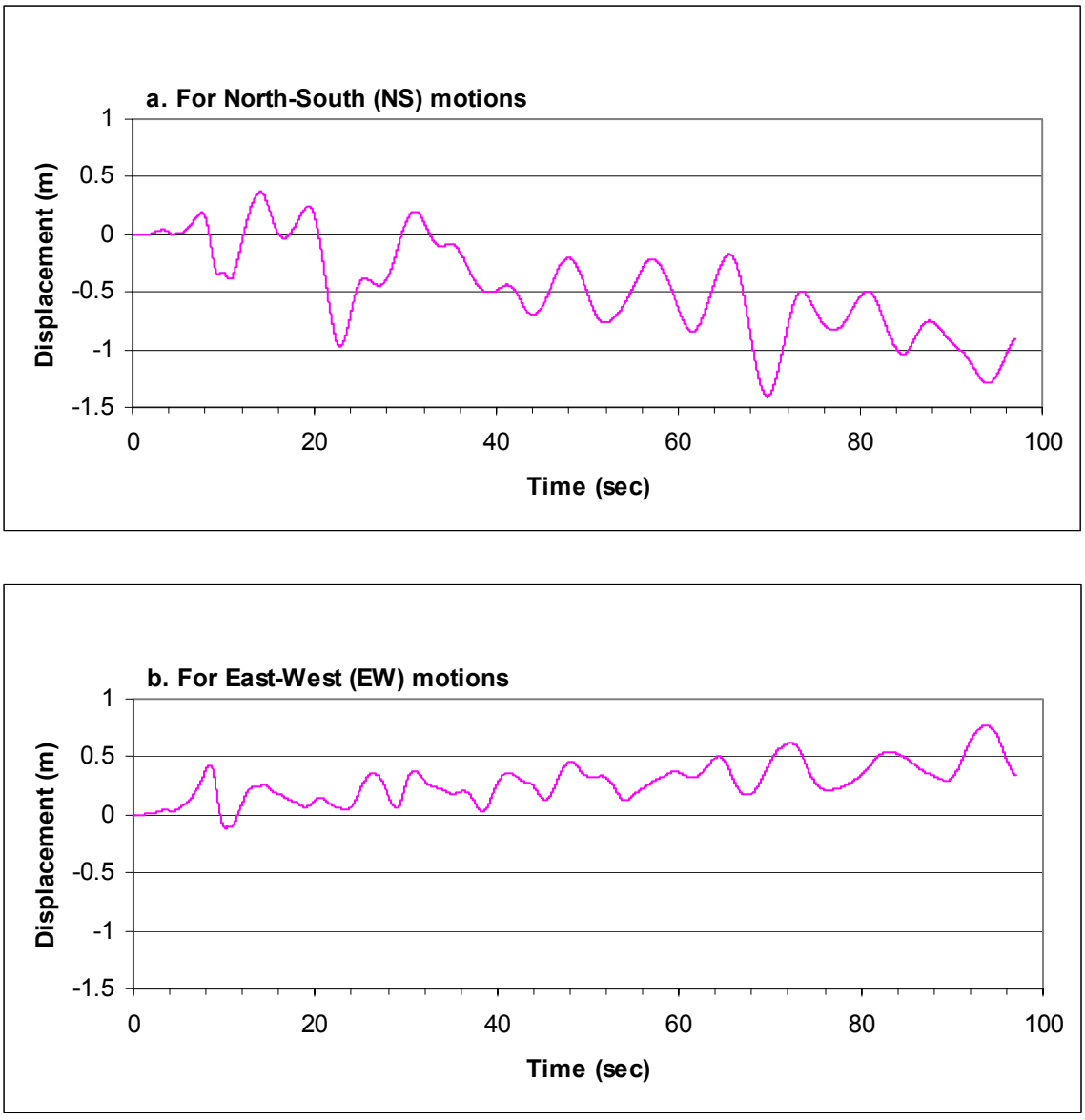

Figure 7.6. Actual displacement time histories for NJ site during 1964 Niigata, Japan earthquake (M=7.5)

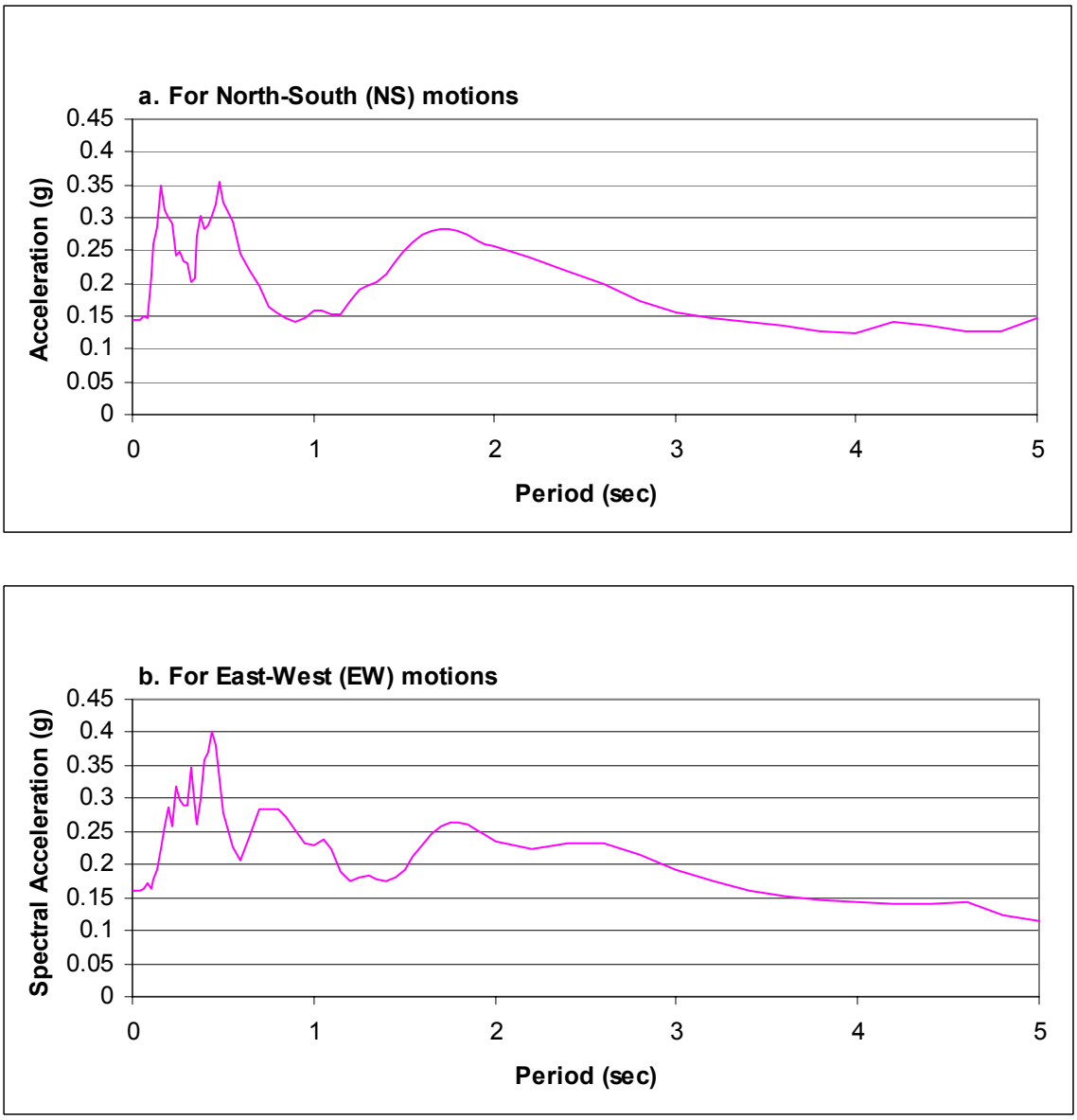

Figure 7.7. Actual response spectra for NJ site during 1964 Niigata, Japan earthquake (M=7.5)

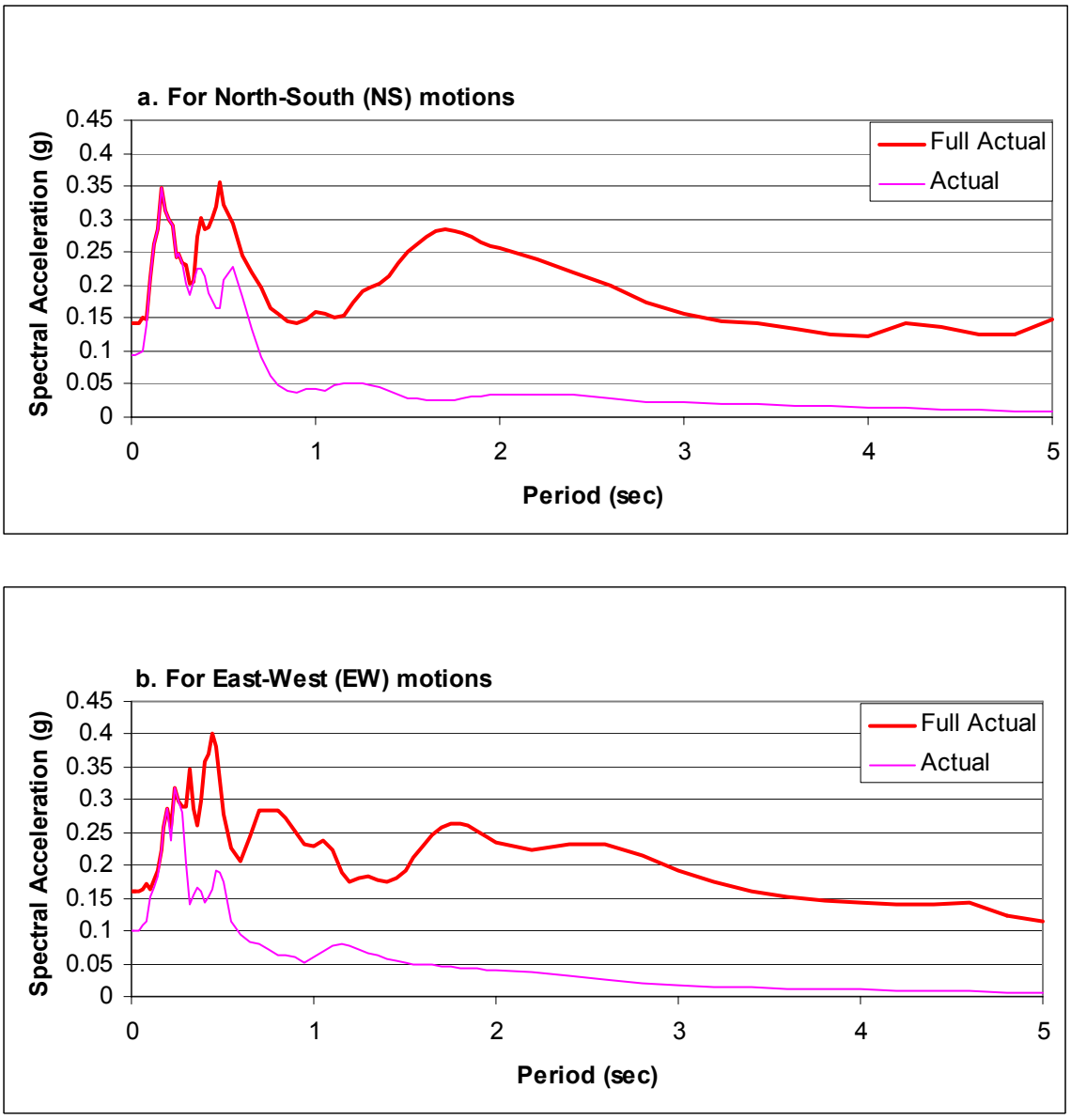

Figure 7.8. Actual response spectra calculated from the first 5 sec of acceleration record for NJ site during 1964 Niigata, Japan earthquake (M=7.5)

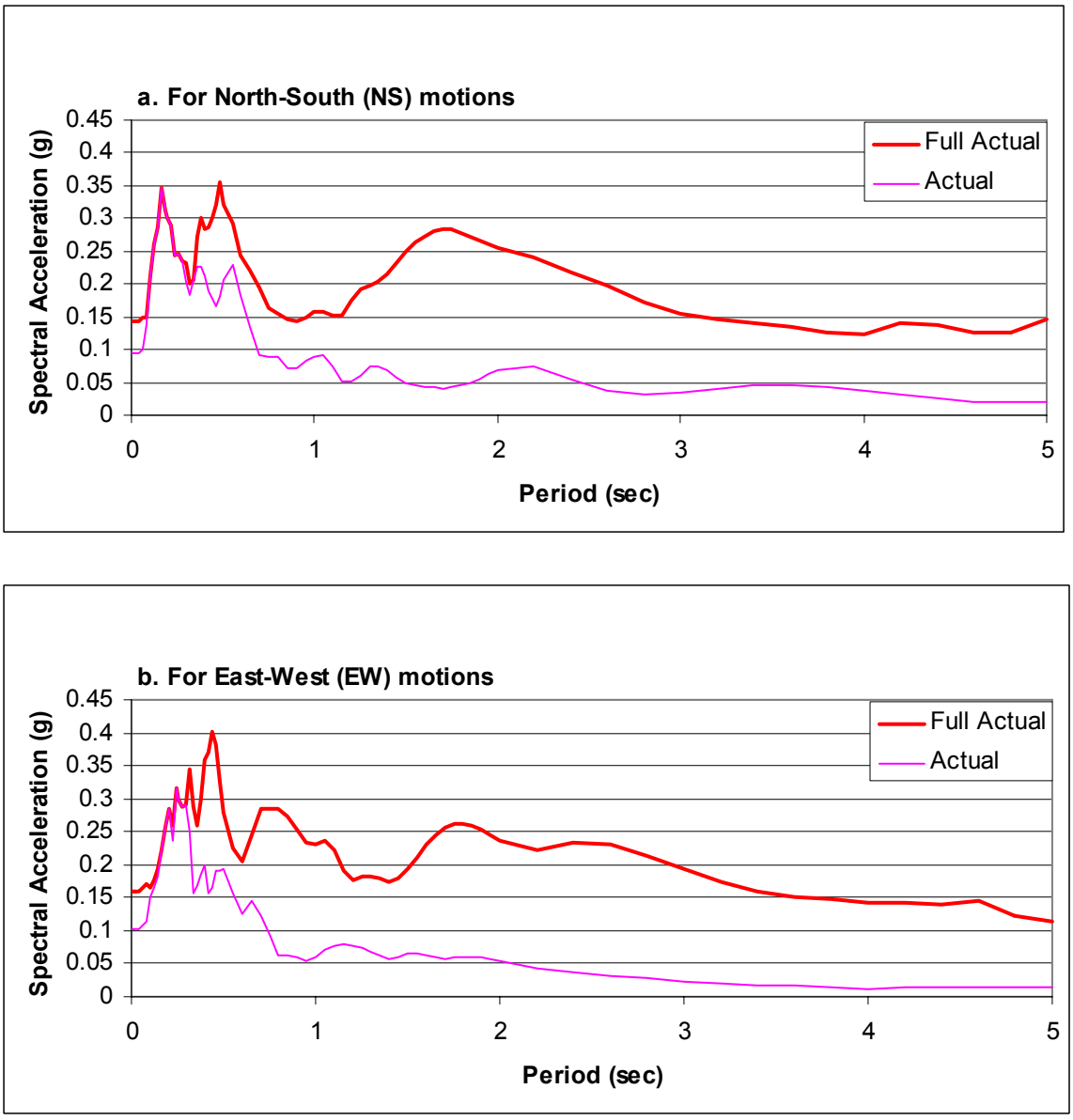

Figure 7.9. Actual response spectra calculated from the first 8 sec of acceleration record for NJ site during 1964 Niigata, Japan earthquake (M=7.5)

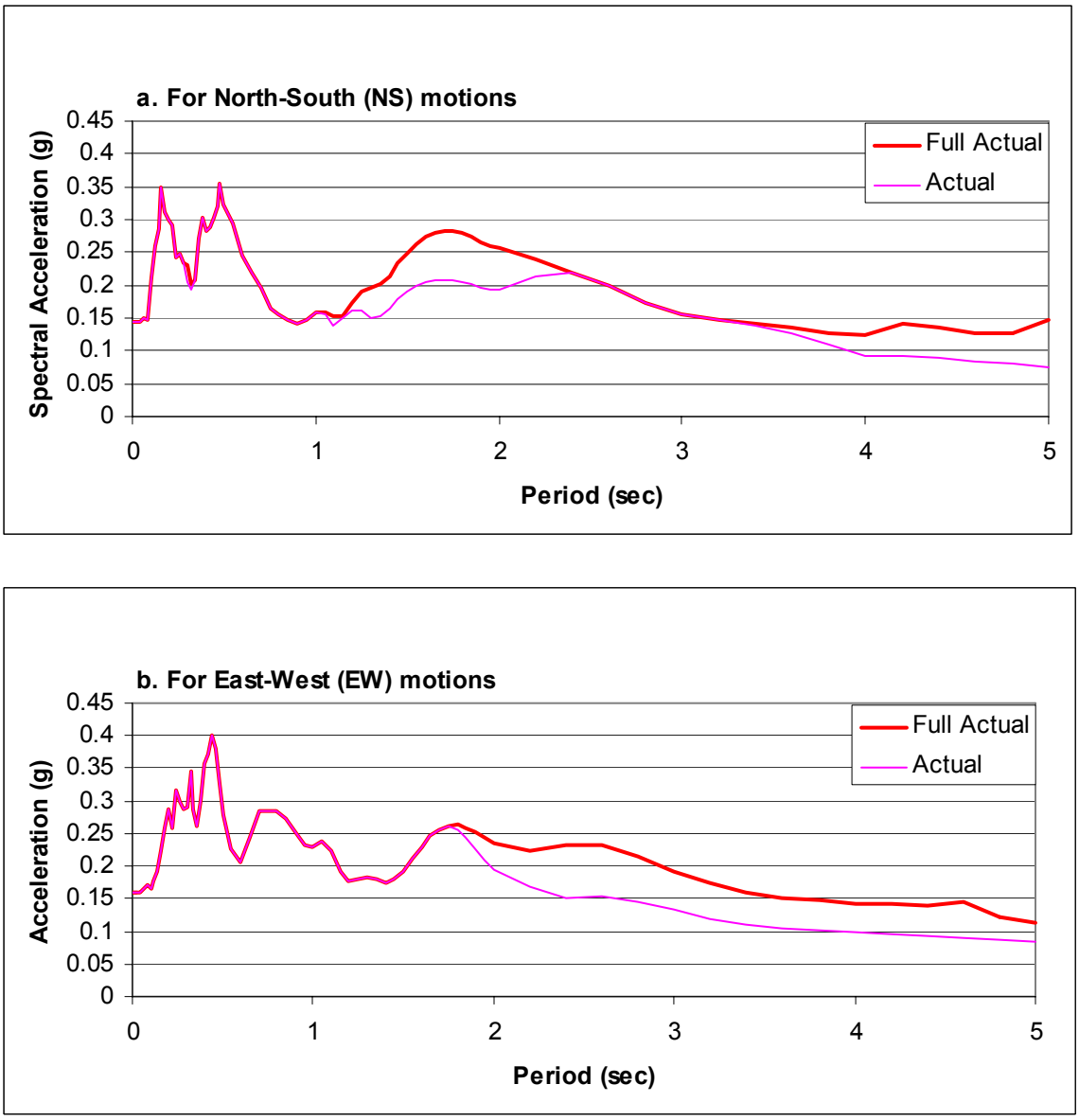

Figure 7.10. Actual response spectra calculated from the first 10 sec of acceleration record for NJ site during 1964 Niigata, Japan earthquake (M=7.5)

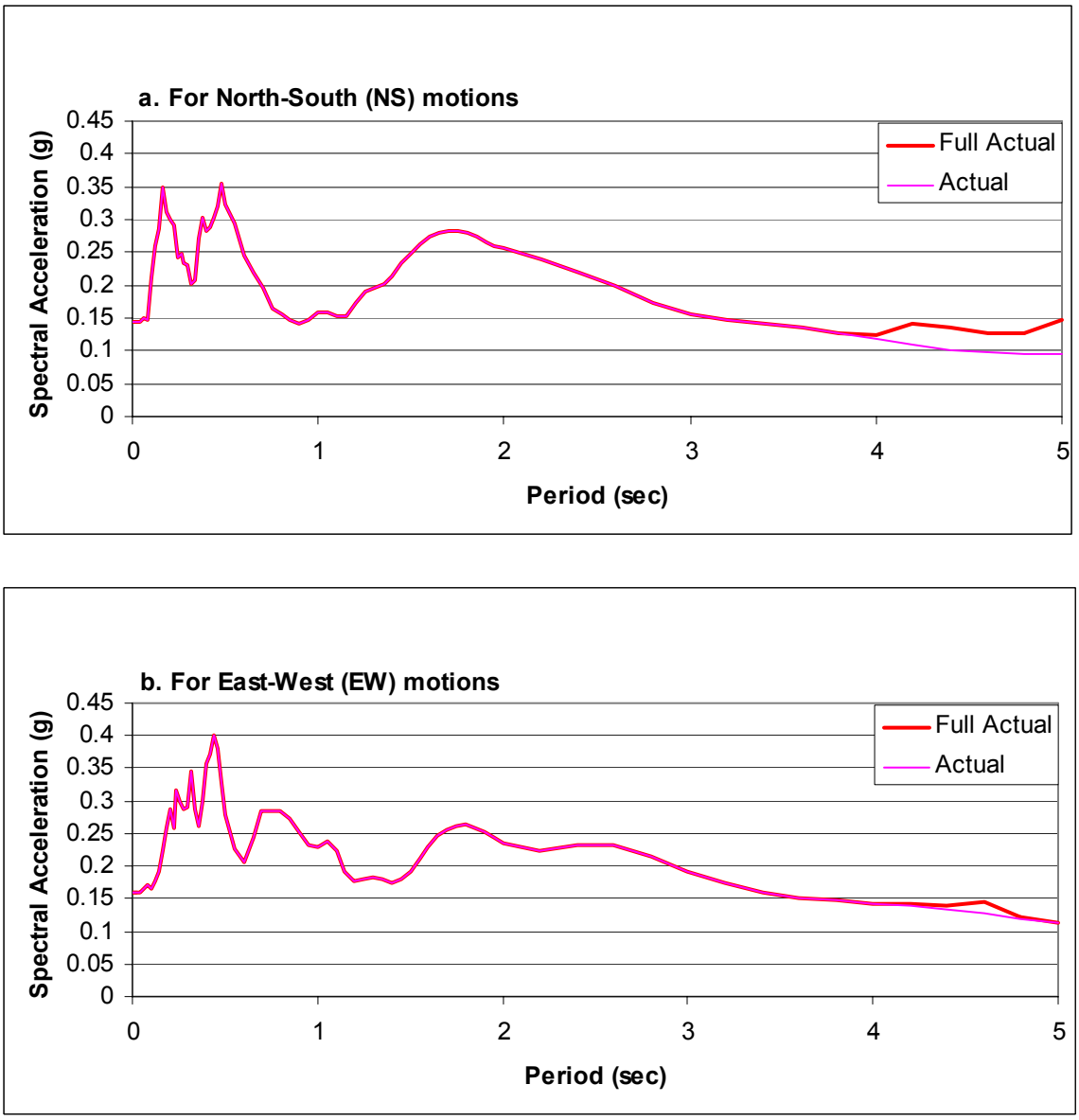

Figure 7.11. Actual response spectra calculated from the first 12 sec of acceleration record for NJ site during 1964 Niigata, Japan earthquake (M=7.5)

SECTION 8

Influence of Liquefaction on Design Response Spectra

In the previous sections, the influence of liquefaction on ground response has been analyzed for five instrumented sites by comparing actual and predicted motions and spectra. The predicted motions and spectra are those that should have occurred in the absence of soil softening and liquefaction. The following sections (1) summarize principal findings from these analyses, (2) compare response spectra that were influenced by soil softening and liquefaction with design response spectra, (3) evaluate the need to adjust design response spectra to account for the influence of liquefaction, and (4) consider other effects that need to be addressed in bridge design such as increased ground displacement due to soil softening.

Influence of Liquefaction on Short-Period Motions (Periods Less than about 0.7 Sec)

At sites where increased pore water pressures and soil softening occurred early in the sequence of ground motions that propagated through the site, comparisons between actual and predicted response spectra indicate that soil softening caused considerable reduction of short period (< 0.7 sec) spectral accelerations. These reductions occurred at sites with both moderately intense (WLA) and very intense (PIDA) ground motions.

WLA Site

At WLA, where predicted peak horizontal ground accelerations (PHA) of 0.29 g and 0.28 g in the NS and EW direction, respectively, during the 1987 Superstition Hills earthquake (Figure 3.10), actual spectral accelerations are less than predicted spectral accelerations at nearly all periods less than 0.7 sec (Figure 3.13). Only at periods

between 0.1 and 0.2 sec are actual spectral accelerations greater than the predicted values. This inconsistency was more likely due to an anomaly in the calculation procedure than to short-period amplification of motions as a consequence of soil softening. As noted in Section 2, the calculation procedure is less reliable for very short period motions than at longer periods.

The most noticeable difference between the predicted and actual spectra at WLA is the absence of spectral peaks of 1.2 to 1.3 g in the actual spectra for periods between 0.2 to 0.4 sec (Figure 3.13). Actual spectral values are muted in this period range compared to the predicted spectral values and vary from 0.4 g and 0.8 g. For the WLA records, soil softening had the effect of reducing short-period (< 0.7 sec) spectral accelerations with major reductions in peak spectral values, as noted above.

PIDA Site

As at WLA, soil softening at the PIDA site led to smaller actual than predicted spectral accelerations for periods less than 1.0 sec. Major predicted spectral peaks of 2.0 g and 1.5 g in the NS and EW directions, respectively, at periods between 0.2 sec and 0.4 sec are absent or muted in the actual spectra (Figure 4.6). Actual spectral values for periods between 0.2 sec and 0.4 sec are 0.4 g to 0.5 g, less than one-third of the predicted values. In summary, soil softening at PIDA had a beneficial structural effect of reducing short period motions (<1.0 sec).

TI and ANAS Sites

If significant pore pressure generation and consequent soil softening does not occur early in the ground motion sequence, there likely will be little effect on short-period spectral accelerations. The reason for this lack of influence is that intense short

period motions commonly propagate through soil sites before the arrival of the peak ground acceleration. Thus, softening would not influence these early arriving motions and consequently would have little effect on short-period parts of the response spectrum.

This lack of influence on short-period spectral acceleration is demonstrated in the EW spectra calculated for both the TI and ANAS sites (Figures 5.7 and 6.5). The motions at these sites during the 1989 Loma Prieta earthquake were only moderately intense, with predicted PHA of 0.20 g to 0.25 g. No soil softening occurred at either the TI or ANAS sites before the arrival of the peak ground acceleration. Because the greatest intensities of short period motions propagated through the site with or before the arrival of the peak acceleration, soil softening had little influence on these motions. This lack of influence is demonstrated by the nearly matching peaks in the predicted and actual spectra between periods of 0.5 sec and 0.8 sec in both spectra. Thus, soil softening had little influence on short period response at these sites.

Influence of Liquefaction on Long-Period Motions (Periods Greater than about 0.7 Sec)

For the five sites investigated, soil softening had considerable influence on long-period spectral accelerations (periods greater than about 0.7 sec). The influences for each site are discussed below.

WLA Site

At the WLA site, actual spectral accelerations are much greater than the predicted values for all periods greater than 0.7 sec (Figure 3.13). This enhancement of the actual spectra compared to the predicted spectra was largely due to persistent ground

oscillations that developed after the arrival of the peak acceleration as noted in Section 3. Because the amplitudes of ground oscillations were greater in the NS than in the EW direction, NS spectral values were greater than EW spectral values. Thus for the WLA site, spectral values that would be required for the design of long period (>0.7 sec) structures are greater due to soil softening than those that might have been required for an unsoftened site.

PIDA Site

At the PIDA site, actual spectral accelerations only exceeded predicted spectral accelerations over a narrow range of periods (between 1.0 sec and 1.5 sec) in both the NS and EW directions (Figure 4.6). For periods greater than 1.5 sec, predicted spectral accelerations are somewhat greater or nearly the same as actual accelerations. The lack of development of persistent ground oscillations at PIDA apparently lead to the relatively smaller spectral values at these long periods compared to the WLA site. The slight increases of spectral values in the 1.0 sec to 1.5 sec period range, apparently was due to shift of energy from shorter period (<1.0 sec) motions to longer period (>1.0sec) motions. Based on these comparisons, little difference would be required in selecting spectral values for design of long period structures (>1.0 sec) for either softened or unsoftened site conditions at the PIDA site.

TI and ANAS Sites

At the TI and ANAS sites, with moderately low PHA (approximately 0.2 g) during the Loma Prieta earthquake, the actual spectral accelerations were greater than the predicted spectral accelerations in the 1.5 sec to 4.0 sec range in the NS direction (Figures 5.7 and 6.5). As at WLA, these greater actual spectral values were largely due

to the development of ground oscillations that persisted for at least 30 sec after the cessation of strong ground shaking. Thus, for design applications, greater spectral values would be required for the softened site than the unsoftened site for structures with fundamental periods greater than 1.5 sec.

As noted in sections 5 and 6, predicted and actual response spectra calculated for the NS directions at TI and ANAS are too divergent to be useful for deducing influences of soil softening on ground response. Apparently this divergence was due to major differences in the seismic energy content of motions reaching YBI in the NS direction compared to that reaching TI and ANAS in the NS direction.

NJ Site

Because no reference accelerometers were in place below the liquefiable layer at NJ or on bedrock outcrops in the vicinity of NJ, no reference records are available from which predicted spectra could be developed. The actual acceleration, velocity and displacement time-histories plotted on Figures 7.4 - 7.7, however, clearly show that a long sequence of near-harmonic ground oscillations developed at the NJ site following an initial sequence of strong short-period accelerations. These time histories indicate that amplitudes of the induced ground oscillations were greater in the NS direction than in the EW direction. As a consequence of these oscillations, broad peaks developed in the NS and EW response spectra between periods of 1.0 sec and 3.0 sec with maximum spectral values of about 0.28 g and 0.26 g respectively. Based on comparisons of response spectra with other sites where ground motion developed, spectral values at the NJ site appear to have been greatly enhanced due to soil softening for periods greater than about 1.0 sec.

Comparison of Calculated Spectra with LRFD Bridge Code Seismic Provisions

Seismic load factors for application in bridge design are specified in Section 3, Loads and Load Factors, of the LRFD Bridge Code (AASHTO, 1998). The general provisions of the code call for the calculation of a seismic response coefficient, C_{sm}, which is applied as a lateral force coefficient for calculation of lateral seismic in bridge design. C_{sm} is calculated via the following equation (LRFD Equation 3.10.6.1-1):

$$C_{sm} = 1.2AS/T_m^{2/3} \# 2.5\ A \qquad (1)$$

Where:

T_m = period of vibration for the m^{th} mode

A = acceleration coefficient specified in Article 3.10.2

S = site coefficient specified in Article 3.10.3 and Table 8.1

The following note of exception with respect to Equation 1 is given in Section 3.10.6.2 of the LRFD code: "For bridges on soil profiles III or IV and in areas where the coefficient "A" is not less than 0.30, C_{sm} need not exceed 2.0 A."

A normalized form of the equation is generated by dividing both sides of the equation by the factor A:

$$C_{sm(normalized)} = 1.2S/T_m^{2/3} \# 2.5 \qquad (2)$$

This form of the equation is plotted in Figure 8.1 to provide normalized C_{sm} values for use in design. Figure 8.1 (adapted from Figure C3.10.6.1-1 of the LRFD code) contains normalized C_{sm} curves for Code Soil Profile Types (CSPT) III and IV. These softer soil types (CSPT III and IV), by definition, are the only soil profile types that could incorporate subsurface layers of liquefiable sediment.

Comparisons of Spectra with LRFD Code Coefficients

Three procedures were applied in this study to compare LRFD code coefficients to response spectra calculated from instrumental records at the five liquefaction sites analyzed. First, both the predicted and actual response spectra developed in Sections 3 through 6 are compared with code coefficients that would be required for bridge design in highly seismic areas such as the coastal parts of California. An LRFD acceleration coefficient, A, of 0.60 g, is required in such seismic areas, which include the localities of the WLA, TI, and ANAS sites. If the Wasatch front area of Utah were to use an acceleration coefficient with 2% probability of exceedance in 50 years, rather than a 10% probability of exceedance as used in the maps in LRFD code, the acceleration coefficient would also be about 0.60 g. The International Building Code (IBC), required for design of buildings in Utah, requires use of ground motions with 2 percent probability of exceedance in 50 years, which equates to an acceleration coefficient of about 0.60 along the Wasatch Front.

Second, the response spectra are compared with an LRFD acceleration coefficient of 0.30 g, the LRFD coefficient required for sites that are along the Wasatch Front (LRFD Code Figure 3.10.2-1). The acceleration coefficients in the LRFD code correspond approximately to accelerations with 10 percent probability of being exceeded in 50 years.

Third, the predicted PHA for each component of motion at each site was substituted for the coefficient A in Equation 1. This substitution provides a test of the conservativeness of the bridge coefficients for sites where the PHA is equal to the

acceleration coefficient, A. The Predicted PHA was used in this comparison, rather than the actual PHA, because the predicted PHA should have occurred at the sites in the absence of soil softening and liquefaction. The actual PHA, which is the measured PHA at ground surface, was not used because in most instances the actual PHA is usually less than the predicted PHA due to soil softening.

Comparison of Code Coefficients and Calculated Response Spectra for WLA

Predicted and actual response spectra calculated for the WLA site from the 1987 Superstition Hills strong motion records are plotted on Figure 8.2 along with LRFD code coefficients for A of 0.60 g, 0.30 g and predicted PHA which are 0.31 g and 0.26 g (for NS and EW directions respectively). These comparative curves indicate that the calculated spectra for both NS and EW directions are very conservatively enveloped by code coefficients based on an A of 0.60 g. This conservative result was expected because the PHA for the site was much less than 0.60 g. The code coefficients for A = 0.30 g also conservatively envelope the actual response spectra for both the NS and EW directions. A predominant peak in the predicted spectra, which was muted in the actual spectra due to soil softening, exceeds the code coefficients, however, for periods between 0.3 and 0.5 sec. Reasons for this predicted spectral peak exceeding design coefficients in this instance, and any hazards that exceedence might cause, are beyond the scope of this research project, and are not discussed further here.

The code coefficients based on predicted PHA values for WLA for CSPT IV exceed the actual response spectral values at all periods for both the NS and EW spectra. Similarly, the CSPT III code coefficients exceed the actual spectra at all periods except

for a narrow segment between periods between 2.2 sec and 2.3 sec in the NS direction (Figure 8.2a). This near complete enveloping of the actual response spectra is true even though the actual spectra are much greater than the predicted spectra at periods greater than 1.0 sec. The LFRD curves for PHA in the NS direction (Figure 8.2a) were calculated using a constant of 2.5 in Equation 1, even though the PHA of 0.31 g slightly exceeds the limit of 0.30 g, which should require a constant of 2.0. The constant of 2.5 was used because 0.31 g only slightly exceeds the limit of 0.30 g and for consistency with the east-west curves plotted on figure 8.2.b. Use of a constant of 2.0 would lead to a flat cap on the PHA curve at an ordinate of 0.62 g. The actual response spectrum would exceed this cap between periods of 0.3 and 0.5 sec, leading to possibly unconservative design in this period range.

The peaks in the predicted spectra between periods of 0.3 sec and 0.5 sec in both the NS and EW components of motion greatly exceed the code coefficients based on PHA. As noted previously, soil softening served to greatly reduce those peaks so that these peaks are muted or do not appear in the actual spectra. Thus, for this site and earthquake, soil softening had a significant beneficial effect of reducing short-period spectral accelerations to values that generally meet LRFD code requirements.

Comparisons of Code Coefficients and Response Spectra for PIDA

Even though the PIDA site is in Japan, we made comparisons of spectra from that site with LRFD coefficients as though the site were in the US. Response spectra calculated for the PIDA site for the 1995 Kobe earthquake are plotted on Figure 8.3 along with the LRFD code coefficients, A, of 0.60 g, 0.30 g and the predicted PHA. The

predicted PHA for this site are 0.63 g and 0.56 g in the NS and EW directions respectively. Thus, this site provides a test of the code coefficients for a site that was heavily shaken and liquefied by a strong earthquake.

For A = 0.60, the code coefficients plotted in Figure 8.3 very conservatively bound the actual NS and EW spectra for site periods less than 0.9 sec. For periods between 0.9 sec and 2.0 sec, the actual spectra in the NS direction slightly exceed the code coefficients for both CSPT III and IV, indicating that the code coefficients are slightly unconservative for this part of the spectrum. For periods greater than 2.0 sec, code coefficients again envelope the actual response spectra. The general bounding of the actual curve indicates that code coefficients, based on an A of 0.60 g, are generally conservative for this site which was subjected to very strong motions and soil softening and liquefaction.

As at the WLA site, peaks in the predicted spectra between periods of 0.3 sec and 0.5 sec in both the NS and EW components of motion greatly exceed the code coefficients for an A of 0.60 g. Because of soil softening, short-period predicted spectral values were greatly reduced so that these peaks are muted or do not appear in the actual spectra. Thus, for this site and earthquake, soil softening had a significant beneficial effect of reducing short-period spectral accelerations to values that meet LRFD code requirements for an A of 0.60 g.

The code coefficients an A of 0.30 also adequately bound the actual spectra for periods less than 0.9 sec. Again, soil softening reduced predicted spectral values in this period range so that the actual spectral values are conservatively enveloped by the code coefficients. For periods greater than 0.9 sec, the code coefficients for A = 0.30 g

generally lie well below the actual spectra, indicating that these code coefficients are unconservative and inadequate for long-period structures at this site.

The code coefficients calculated for predicted PHA values of 0.63 g and 0.56 g in the NS and EW directions, respectively, are only slightly greater than those noted above for an A-value of 0.60 g. The PHA-based coefficients for CSPT IV exceed the actual response spectra for the PIDA site for all periods for both the NS and EW directions. Similarly, the CSPT III code coefficients exceed the actual spectra at all periods except for periods between 1.2 sec and 1.5 sec in the NS direction. This near complete enveloping of the normalized actual response spectra is true even though spectral values 0.9 to 2.0 sec range appear to have been enhanced by soil softening.

Comparisons of Code Coefficients and Response Spectra for TI and ANAS

Predicted and actual response spectra calculated for the TI and ANAS sites for the 1989 Loma Prieta earthquake are plotted on Figure 8.4 and 8.5, respectively, along with the LRFD code coefficients. As noted previously, soil softening and liquefaction developed late in the sequence of ground motions that passed through these sites. The short period (< 0.9 sec) response spectra showed little affected by soil softening during the 1989 Loma Prieta earthquake. Because soil softening and liquefaction induced ground oscillations persisted after the cessation of strong ground accelerations at these sites, enhancement of spectral accelerations occurred at longer periods (> 2.0 sec) at both of these sites.

As noted in Section 5 and 6, predicted spectra in the NS direction for both TI and ANAS, determined from the YBI NS strong motion accelerogram, are very dissimilar to

actual NS spectra at these two sites. This large variance was apparent due to an anomaly in NS component of motion recorded at the YBI site. For this reason, no comparisons are made here for the NS component of motion for these sites and all of the discussion below applies only to EW motions.

Code coefficients based on an A of 0.60 g very conservatively envelope both the predicted and actual response spectra for both the TI and ANAS sites for either CSPT III or IV site criteria. This conservatism would be expected because of the moderate intensity of the ground motions that shook these sites during the 1989 Loma Prieta earthquake.

Code coefficients based on an A of 0.30 g also envelope the response spectra for both of these sites except for the spectral peak in the ANAS actual and predicted spectra between periods of 0.6 sec and 0.8 sec. Again, those spectral peaks were little affected by soil softening. Had the motions been more intense, soil softening would likely have occurred earlier in the ground motion sequence at these sites and the influence of softening might have reduced the short-period motions, as occurred at other sites studied in this investigation.

The code coefficients based on predicted PHA from the TI and ANAS sites do not envelope the strong spectral peaks in the actual and predicted response spectra between 0.6 and 0.8 sec. Other than this omission, code coefficients for CSPT IV envelope actual response spectra at all other periods. Similarly, the CSPT III code coefficients envelope the actual spectra at all periods greater than 0.8 sec except for a segment in the TI actual spectra between 1.3 sec and 2.3 sec. This near complete enveloping of the normalized actual response occurred even though the actual spectra are much greater than the

predicted spectra at all periods greater than about 1.5 sec due to soil softening.

Comparisons of Code Coefficients and Actual Spectra for NJ

Because there were no instrumented downhole or bedrock sites in Niigata, Japan during the 1964 earthquake, predicted ground motions and response spectra in the absence of soil softening could not be calculated for the NJ site. Thus, only the actual spectra are compared with LRFD code coefficients for the NJ site. As plotted on Figure 8.6, LRFD code coefficients based on A-values of 0.60 g and 0.30 g for CSPT III and IV site criteria conservatively bound the actual spectra at all periods. This conservatism might be expected because the actual (measured) PHA at this site was only 0.16 g much smaller than the A-values of 0.6 g and 0.3 g used to generate the code coefficients for this plot.

The code coefficients calculated for A-values equal to the actual PHA of 0.15 g and 0.16 g in the NS and EW directions respectively and for CSPT IV site criteria conservatively bound the actual spectra for this site and earthquake for periods less than 1.5 sec. For CSPT III criteria, the code coefficients conservatively bound the actual spectra for all periods less than 1.4 sec. For periods greater than 1.5 sec, code coefficients for CSPT IV site criteria very nearly match the actual spectra in both the NS and EW directions. For periods greater than 1.4 sec, code coefficients for the CSPT III site criteria uniformly lie below calculated response spectra in both the NS and ES directions. However, our recommendation is that this comparison should have been based on predicted rather than actual PHA.

Had predicted PHA values been substituted for A in equation 8.1 the calculated

code coefficients for PHA substitution would likely have plotted much higher on Figure 8.6. That enhancement would be due to the fact that predicted PHA, which are estimated for unsoftened site conditions, are generally much larger than the actual PHA at sites that significantly soften and liquefy. Had the predicted PHA been 33 percent greater than the actual PHA, approximately 0.20 g to 0.22 g at the NJ site, then coefficients for the CSPT IV site criteria would have uniformly enveloped the actual response spectra, and the coefficients for the CSPT III site criteria would have been nearly congruent with the actual spectra for periods greater than 1.4 sec.

Findings, Recommendations and Cautions

General Findings

The comparisons of LRFD code coefficients and actual response spectra presented in Figures 8.2 through 8.6 indicate that an acceleration coefficient, A, of 0.6 g with CSPT IV site criteria fully envelope the actual response spectra for all of the instrumented liquefaction sites investigated herein. Code coefficients for an A of 0.6 g and CSPT III site criteria also fully envelope all of the actual spectra, except for long period motions between 1.1 sec and 1.4 sec in the NS actual spectra calculated for PIDA. The input motions at PIDA were very intense with predicted PHA of 0.63 g and 0.56 g for the NS and EW records respectively. These comparisons lead to a firm finding that application acceleration coefficients of 0.60 g with either CSPT III or IV site criteria should conservatively envelope response spectra for nearly all sites susceptible to soil softening or liquefaction, even for very intense seismic ground motions.

Because soil softening generally leads to reduction of short-period spectral

accelerations compared to the unsoftened site response, LRFD code coefficients based on an A of 0.3 g conservatively envelope actual spectral accelerations for short period motions (<0.7 sec) for all of the five sites investigated, except TI and ANAS, where soil softening did not occur until most of the short-period energy had passed through the site. Even the actual response spectra for PIDA, where input ground motions were very intense, are conservatively enveloped up to periods of about 1.5 sec by code coefficients based on an A-value of 0.30 g. Thus, code coefficients based on an A-value of 0.30 g are likely to be conservative at liquefiable sites where soil softening occurs early in the sequence of strong ground motions.

Where the predicted PHA were substituted for the acceleration coefficient, A, the code coefficients conservatively enveloped actual response spectra at short periods (< 0.7 sec) for all sites except TI and ANAS where soil softening did not occur until late in the sequence of strong ground motions as noted above. Even at longer periods (>0.7 sec), the code coefficients for CSPT IV conservatively enveloped the response spectra for all of the sites, including NJ if the predicted PHA were about 33 percent larger than the actual PHA. Thus, a viable alternative to selecting an A-value from the LRFD acceleration coefficient maps for liquefiable sites would be to deterministically determine PHA for liquefiable sites and then substitute that PHA for the acceleration coefficient, A, in Equation 8.1 to generate generally conservative code coefficients on a site specific basis.

Recommendations for Utah

Based on the findings above, several options are available for the Utah Department of Transportation to generate conservative response spectra for liquefiable

sites. These recommendations require no special treatment of standard design criteria to account for soil softening.

The first option would be to require bridge design to be based on PHA with 2 percent probability of not being exceeded in 50 years, rather than 10 percent probability of not being exceeded, the exceedance level adopted in the LRFD code. For the Wasatch Front area, which is the area with the greatest seismic hazard in the state, the required acceleration coefficient, A, would be approximately 0.6 g. By applying this acceleration coefficient, the code coefficients generated from Equation 8.1 should be sufficiently conservative to envelope response spectra for liquefaction sites for all spectral periods. Thus, no special adjustments to the response spectra or code coefficients would be required to account for the effects of soil softening and liquefaction on ground response. This option may be more important, however, for design of structures on typical nonliquefiable sites than on liquefiable sites, because of the significant threat of large (M=7) earthquakes on the Wasatch fault could generate PHA that greatly exceed the 0.3 g acceleration coefficient that is suggested in the code for the Wasatch front area.

A second possible option would be to continue using the LRFD recommended acceleration coefficient maps, which suggest an acceleration coefficient of about 0.30 g for the Wasatch front. As noted for each of the investigated sites where soil softening occurred early in the sequence of strong accelerations (WLA, PIDA, and NJ), the softening caused sufficient reduction of short-period spectral accelerations that code coefficients calculated using an A-value of 0.30 g conservatively enveloped spectral values for all structural periods less than 0.7 sec. Most bridges in the Utah highway system are short-period structures and would fit within this period range. For longer

period structures, assigning a CSPT of IV to all sites underlain by liquefiable layers would add additional conservatism without requiring other specialized adjustments to the code. However for strongly shaken sites that soften or liquefy, long-period spectral accelerations would likely exceed code coefficients based on an A-value of 0.30 g.

A third possible option would be to require a site specific or deterministic analysis of ground motions for bridge sites underlain by liquefiable layers. These analyses could develop expected PHA in the absence of soil softening or liquefaction. Those PHA could then be applied as the acceleration coefficient, A, in Equation 8.1 to generate generally conservative code coefficients that would be applicable even if the ground response during large earthquakes were influenced by softening and liquefaction. Deterministic peak accelerations taken from the map compiled for Utah by Halling et al. (2002), could be applied in this manner. Because the accelerations contoured on those maps are for bedrock accelerations, modification for site effects would be needed for bridges founded on soil sites.

For general application in Utah, the authors of this report recommend Option 1 because of the added measure of safety for all bridges, including those sited over liquefiable layers. As alternative recommendations, we suggest Options 3 and 2, in that order, to assure that code coefficients used in bridge design are adequate to account for the influence of soil softening and liquefaction should they occur.

Cautions

An important phenomenon associated with soil softening and liquefaction that has not been addressed in previous sections of this report is increased transient ground

deformations or displacements that occur at liquefaction sites. Softening of liquefiable layers generally concentrates these displacements within the liquefiable layer. These displacements could cause serious damage to deep foundations that transect the liquefiable layer. The large differential displacements associate with these enhanced motions could also damage bridges on shallow foundations due to the large differential movements.

Peak-to-peak ground displacements at ground surface estimated by integrating the acceleration records for the 5 instrumented sites investigated herein are tabulated in Table 8.2. The magnitudes of the peak to peak displacements range from 0.2 m at WLA, TI and ANAS, to 0.5 m at PI, to as much as 1.2 m at NJ. Assuming that the displacements were concentrated across the thickness of the liquefiable layer, approximate soil strains can be calculated by dividing these estimated displacements by the thicknesses of the liquefiable layer. The average strains so calculated range from 5% to 10%. Thus, piles driven through liquefiable layers at these and other liquefiable sites should be able to withstand several cycles of cyclic shear strain, with amplitudes as great as 5%, without adversely affecting the load-carrying capacity of the piles.

Table 8.1 Site coefficients specified in LRFD Code

Site Coefficient	Code Soil Profile Type (CSPT)			
	I	II	III	IV
S	1.0	1.2	1.5	2.0

Table 8.2. Estimated peak-to-peak ground displacements at instrumented liquefaction sites

Site	WLA		PIDA		TI		ANAS		NJ	
Direction	NS	EW	NS	EW	NS	EW	NS	EW	NS	EW
Displacement (m)			0.5	0.4	0.07	0.2	0.08	0.2	1.2	0.5

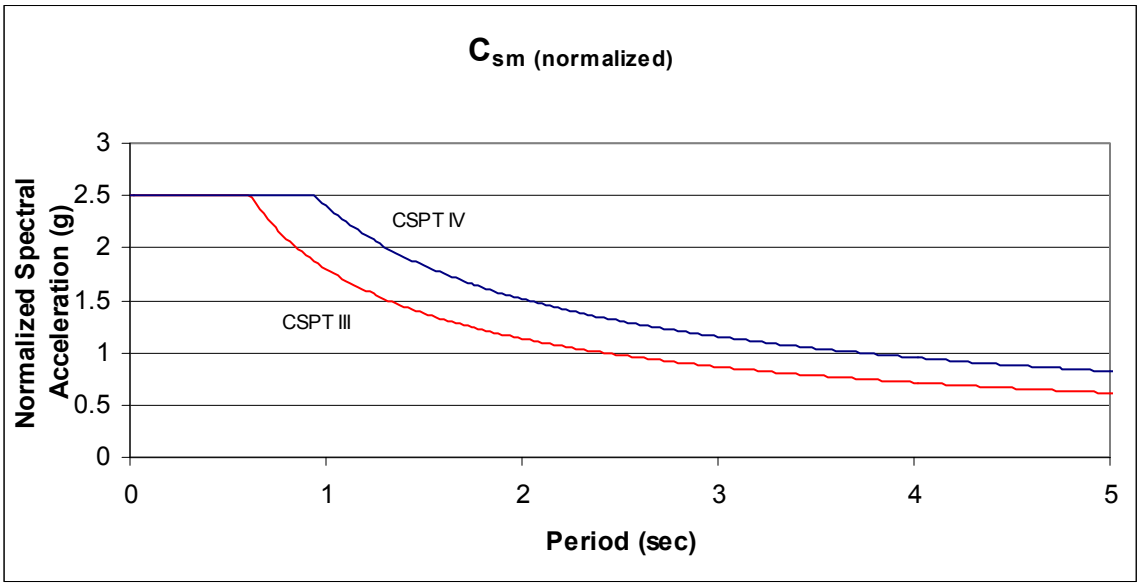

Figure 8.1. Normalized seismic response coefficent, C_{sm}, values as used in design for Code Soil Profile Types (CSPT) III and IV

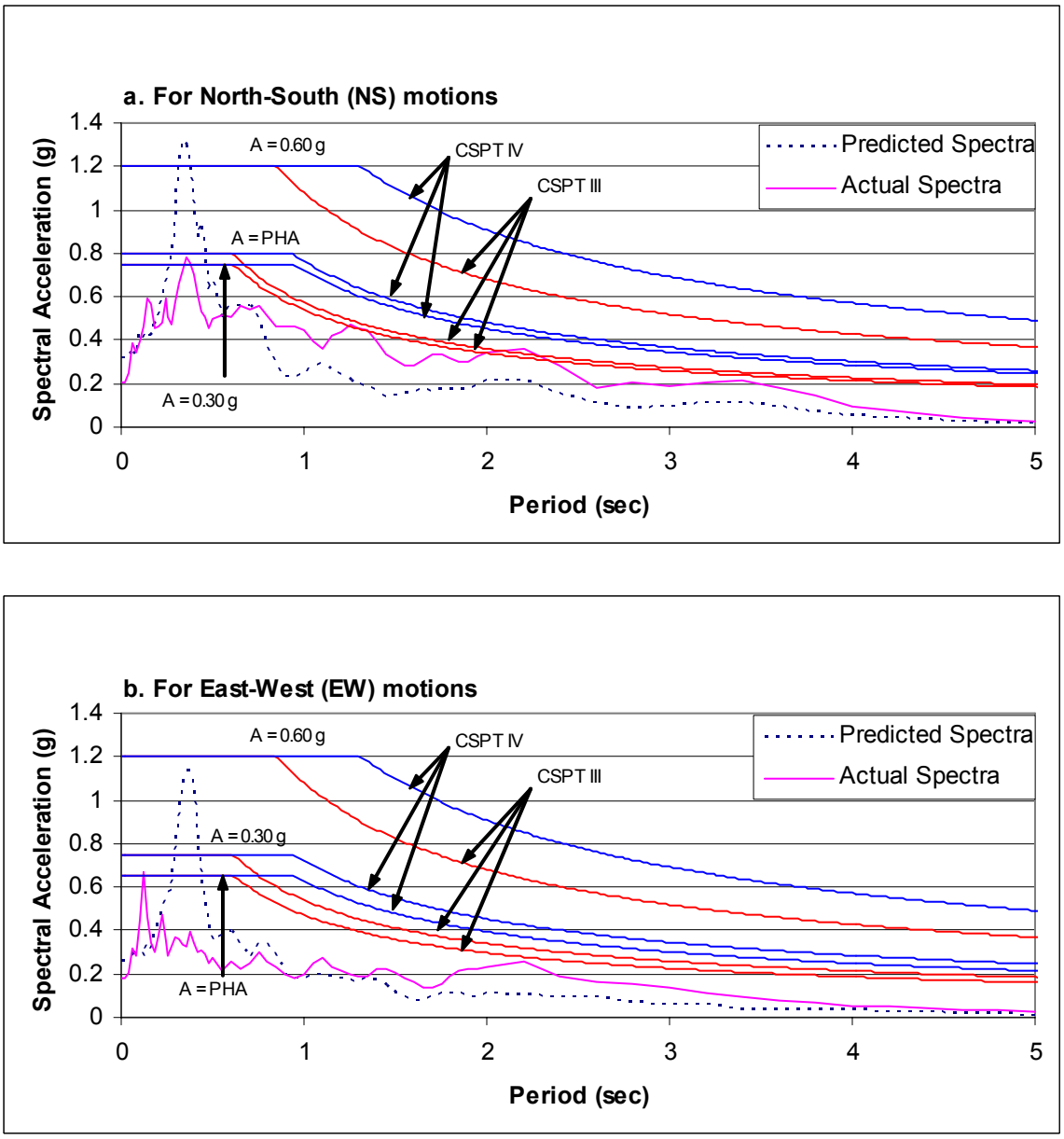

Figure 8.2. Predicted and actual response spectra for WLA site during 1987 Superstition Hills earthquake (M=6.6) with LRFD code coefficient response spectra

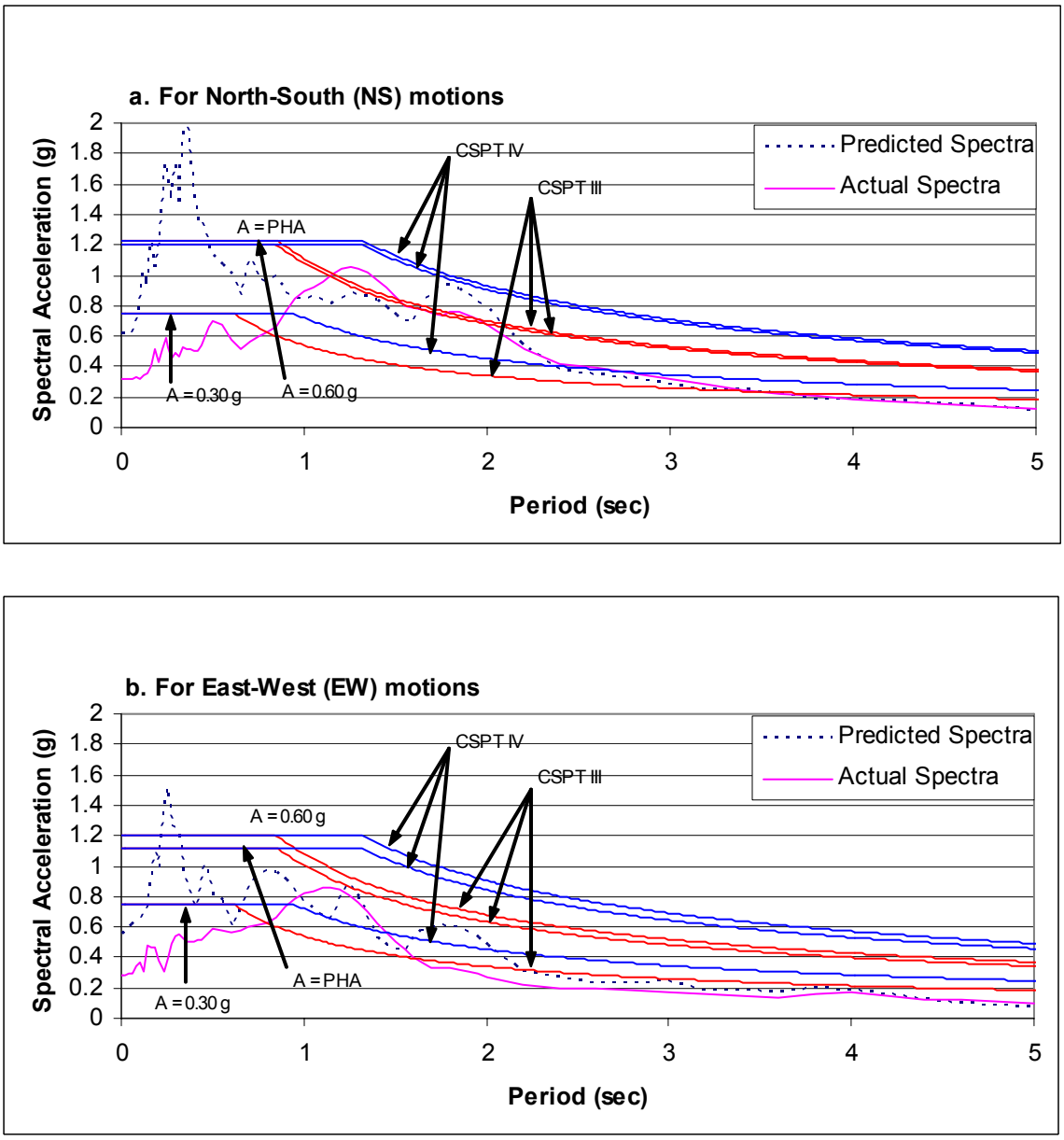

Figure 8.3. Predicted and actual response spectra for PIDA site during 1995 Kobe earthquake (M=7.2) with LRFD code coefficient response spectra

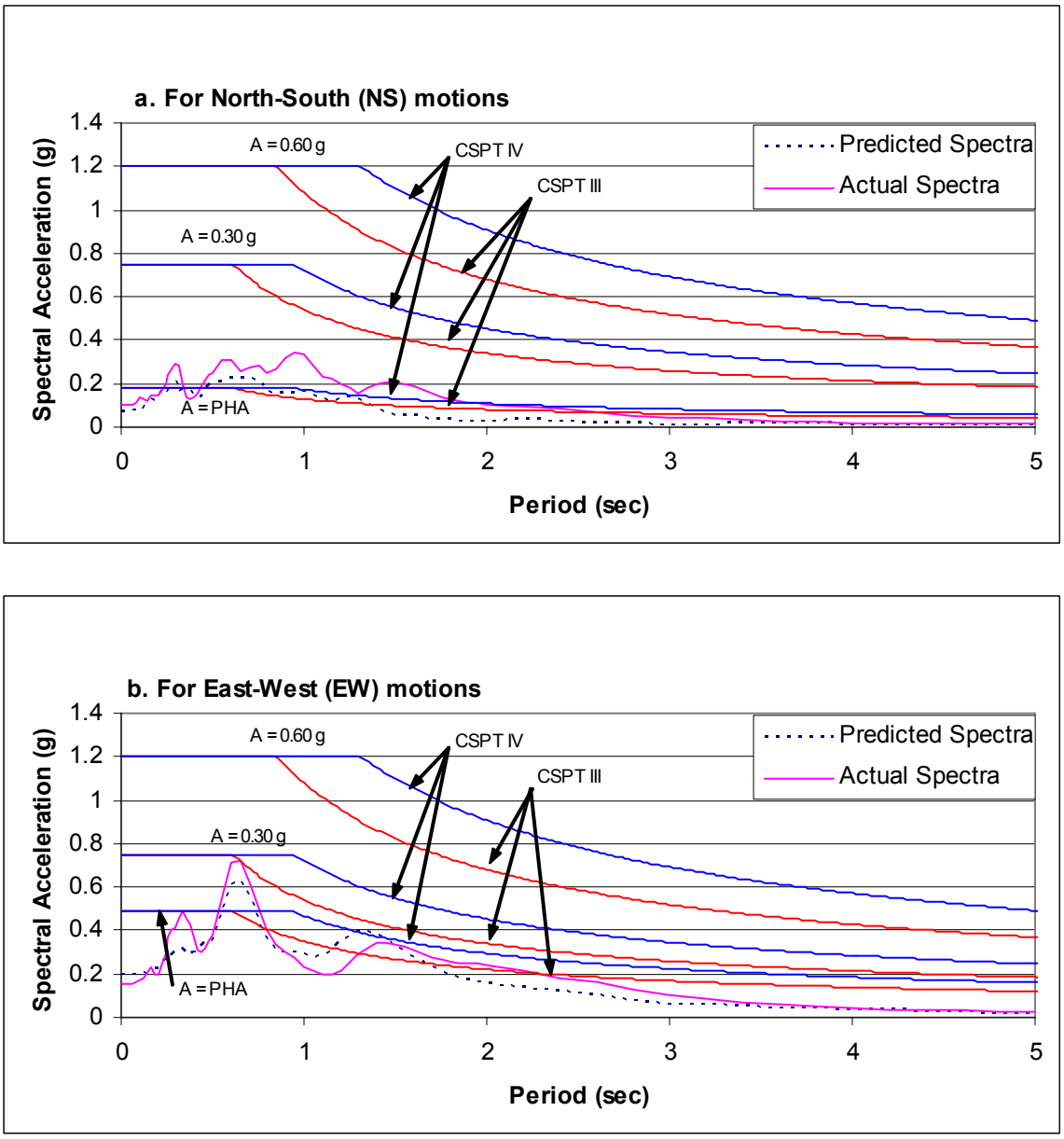

Figure 8.4. Predicted and actual response spectra for TI site during 1989 Loma Prieta earthquake (M=6.8) with LRFD code coefficient response spectra

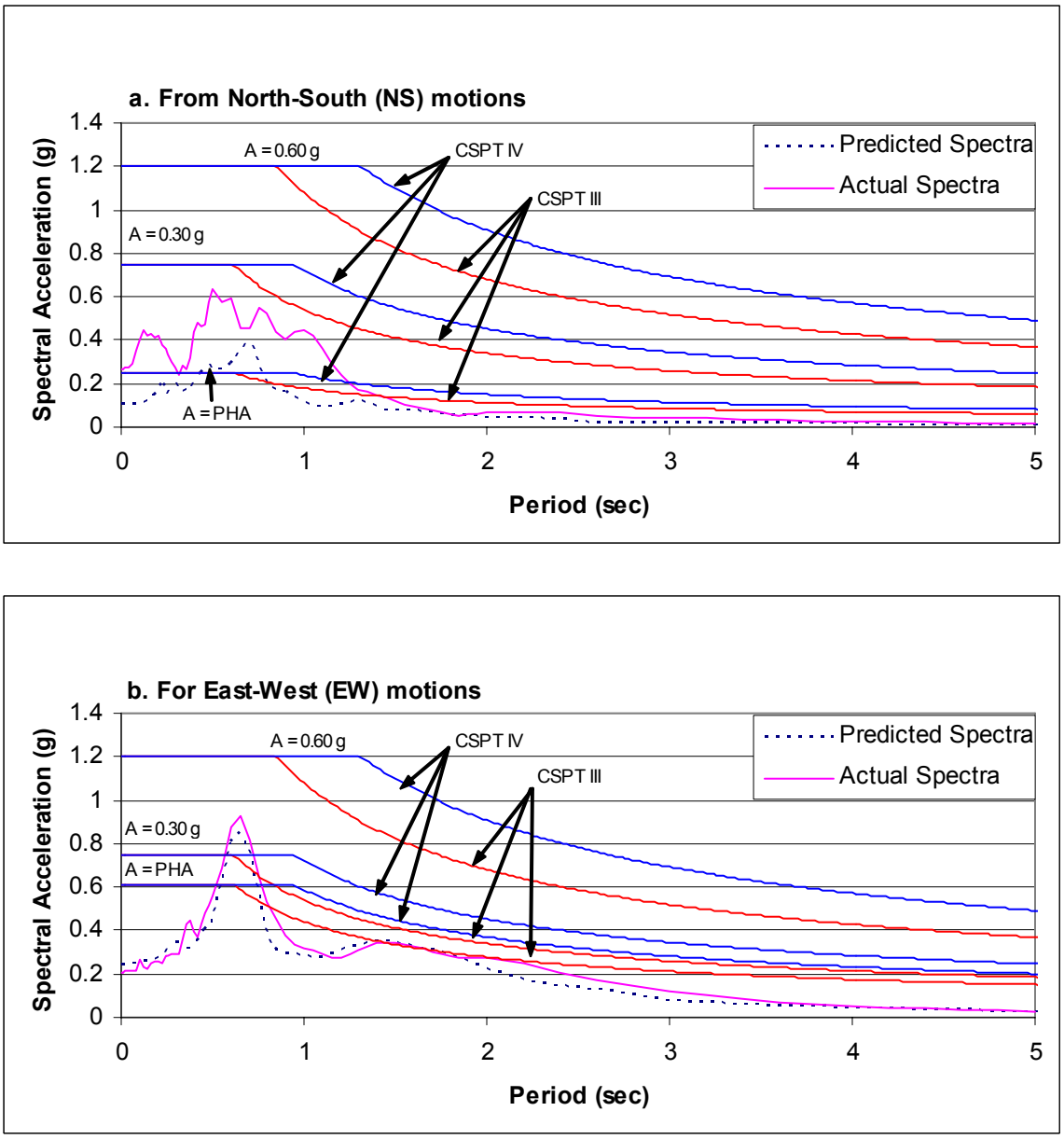

Figure 8.5. Predicted and actual response spectra for ANAS site during 1989 Loma Prieta earthquake (M=6.8) with LRFD code coefficient response spectra

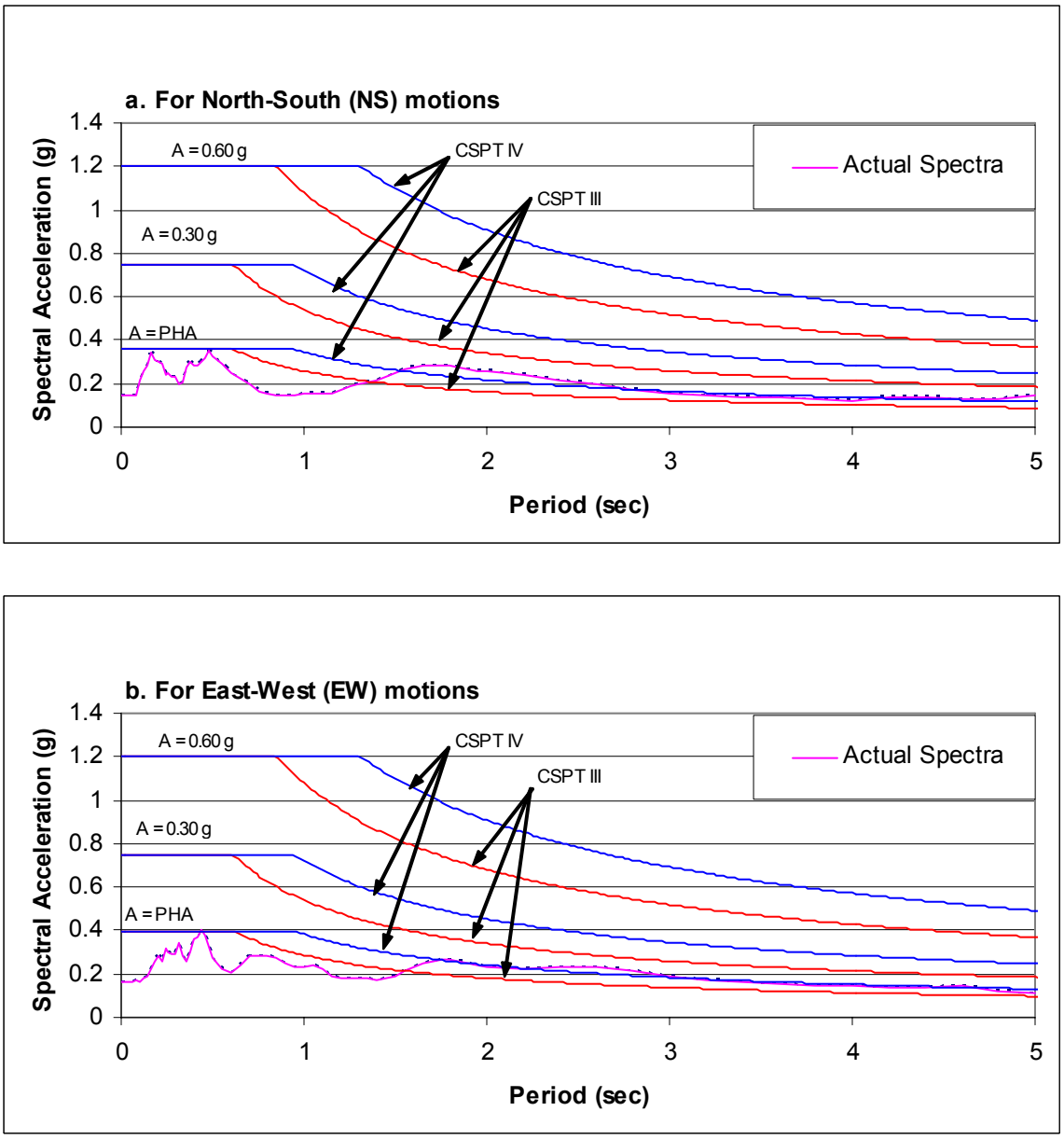

Figure 8.6. Predicted and actual response spectra for NJ site during 1964 Niigata, Japan earthquake (M=7.5) with LRFD code coefficient response spectra

SECTION 9

Conclusions

The analyses and comparisons made in the preceding sections of this report lead to the following general conclusions concerning the influence of soil softening and liquefaction on response spectra required for bridge design.

1. Soil softening due to increased pore water pressure generally causes a reduction of short period (<0.7 sec) spectral accelerations compared to those that would have occurred in the absence of soil softening. This influence is well illustrated by smaller values of response spectra calculated from measured acceleration time histories (termed actual spectra throughout this report) compared to spectra predicted to have occurred in the absence of soil softening (termed predicted spectra) for the WLA and PIDA sites. In both of these instances, significant soil softening began early in the sequence of strong accelerations that propagated through the site and strong spectral peaks that developed in the predicted spectra at periods less than 0.7 sec are muted or absent in the actual spectra. Thus for bridge structures with short fundamental periods (<0.7 sec) soil softening and liquefaction may have a beneficial effect of reducing input lateral forces at the expense of increased ground deformations within the softening soil layer.
2. Where significant soil softening does not occur before the more intense seismic motions propagate through a site, soil softening has little influence on short period (<0.7 sec) ground motions. For example, short period spectral accelerations were little effected at the TI and ANAS sites because of late soil softening and

liquefaction. Longer period motions at these sites were enhanced, however, by soil softening as noted below.

3. Soil softening usually causes enhancement of long-period spectral values (>0.7 to 1.0 sec) due to lengthening of the fundamental site period as the soil softens. In instances where liquefaction-induced ground oscillation persisted after the cessation of strong ground accelerations, considerable enhancement of actual response spectra developed as indicated by greater actual than predicted spectral values for periods between 1.0 sec and 4.0 sec. This enhancement was evident in the spectra calculated for the WLA, TI and ANAS sites, but was absent in the PIDA spectra. The reason for the absence at PIDA was apparently due to the very strong ground motions that quickly liquefied the soils beneath the site, the thick layer of liquefied soil that quickly damped the motions and did not develop resonance with late arriving seismic ground motions, or the near absence of late arriving long-period seismic accelerations. The nearness of the site to the seismic source (approximately 6 km) may have led to both the high intensities of ground motions and the lack of coherent late arriving long-period motions.

4. Comparisons of design spectra embedded within the LRFD Bridge Code (AASHTO, 1998) as elastic seismic response coefficients, C_{sm}, with actual and predicted spectra calculated for the various sites indicate the following relationships:

    A. For structures with short fundamental periods (< 0.7 sec), an acceleration coefficient, A, of 0.60 g and either Code Soil Profile Type (CSPT) III or IV generate C_{sm} that very conservatively envelope all of the actual spectra

calculated for the five sites investigated. This enveloping is true even for the intensely shaken PIDA site where predicted PHA are 0.63 g and 0.56 g, respectively, in the NS and EW directions. (Had soil softening not occurred at this site and the predicted spectra would have exceeded the C_{sm} values at periods between 0.2 sec and 0.5 sec. Soil softening, however, prevented these large spectral peaks from developing.) Thus for structures with short fundamental periods (<0.7 sec), C_{sm} based on an A of 0.60 g are likely to be very conservative for bridge design at liquefaction sites due to the beneficial influence of soil softening. Again this benefit may occur at the expense of greater ground deformation within the softened soil layer. By way of commentary, an A of 0.60 g is compatible with mapped A-values for most highly seismic areas of California, including the sites at WLA, TI, and ANAS. An A of 0.60 g is also applicable to the Wasatch front area of Utah if a probability of exceedence of 2 % in 50 years is applied rather than the code specified 10 % probability of exceedence in 50 years in the LRFD code. UDOT engineers have adopted a 2 % probability of exceedance criterion for all UDOT bridges. A 2 % probability of exceedence is also required by the International Building Code (IBC), the code adopted by the State of Utah for building design.

B. For structures with short fundamental period (<0.7 sec), C_{sm} based on an A of 0.30 g (the LRFD code value for the Wasatch front) and either CSPT III or IV also conservatively envelopes actual response spectra calculated

for each of the investigated sites, except ANAS where soil softening did not significantly reduce predicted short-period spectral accelerations. Again this enveloping occurs only because soil softening greatly reduced most of the predicted short-period spectral accelerations.

C. For structures with long fundamental periods (>0.7 sec) an A of 0.60 g and a CSPT IV generates C_{sm} that conservatively envelope all of the calculated actual response spectra. Thus, code coefficients based on this level of ground motion and for soft site conditions (CSPT IV) should be conservative for application at liquefaction sites.

D. If CSPT III site criteria are applied with an A of 0.30 g, the generated C_{sm} conservatively envelope all of the response spectra calculated for the five sites, except for the actual NS spectrum calculated for PIDA. The PIDA spectrum exceeds C_{sm} values by as much as 20 % for periods between 1.0 sec and 2.0 sec. The predicted peak horizontal acceleration (PHA) for the NS component of motion at PIDA is 0.63 g, which is relatively strong and exceeds the applied A-value of 0.6 g; thus this site represents a very intensely shaken site. Based on this one important comparison, CSPT III criteria may be inadequately conservative for long-period bridges founded on liquefiable deposits. On the other hand, the CSPT III criteria adequately envelope the PIDA spectra in the EW direction, which also had a high predicted PHA of 056 g.

E. Where predicted PHA were substituted for A, the code coefficients conservatively enveloped actual response spectra at short periods (< 0.7

sec) for all sites except TI and ANAS where soil softening did not occur until late in the sequence of strong ground motions as noted above. Even at longer periods (>0.7 sec), the predicted PHA-based code coefficients for CSPT IV site criteria conservatively enveloped the response spectra for all of the sites, including PIDA.

5. As suggested above, a caution that must be considered at liquefiable sites is the possibility of increased ground deformation within the liquefied zone. Peak-to-peak ground displacements at ground surface estimated from calculated displacement time histories for the 5 sites investigated herein are tabulated in Table 8.2. The magnitudes of the peak to peak displacements range from 0.2 m at WLA, TI and ANAS, to 0.5 m at PI, to as much as 1.2 m at NJ. Assuming that the displacements were concentrated across the thickness of the liquefiable layer, approximate average strain amplitudes range from 2 % to 5 %. Thus, piles driven through liquefiable layers at liquefiable sites should be able to withstand several cycles of cyclic shear strain, with amplitudes as great as 5 %, without adversely affecting the load-carrying capacity of the piles.

Section 10
References

AASHTO, 1998, LRFD Bridge Design Specifications: American Association of State Highway and Transportation Officials, Washington, D.C.

Bennett, M.J., McLaughlin, P.V., Sarmiento, John, and Youd, T.L., 1984, Geotechnical investigation of liquefaction sites, Imperial Valley, California: U.S. Geological Survey Open File Report, 84-252, 103 p.

Brady, A.G., and Shakal, A.F., 1994, Strong-Motion Recordings: The Loma Prieta Earthquake of October 17, 1989—Strong Ground Motion, US Geological Survey Professional Paper 1551-A, p. 9-38.

Carlisle, H., and Rollins, K.M., 1994, Ground response studies at the Alameda Naval Air Station: The Loma Prieta Earthquake of October 17,1989—Strong Ground Motion, US Geological Survey Professional Paper 1551-A, p. 123-143.

EERC, 1995, Liquefaction and related effects: Geotechnical Reconnaissance of the Effects of the January 17, 1995 Hyogoken-Nanbu Earthquake, Japan, University of California,Berkeley, Report no. UCB/EERC-95/01, p. 27-71.

Elgamal, A.W., Zeghal, M.,and Parra, E., 1996, Liquefaction of reclaimed island in Kobe, Japan: Journal of Geotechnical Engineering, v.122, no. 1, p. 39-49.

Halling, M.W., Keaton, J.R., Anderson, L.R., and Kohler, W., 2002, Deterministic Maximum Peak Bedrock Acceleration Maps for Utah: Miscellaneous Publication 02-11, Utah Geological Survey (in cooperation with Utah Department of Transportation), 57p.

Hamada, M., Yasuda, Y., Isoyama, R., and Emoto, K, 1086, Study on Liquefaction Induced Permanent Ground Displacements: Association for the Development of Earthquake Prediction, Tokyo, Japan

Holzer, T.L., Youd, T.L., and Hanks, T.C., 1989, Dynamics of liquefaction during the Superstition Hills Earthquake (M = 6.5) of November 24, 1987: Science, v. 244, p. 56-59.

Hirono, T., 1968, Seismometrical Features: General Report on the Niigata Earthquake of 1964: Electrical Engr. College Press, Univ. of Tokyo, Japan.

Hamada, M, Isoyama, R., and Wakamatsu, K, 1996, Liquefaction-induced ground displacement and its related damage to lifeline facilities: Soils and Foundations, Special Issue, p. 81-97.

Ishihara, K., Yasuda, S, and Nagasi, H, 1996, Soil characteristics and ground damage: Soils and Foundations, Special Issue, p. 109-118.

Iwasaki, Y, and Tai, M, 1996, Strong ground motion records at Kobe Port Island: Soils and Foundations, Special Issue, p. 29-40.

Kawasumi, H., (ed),1968, General Report on the Niigata Earthquake of 1964: Electrical Engr. College Press, Univ. of Tokyo, Japan.

Morimoto, R., 1968, Geologic background of the Niigata earthquake: General Report on the Niigata Earthquake of 1964: Elctrcl Engr Coll Press, Univ of Tokyo, Japan.

Rollins, K.M., McHood, M.D., Hryciw, R.D., Momolka, M., and Shewvridge, S.E., 1994, Ground response on Treasure Island: The Loma Prieta Earthquake of October 17,1989—Strong Ground Motion, US Geological Survey Professional Paper 1551-A, p. 109-122.

Seed, H.B., and Idriss, I.M., 1970, Seismic response of soil deposits: Journal of the Soil Mechanics and Foundations Division, ASCE, v. 96, no. SM2, p. 631-638.

Youd, T.L., 1978, Major cause of earthquake damage is ground failure: Civil Engineering, v. 48, no. 4, p.47-51.

Youd, T.L., 1993, Liquefaction-induced damage to bridges: Transportation Research Record No. 1411, p. 35-41.

Youd, T.L., 1998, *Screening Guide for Rapid Assessment of Liquefaction Hazard at Highway Bridge Sites:* Multidisciplinary Center for Earthquake Engineering Research Technical Report MCEER-98-0005, p. 58.

Youd, T.L. and Bartlett, S.F., 1989, US case histories of liquefaction-induced ground displacement: Proceedings, First U.S.-Japan Workshop on Liquefaction, Large Ground Deformation and Their Effects on Lifeline Facilities, US National Center for Earthquake Engineering Research, p. 22-31.

Youd, T.L. and Holzer, T.L., 1994, Piezometer performance at the Wildlife liquefaction site: Journal of Geotechnical Engineering, American Society of Civil Engineers, v. 120, no. 6, p. 975-995.

Youd, T.L. and Wieczorek, G.F. 1984, Liquefaction during the 1981 and previous earthquakes near Westmorland, California: U.S. Geological Survey Open-File Report 84-680.

Youd, T.L., Willey, P.S., and Gilstrap, S.D.,1997, Liquefaction hazard screening for Utah highway bridges: Fnl Rprt, UDOT Task Order 7RE0383 SPR-0012(018), Cntrct No. 93-8476, and FHWA (NCEER) Proj DTFH61-92-C-00106, Task 106-F-6.1